Lignin valorization through heterogeneous photocatalysis towards a sustainable circular-economy mindful approach

Filipe Matos Pereira Lima

Thesis submitted to the University of Ottawa
in partial Fulfillment of the requirements for the
master's degree in Chemistry

Department of Chemistry and Bimolecular Sciences
Faculty of Science
University of Ottawa

Abstract

Renewable materials have been put into the spotlight as the demand for environmentally responsible feedstocks grows yearly. Lignin, an abundant and renewable aromatic polymer, which can source a diverse cast of derivative structures, has yet to rise to the potential it possesses as a material in high technological applications. The expansion of studies and growing interest in its versatility has brought forth materials such as lignin nanoparticles, coatings, films, second generation alcohols, phenolic building blocks for drug synthesis, and many others. Among the many valorization methods thus far pursued, photochemical methods have received relatively low representation, incurring several challenges stemming from less desirable interactions of lignin as a substrate directly with light. As the search for clean, low-emissive processes with high scale-up potential for lignin valorization continued, advances and studies on the benefits and challenges on the use of photochemistry with this class of compounds became the focus of this work.

This thesis will primarily aim to highlight our efforts to find photocatalytic materials and systems to achieve lignin valorization, discuss its limitations and benefits, and provide a pathway towards potential applications of these reactions. Our core values were to find conditions that worked well, but also translating that success into systems that could be greener and less dangerous or environmentally impactful.

We can report to have achieved single-product yields of over 2% in protolignin valorization reactions using Pd and Au based nanoparticles, supported on niobium-based materials. We have also reached up to 2% yields in visible-light reactions using CdSe quantum dots. While literature reports tend to overwhelmingly focus on lignin models, we have kept ours on real lignin, which while more complex and challenging, does present more relevant results in the long run for this field. These results, in addition to molecular model valorization experiments, present a promising prospect for the application of photocatalysis in lignin valorization for the future.

Dedicated to my partner Sarah A. Borys, my family and friends for supporting me in the best and worst times

&

To my mentors Dr. Juan C. Scaiano, Dr. Anabel Lanterna and Dr. Rashmi Venkateswaran

Acknowledgments

The journey that culminates with the writing of this thesis may be an academic one in principle, but it has been a personal journey just as much. I have grown to the point where I can scarcely recognize the teenager who hastily changed his mind on studying History and applied to study Chemistry in University instead in late 2008. I decided in that moment that I wanted to understand ways to affect change in the world, more than the changes that affected who we are now. To my surprise, I ended up learning through the lens of science.

After spending over a third of my life in academia, one of the most important things I've learned was the value of true mentorship. Tito Scaiano has been a true mentor for many years, and I am honored to be counted among his students, being challenged to overcome adversities, and deliver the best work that I could.

I would also like to thank Dr. Anabel Lanterna and Dr. Bowen Wang, for being great teachers inside the laboratory, and good friends outside of it as well. Lastly, I would like to thank all my friends and colleagues from the Scaiano Group and from the department. A special thank you to Kelsey Fournier, Connor Bourgonje, and other close friends who made me feel like one of them. For all the shared pains and victories, for the sleepless nights of marking, studying, and the fun ones too, everything became easier together with you.

Table of Contents

List of Figures

List of Tables

List of Schemes

List of Abbreviations

[ ]	Concentration
ζ Potential	Zeta Potential
0D	Zero dimensional
1D	One dimensional
2D	Two dimensional
3D	Three dimensional
Au	Gold
AuNP	Gold nanoparticle
Aq	Aqueous
Br	Bromine
C	Carbon
Cu	Copper
CTAB	Hexadecyltrimethylammonium bromide
°C	Degrees Celsius
CB	Conduction band
DCM	Dichloromethane
DR	Diffuse reflectance
EDS	Energy- dispersive X-ray spectroscopy
eV	Electron volt
EWG	Electron withdrawing group
EDG	Electron donating group
GC-FID	Gas Chromatograph coupled to a Flame Ionization Detector
GC-MS	Gas Chromatograph coupled with Mass Spectrometer
HCl	Hydrochloric acid
THF	Tetrahydrofuran
H+	Proton
HOMO	Highest occupied molecular orbital
hv	Light
ICP-OES	Inductively coupled plasma optical emission spectroscopy
IR	Infrared
I-2959	Irgacure 2959
LED	Light emitting diodes
LSPR	Localized Surface Plasmon Resonance
LUMO	Lowest occupied molecular orbital
MeCN	Acetonitrile

MeOH	Methane
mM	Millimolar
mmol	Millimole
N	Nitrogen
$NaBH_4$	Sodium borohydride
NaOH	Sodium hydroxide
nm	Nanometer
NP	Nanoparticles
NMR	Nuclear magnetic resonance
P	Product
PC	Photocatalyst
Pd	Palladium
Pt	Platinum
QD	Quantum dots
R	Reactant
rpm	Revolutions per minute
S	Substrate
SEM	Scanning Electron Microscopy
SPP	Surface Plasmon Polariton
TEM	Transmission Electron Microscopy
TiO_2	Titanium dioxide
TLC	Thin layer chromatography
UV	Ultraviolet
VB	Valence band
VIS	Visible
XPS	X-ray Photoelectron Spectroscopy

Chapter 1 Introduction

1.1 Historical Context

The Discovery of Lignin

Wood has been for thousands of years one of the most important resources to our species. From the construction of shelter, its use for energy and heat generation, and later all of its finer applications, its safe to say that harvesting this renewable material has shaped the advance of society and the hold of our species over nature. Paper is a finer application of wood, and one that revolutionized the keeping of recorded history and stories, starting with its discovery by Ts' Ai in China, around 105 AD[(1)]. For over a thousand years afterwards, plant fibers were mechanically separated in a rudimentary process to produce paper, which used no chemical enhancement processes, and all of which happened before any components of wood had ever been discriminated or chemically described.

In 1838, a wealthy chemical manufacturer in France named Anselme Payen performed experiments for the extraction of chemical derivatives from wood[1]. He discovered a new treatment in which he used a concentrated nitric acid solution to oxidize wood, followed by a wash with alkaline solution of diluted sodium hydroxide to separate the resulting extract into two fractions. This method produced an insoluble product which he denominated "cellulose", and a secondary fraction that dissolved upon alkaline treatment, which he referred to as "dissolved incrustant". According to most sources, that dissolved by-product was later named "lignin" by Schulze in 1857[1,2].

A few years prior to Payen's experiments, great advances had been made in the field of organic chemical analysis, and of notable influence on him, combustive processes discovered by Antoine Lavoisier in the 1780's were of special importance. Lavoisier's method was a rudimentary experiment to determine mostly carbon and

oxygen content by burning a sample in a controlled manner, though it required multiple operators and was very time consuming and expensive. Through the contributions of other researchers, combustive analytical methods evolved slowly over the following decades, and by the time of Payen's experiments, Justus von Liebig had reduced the previously cumbersome and costly process to a bench experiment, requiring only one operator and only half a gram of analyte. Liebig's method for carbon, hydrogen and oxygen determination was then used by Payen to produce an early account of the chemical difference between raw wood and lignin.

It wasn't until over thirty years after the original discovery of lignin that the first patent was filed for an industrial process for the pulping of wood by extracting lignin, yielding isolated cellulose fibers.

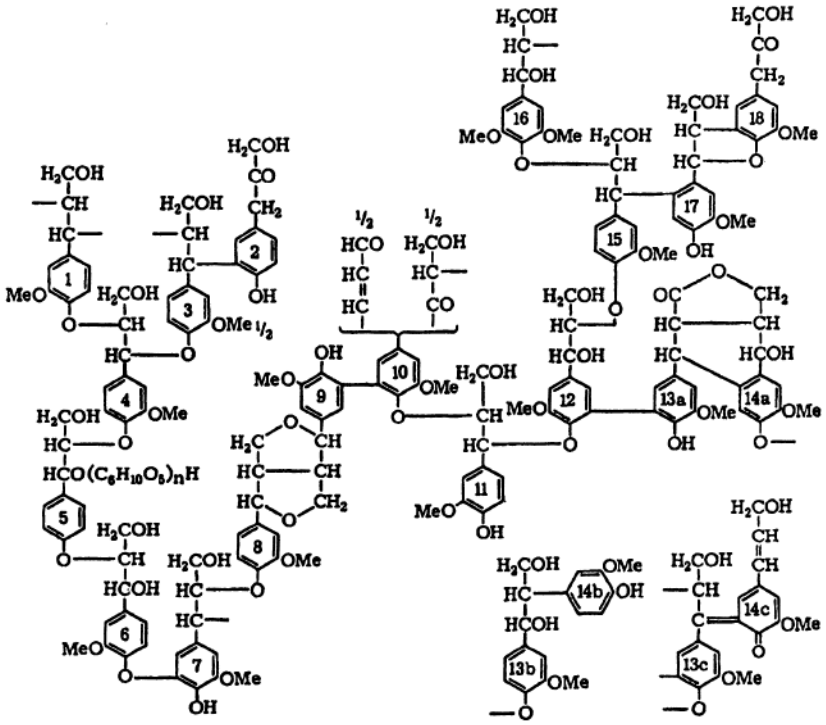

Figure 1.1: Later model proposed by Freudenberg for the structure of Spruce lignin in 1968. Reprinted with permission from McCarthy, J. L., & Islam, A. (1999). Lignin chemistry, technology, and utilization: A brief history. *ACS Symposium Series*, *742*, 2–66. Copyright 1999 American Chemical Society.

Studies on Structure and Natural Formation

The continuation of the historical background of lignin is one of its structures, and the extensive studies made to reach an accurate and complete description of its chemical bonds and monomeric unit structures. Little more than the aromatic nature of lignin was known for at least 2 decades after its initial discovery, until further extractions started to reveal possible monomeric products that were theorized as being related to the structure of lignin. A significant leap in this era was the isolation of coniferin, a glucoside of coniferyl alcohol, by Tiemann and Mendelsohn in 1875[1,11], which they obtained by treating wood with emulsin (β-glucosidase), obtaining coniferyl alcohol and glucose. They attributed the presence of coniferin to lignin, constituting one of the first hints at the monomers present.

It is pertinent to mention that in 1880, Cross and Bevan[12] used a modified extraction on wood to yield purified cellulose. Their method involved the extraction of several bast fibers, such as flax, hemp, manilla and others, by way of boiling it with a hydrochloric acid solution, yielding cellulose and “an aromatic body”, isolated as a chlorinated derivative with similar structure to that of a tetrachloroquinone. The mixture of extracts was then treated with nitric acid to yield a stable and isolated cellulose and a nitro-derivative of the aromatic compounds. This development is noted since we know it by the name of kraft pulping, and it is the most significant method of cellulose isolation, thus one of the many processes that result in large amounts of leftover lignin, that being the aromatic compounds the authors referred to.

Progress in elucidating a sensible structure for lignin was slow, as pointed out by Freudenberg in his article Biosynthesis and Constitution of Lignin[10]. A hurdle during early compositional analysis was to determine whether lignin was an ordered structure or repeated units, such as cellulose, or if it was a “compost heap”.

A large contribution to lignin studies was realized when H. Erdtman’s experiments[1] on oxidizing isoeugenol using mushroom oxidases generated phenylcoumaran, which had similar structure and composition to those believed at

the time to compose lignin. Based on this, and by using an oxidation reaction as a model for the formation of lignin, Erdtman postulated in 1933 that lignin is most likely a product of the dehydrogenation of guaiacyl-propane, with oxidized sidechains. This was a very influential and important account of lignin characterization/definition via its rationalized mechanism of formation and this approach, as will be discussed next, had very lasting consequences.

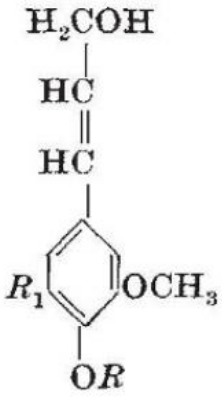

(I) R and R_1 = H: coniferyl alcohol

(II) R = $C_6H_{11}O_5$; R_1 = H: coniferin

(III) R = H, R_1 = OCH_3: sinapinic alcohol

(IV) R = $C_6H_{11}O_5$; R_1 = OCH_3: syringin

Figure 1.2: Freudenberg condensed the structures of the different monomers then estimated to compose lignin in this schematic. More possible structures would be added, as complex moieties were found, but the theories around lignin formation stem from the interactions of these compounds. Reprinted by permission from: Springer Nature, Nature. Biosynthesis and Constitution of Lignin, Freudenberg, Karl, 1959.

This then led Freudenberg, among many other researchers, to start investigating the formation of lignin as the means of fully comprehending its structure. The methodology chosen was to introduce radioactive compounds into spruce saplings to be used as a tracer, or marker. After a few days, the area that was left absorbing the marker is tested for radioactive lignin. If the compound infused with the radioactive material is similar enough in structure that the plant can biosynthesize it into lignin, they would then obtain a building block for lignin itself. The conclusions of this study were that from a C_6C_3 acid, plant metabolism generates coniferin, which is later converted by β-glucosidase into coniferyl alcohol, which is then converted into lignin by laccase and peroxidase.

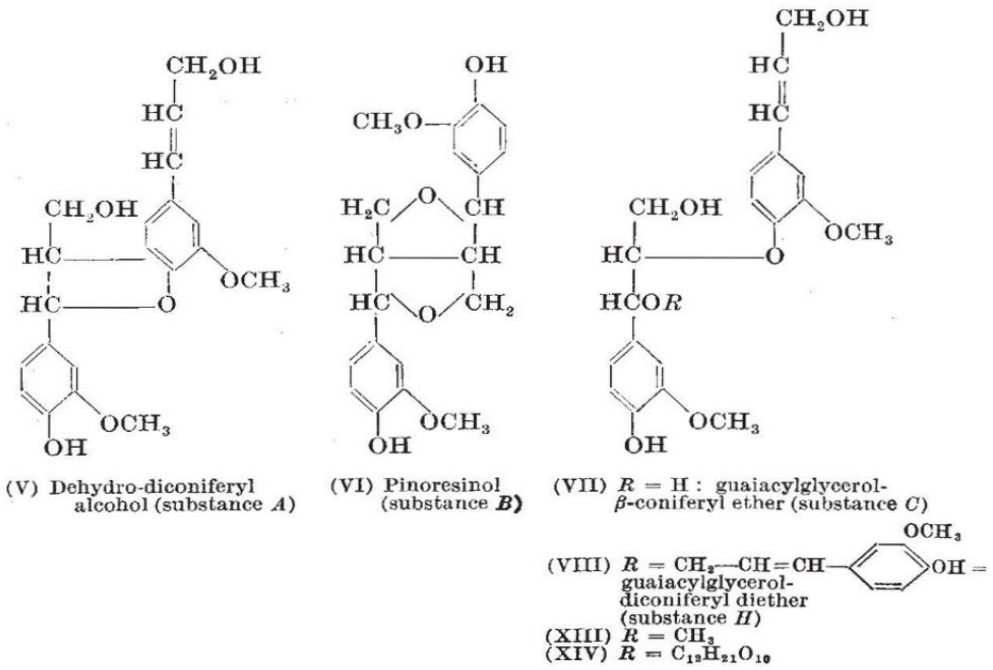

Figure 1.3: Intermediary structures obtained by the production of lignin in vitro. Reprinted by permission from: Springer Nature, Nature. Biosynthesis and Constitution of Lignin, Freudenberg, Karl, 1959.

It was also found that different bindings of the alcohols were possible when different conditions or slightly different structures were introduced, such as the examples shown in Figure 1.4.

Lignocellulose has since been the name given to the bulk of dry plant matter, also referred to as lignocellulosic biomass, and as such it is one of the most abundantly available organic-based raw materials on Earth. It is composed of three major polymeric structures, divided under two categories. Cellulose and hemicellulose are carbohydrate polymers, while lignin is an aromatic polymer. Lignin is considered a macromolecule, which in short is a molecule with a large structure, usually ranging from 100 to 10,000 angstroms[4].

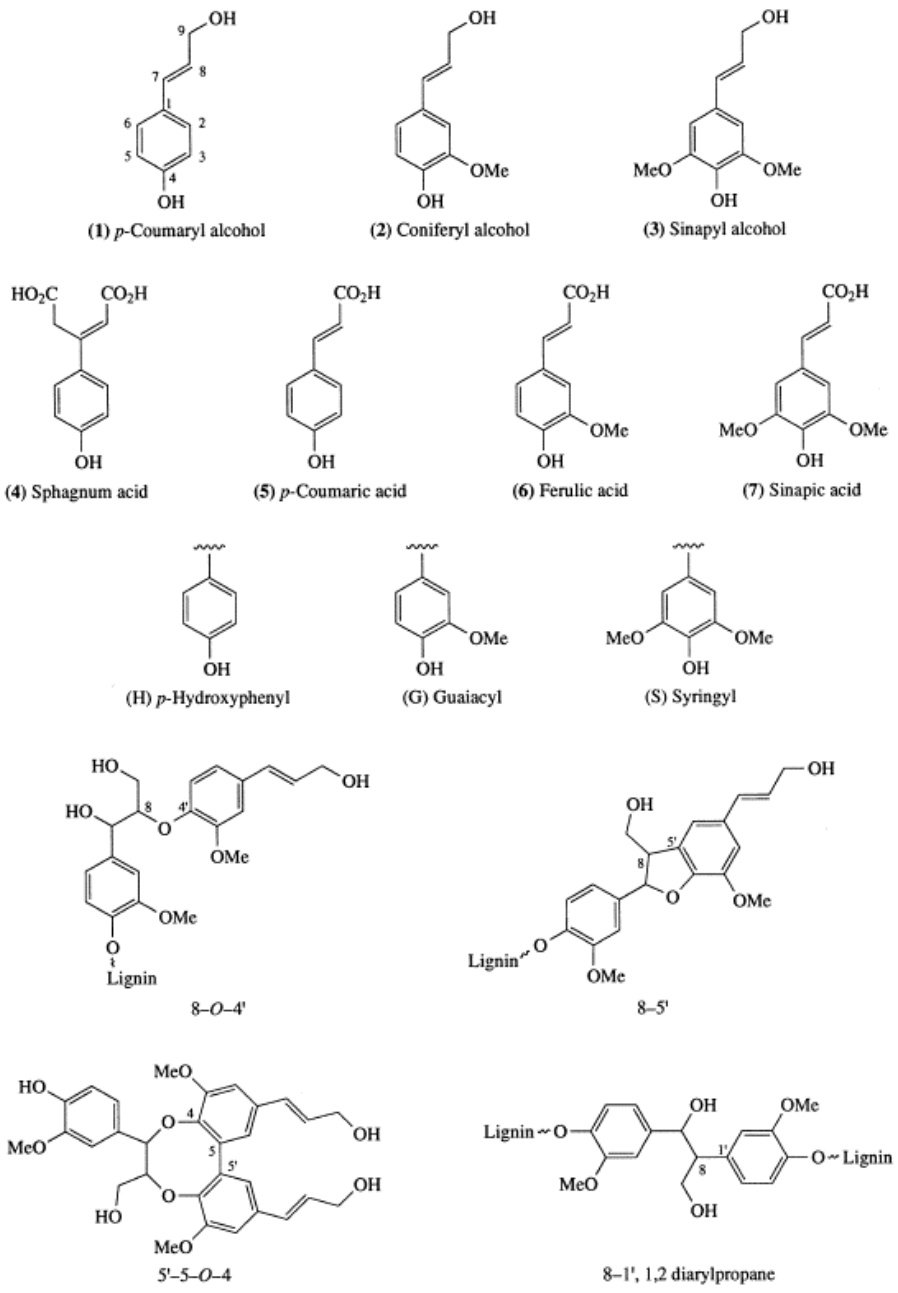

Figure 1.4: A more complete representation of the possible aromatic constituents of lignin, including their common names, as well as dimers and trimers present. Reprinted from Comprehensive Natural Products Chemistry, Vol. 3, Lewis, N. G., Davin, L. B., The Nature and Function of Lignins, 617-745, Copyright 1999, with permission from Elsevier

1.2 Lignin Characterization and Classification

As highlighted in the previous section, lignin exists in nature as a polymer bound to cellulose and hemicellulose to constitute both structural and certain active

portions of plants. To describe it in modern terms, lignin can be considered an amorphous heteropolymer, referring to the different types of moieties and linkages which compose its overall structure[13]. Lignin has an assortment of phenylpropane units, joined by a variety of linkages, and in its native form is highly insoluble in water. The heteropolymer nature of lignin gives it resistances to microbial attacks and oxidative stress. The demand for separation of lignin from its neighbouring polymeric structures has historically favored the recovery of cellulose and hemicellulose in their native form, as both had been developed early on into massively important industrial starting materials of the paper industry.

As there is no current method to obtain lignin without extraction which, by nature, modifies its structure, it is widely accepted that there is no one universal model or “correct” structure for lignin, and therefore the study of this class of compounds is highly complex.

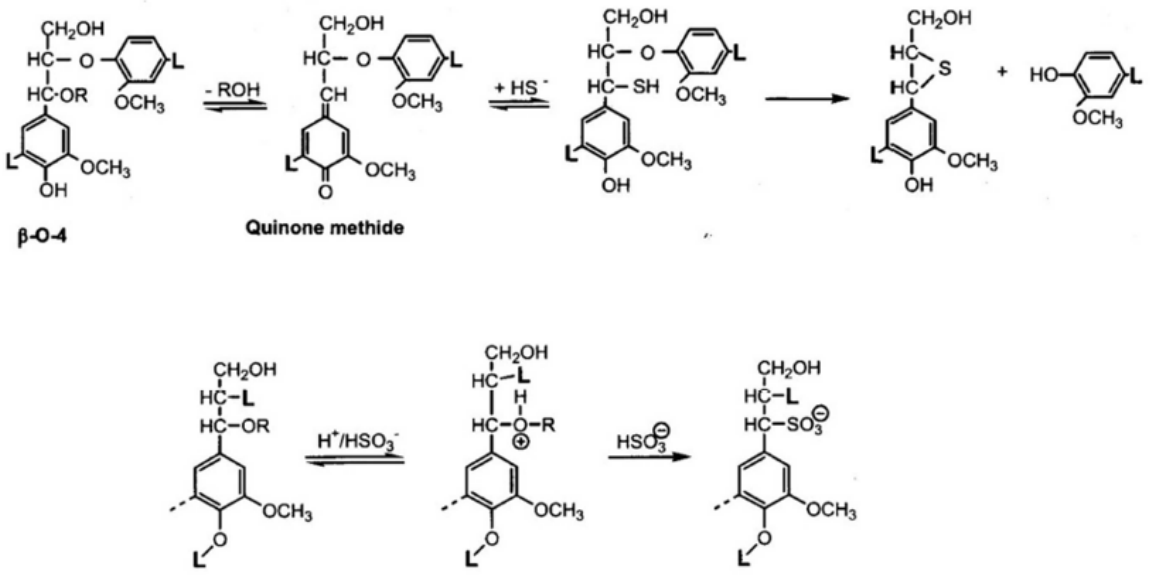

Figure 1.5: Lignin modification during pulping processes. Reproduced with permission from Glasser, W. G., Copyright 2019

Despite the extensive compositional variabilities, we can sort lignins into two primary groups, the first of which being extracted or technical lignins, and the second group is that of protolignins.

Technical Lignins

Isolated lignin is obtained as a product of an extraction process from wood, leading to a material of either more narrow characteristics, such as a specific gain in solubility, or just a generally smaller molecular weight upon the breaking and modification of a certain linkage to separate it from hemicellulose and cellulose, such as the process shown in Figure 1.5.

Traditional pulping reactions give us insight into some form of modifications that can be expected when extracting lignin. In Figure 1.5, two typical extractions used in the pulping of wood, one alkaline and one with acid treatment, are represented. At the top section, Alkyl-aryl ether cleavage and phenolic OH generations are achieved through quinonemethide intermediates in alkaline media. Presence of bisulfide ions prevents side-reactions, maximizing alkali-solubility and achieving a more complete depolymerization. At the bottom, water-soluble lignin sulfonates are produced through benzylium ion intermediate aromatic structures, which represents a typical acid pulping condition, again with bisulfite present.

Technical lignins can also be subclassified in two major groups[6], depending on the separation method used to obtain them. The first encompasses extracted lignin, such as Kraft, organosolv lignin, dioxosolv lignin, sulfonated lignin, among others, while the second is the result of hydrolysis reactions to remove carbohydrates from raw wood, also called hydrolytic lignin. Dioxosolv and organosolv lignin are worthy of special note, as they are selectively extracted to isolate components that are each especially soluble in aqueous or organic solutions, respectively.

Protolignins and Compositional Analysis

A widely used terms to categorize lignin is the source by which it was obtained, meaning the type of wood from which it was extracted, such as beech, spruce, or pine. This can give some general information about the expected aromatic composition of lignin, and the general yield of lignin from the sourcing wood. Statistical and compositional analysis done by Ragauskas and Ralph[47,77] generated three major divisions of lignin, so that the use of individual tree species was

unnecessary. The new classifications are hardwood lignin, sourced from dicotyledon angiosperms, softwood lignin, sourced from gymnosperms, and herbaceous lignin, sourced from monocotyledon angiosperms.

The name given to the group of structures being characterized and classified by this methodology is that of protolignin[6]. Classifying protolignins is a much more modern process than classifications of extracted lignins, and much of its advancements came with progress made in the field of 2D NMR. Thanks to this technique, individual moieties could be identified without the need for breaking the polymer into its fractionating compounds, and thus a more accurate description of their structure is achieved

Though knowing the type of lignin can be insightful towards applications and preferable experimental conditions, it is not enough to understand the chemical makeup contained in a specific source, or even batch of lignin. Therefore, compositional analysis of aromatics and structures is essential, since it provides more clear distinctions as to what can be expected in terms of monomer yields, antioxidant capability, and other relevant outcomes.

Table 1.1: Historical studies on lignin composition from different sources and authors. Adapted from McCarthy, J. L., & Islam, A. (1999)[1]

Author	Reference	Species	C_6C_3 Units	β-O-4	α-O-4	Aliphatic OH	Phenolic OH	Ketones	Aldehydes	Methoxyl
*Freudenberg		S	18	38.9	16.7	97.1	33.3	13.9	2.7	97.2
*Adler		S	16	43.8	18.8	19.5	4.5	1.0	1.5	16.0
*Nimz		H	25	48.0	32.0	81.6	14.4	15.6	16.0	124.0
*Sakakibara		S	28	42.9	21.4	100.0	32.1	7.1	14.3	89.3
*Glasser		S	81	39.5	16.0	104.0	29.0	7.5	16.0	91.4
*Brunow		S	25	64.0	20.0	158.0	12.0	0	6.0	100.0
Jurasek		S	2289	52.3	13.9					

Jurasek		H	2289	58.4	17.0					
Mikscke		S		49-51	6-8					
Mikscke		H		62.0	6-8					
*Glennie		LS	20	50.0	0.0	75.0	35.0	5.0	10.0	100.0
*Marton		KL	21	14.3	0.0	43.9	64.3	14.3	0	78.6

S = Softwood, H = Hardwood, LS = Lignosulfonate, KL = Kraft Lignin

*Values calculated approximately by the authors from the lignin structure figures provided in their work, linkages and functional groups calculated/100 C_9 units

1.3 Advances in lignin valorization and applications

Early studies in lignin valorization included primarily the production of Vanillin by Pearl[1,2], but strategies for lignin valorization have evolved to cover a much wider variety of target molecules. This progression of stratagems has accompanied the energy and sustainability paradigms that modern science is working towards solving. Some of the modern lignin valorization techniques are here described.

Pyrolysis

Pyrolysis of lignocellulosic biomass is a process that through the application of high temperatures, from 350 to 800°C, lignocellulosic decomposition is obtained. Product composition in reactions such as this are usually a biogas, a liquid bio-oil and solid residue called bio-char. The “bio” denomination stems from the high amounts of carbonaceous and carbohydrate molecules contained in each of the previous products, however, due to the complex nature of the lignocellulosic feedstock and the non-selective process that is pyrolysis, product variety and distribution of this process has proven to be extremely difficult to control. This is not the only limitation of the technique, since the temperatures used for pyrolysis also accrue a higher energy demand than competing methodologies, making it an uneconomic choice. [51,52]

Despite that, direct pyrolysis of raw biomass is still a methodology capable of generating lignin-derived phenols and sugar-derived products simultaneously. The

low selectivity is still a strong limiting factor, since separation of these products is not trivial, and adds another step to an already not cost-effective operation. [53]

Solvolysis

Lignin solvolysis has been performed as both a means to obtain value-added compounds from lignin, and in the development of analytical studies for lignin structure. Historically speaking, acidolysis of lignin was one of the first techniques employed in the characterization of lignin monomers.[54] One early example of monomer studies was the finding of “Hibbert’s ketones” in the early 40’s by Harold Hibbert, those being keto-phenolic monomers generated from the acidolysis of lignin.[55]

Another common solvolysis process for lignin breakage is the base-catalyzed depolymerization of technical lignins, which uses mineral bases to break alkyl-aryl ether linkages.[56] In the past decade, catalytic oxidative or reductive pathways have been prioritized over non-catalytic solvolysis for the depolymerization of the lignin. Both strategies have been developed to promote lignin depolymerization sometimes through C-C cleavage (oxidative cleavage of C_α-C_β) and increase the phenolics yields through reductive stabilization of the intermediates and products.

Catalytic Oxidative Depolymerization

Oxidative depolymerization of technical lignins has mostly been focused on the production of vanillin, which besides having potential immediate commercial applications as a natural vanilla extract, is also considered a key-intermediate for the manufacturing of bio-based polymers.[62] A lasting example of this industrial applicability is the production of vanillin from lignosulfonate under alkaline condition, catalyzed by Cu(II), by the Borregaard company since 1968.[63]

Some of the main compounds used in the catalytic oxidative depolymerization of lignin are based on transition metal ions, such as Fe(III), Mn(II) and (III), Co(II) and Zr(IV). Accounts in the field indicate that these semiconductors can enhance oxygen reactivity, facilitating the cleavage of β-O-4 and pinacol C-C linkages in technical lignins.[64]

It is in the process of catalytic oxidative depolymerization that heterogeneous metal oxides have recently been more commonly employed. Semiconductive metal oxides such as CuO, MnO_2, TiO_2, and ZnO have shown good efficacy in lignin depolymerization under certain conditions, while retaining the benefit of ease of separation and recovery of the catalyst.[65-67]

Another two important groups of catalyst bear mention in this section, those being polyoxometalates (POM)[68] and biomimetic catalysts, including metallosalen complexes and metalloporphyrins[69,70], which have been reported to cleave the β-O-4 linkages. The oxidative approach presents clear advantages over the reductive pathway and others previously discussed, including milder conditions in terms of temperature, which is often just around 100°C, and also the production of more valuable fractions of monomers.[76] The compounds produced often include monomers with active functional groups, such as aldehydes, offering flexibility and modularity afterwards for a wide gamut of applications. A disadvantage of the oxidative pathway so far is the lack of observed C-C linkages that it can cleave, though that is an area for improvement, even if it limits the yield of the reaction in the meantime.[71-73]

The other major drawbacks for the catalytic oxidative pathway to lignin valorization have been limiting the over-oxidation of the lignin when peroxides and other strong oxidants are present, which can cause unwanted ring opening reactions,[74] and radical repolymerization of monomeric and dimeric fragments of obtained technical lignin valorization products, the latter being a consistent issue with this pathway.[75]

Catalytic Reductive Depolymerization

Ni, Ru, Pd-based catalysts have been employed to the reductive catalytic depolymerization of organosolv lignin. The choice of this subsection of technical lignins is important, as lignin solubilization is an essential factor for the success and a strong limitation to these reactions.

Recent work has been able to achieve the catalytic hydrogenolysis of organosolv lignin, obtaining moderate yields of monomers, in the range of 3 to 25%,

when using molecular hydrogen. In these reactions, Ni, Pd, Pt, Ru, and other metals can dissociate molecular H_2, while physicochemical properties of their respective supports, those being acid sites or large surface areas, can contribute to the cleavage of ether bonds. The hydrogen added to the media had two major roles, the first being of course to promote the hydrogenolysis of lignin, but an equally relevant one is the inhibition of condensation reactions, via the hydrogenation of reactive intermediates, reducing the yield of char/coke. [84-86]

As mentioned in the previous section, the presence of side chain functional groups tends to generate more valuable monomers and can limit further functionalization processes. Since this method relies on the reduction of the side chain functional groups, the products from this reaction may therefore be less valuable, comparatively speaking. This is very dependent on the intended application and subsequent reaction pathways taken on the valorization of monomeric products.

Major monomeric products from these reactions are variations of 4-alkylguaiacol and 4-alkylsyringol, including either ethyl or propyl para-substituted sidechains. Some work has since been done in the tuning of the hydrogen pressure used in these systems, since early indications are that even slightly excessive hydrogen pressures could suppress the catalytic hydrogenolysis of lignin, lowering the yields of monomers/bio-oil and minimizing char formation.[84-86]

Most examples of catalytic reductive depolymerization have been done using exogenous hydrogen, commonly produced from fossil sources (often called “dirty hydrogen” in the renewable field), which is neither ideal nor renewable, and the presence of large reserves of H_2 also presents a fire-hazard and adds costly maintenance additions to the work environment necessary for its manipulation and safe use.[87,88] In response to that, catalytic transfer of lignin in hydrogen-donor solvents (methanol, ethanol, isopropanol) without external hydrogen has been gaining traction in this field, and many combinations of hydrogen donors, including sustainable alternatives, have been studied by the Scaiano Group in recent years.[61, 89-91]

1.4 Niobium-Based Catalysis

From the myriad of materials that can be chosen as the base of catalysis for lignin valorization, niobium-based compounds bring to the table some unique advantages and have strong implications outside of the laboratory.

Both Canada and Brazil combined possess over 99% of global reserves of niobium and are the major producers of niobium-based compounds worldwide. If sustainable exploitation methods can be observed, the application of this resource for environmental technologies can provide a notable socio-economic benefit to both countries, since thus far few applications of niobium-based compounds have been identified for fine and industrial chemistry.[92] Niobium-based oxide semiconductors, especially, have a hypoallergenic character, possess low cytotoxicity, physiological and chemical inertness, and high thermodynamic stability. These characteristics indicate that niobium-based compounds may be ideal as environmentally friendly supports for catalysis and photocatalysis. [92-94]

The emerging trends with niobium catalysts are the application of their high stability combined with the acid-character of its surface as a highly stable support and co-catalyst in biomass upgrading industries. Although commercial applications are not yet widespread, recent reports highlight their superior lifecycles, higher yields, and other advantages in their catalytic applications.[95-97]. Niobium has a relatively high abundance on Earth, at around 20 ppm, which is comparable to other early transition metals, like cobalt and lithium, except with more limited ongoing applications, the market has a lot more space to grow when compared to already depleting reserves of lithium, for instance.[99]

One last advantage that bears mention is the flexibility offered by using niobium-based supports for catalysis, since these materials possess higher water tolerance than most other semiconductor oxides that compete for this locus.[98] Lignin and its derivatives are naturally wet materials, especially when we consider emerging lignin-first approaches to lignin valorization, and some technical lignins are made

specifically to be more water soluble. The ability to explore water as a solvent in lignin valorization reactions, with advantages in the processing and generation of organic materials from the standpoint of how easy it becomes to reuse the solvent after a trivial separation of the products, it becomes apparent that developing and furthering the understanding of niobium-based supports and catalyst in this space is highly desirable.

Decorating with Metallic Nanoparticles

To complement the properties of niobium-based catalysts, and especially to make use of visible-light photocatalysis, it is common to decorate metallic nanoparticles onto its surface. To explore the effects of doping niobium based photocatalysts with nanoparticles, a few important definitions must be made in order to best understand what they are and what their contribution might be to the catalytic system.

Nanoparticles are one specific case of nanomaterials, where the size of all dimensions of a single particle is between 1 and 100 nanometers[19,20]. Other nanomaterial classes may have one or more dimensions within those limits, this size classification is not always strictly applied, as the most important factor is the appearance of specialized and/or enhanced properties.

Nanomaterials may be composed of either single or multi-phase chemical elements imbuing the material with improved or modified catalytic activity. Other varying properties may occur, such as electrical, magnetic, or thermal properties, but the goal is to tailor the size and shape of the nanomaterial so that the target property is superior to that of the same material in bulk[15]. A first characteristic that has an integral impact on such enhancement is the ratio of surface area available to the nanomaterial per unit of mass. As size decreases, the fraction of atoms composing the surface of their particles increases in relation to the ones with no surface contact[17].

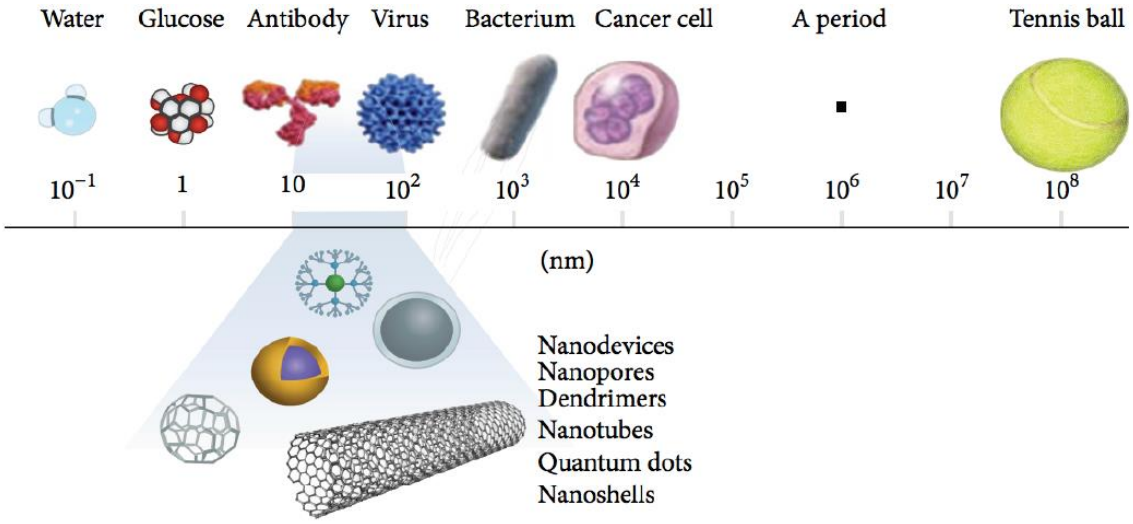

Figure 1.6: A contextualized size comparison of different magnitudes, illustrating where on the scale we can find common nanomaterials. Reprinted with permission from Amim, M. T. et al. (2014)[21]

Another important factor on the specialized or enhanced properties of specialized nanomaterials is due to quantum effects, observed because of their electrons being confined in a more limited space, manifesting a quantized energy spectrum, otherwise not present or detectable in bulk materials. This may result in magnetic moments that will, likewise, not occur in bulk materials, but can be observed in nanomaterials based on metals such as palladium, gold, or platinum.[22,23]

Compositionally speaking, typical nanomaterials may be found to be carbon-based, such as graphite and carbon nanotubes, or NPs of noble transition metals, such as Au, Ag, or Pd, among others. The only class applicable to this work thus far is that of metal nanoparticles.

Synthesis of metal nanoparticles

A common method to classify methodologies for the preparation of metal NP is to group them into top-down and bottom-up approaches. The choice of method depends on the application intended, as well as the scale of material needed, the control over the size distribution, stability of the final particles, and others.

The top-down approach starts with a bulk material which is broken down, or ablated, into smaller units until the desired size to form the target nanoparticles.

Some of the means through which the bulk material may be broken down include mechanical grinding, physical deposition, laser ablation and electro-explosion.[24-25] The top-down approach has significant limitations when controlling particle shape and size is relevant, since the highly energetic means used to ablate the bulk material tend to not be very uniform in the shaping of individual particles, or in the formation of smaller NPs. If the target nanoparticle must have smaller sizes and/or more controlled shapes, the next method is recommended, the bottom-up approach.

The bottom-up approach is based on the formation of the nanomaterial from the atomic or molecular species through a chemical reaction or self-assembly process.[26] The slow formation of the particles, ease of control over variables such as the time of reaction, presence of stabilizing and capping agents, and the possibility of using lower-powered energy sources over a longer period of time combine so that the bottom-up approach may be able to obtain greater control over the uniformity of the size and shape distribution of the nanomaterials.

To expand on the variables mentioned, this synthetic methodology works through the combination of two main parts: nucleation and growth. The synthesis of metal nanoparticles, for instance, can occur with reduction of a metal salt as a precursor to the atomic state (I, C_s). Saturation of precursor solute gradually increases until a critical energy barrier is overcome, that being the activation energy to the self-nucleation stage of the salt (II, C_{min}). Spontaneous nucleation of these nanoparticles is possible, but only under the condition of a supercritical state, such as a supersaturation of the precursor solute. (C_{max}).[27] As the concentration of the precursor solute decreases, the saturation level is leveled below a self-nucleation state, thus ending the nucleation period, marking the start of the second step to nanoparticle formation, the growth period. Growth occurs due to the diffusion of the dispersed nuclei and monomers through the solution, yielding monodispersed particles (III). These steps can be visualized in Figure 1.7.[27-29]

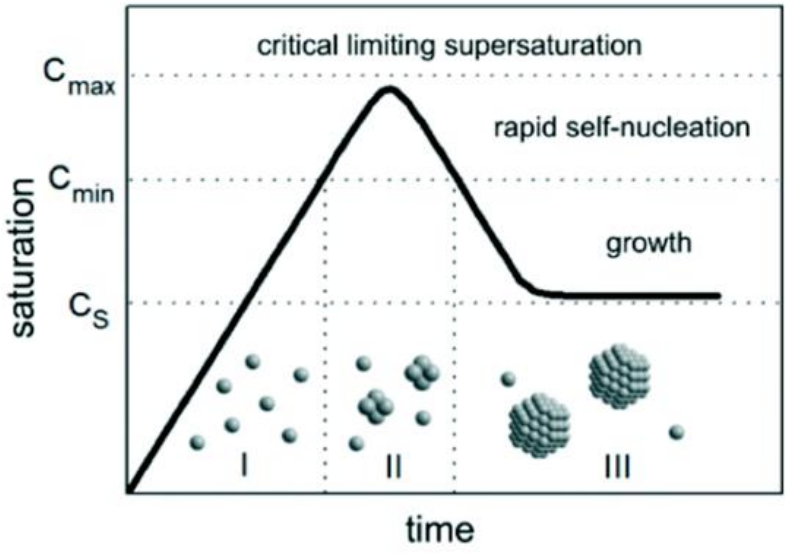

Figure 1.7: La Mer nucleation diagram, outlining steps towards nanoparticle formation. Reprinted by permission from: Springer Nature, Korean Journal of Chemical Engineering, LaMer diagram approach to study the nucleation and growth of Cu_2O nanoparticles using supersaturation theory, Arshadi, S., et al. Copyright 2014.[29]

Photochemical bottom-up approach

There are a variety of methods that are used to synthesize metal NP,[28-31] but the photochemical method offers many advantages over the other methods. It is possible through controlling the time, wavelength of the irradiating light, presence of a photosensitizer, and of a support, to tune the formation of the target nanoparticles to a narrower size and shape distribution, optimizing its optical properties in the final material. The use of a photosensitizer other than the metal salt itself is not always necessary, but in prior experimentation, contributors in the Scaiano Group have found that even in such scenarios the presence of a specialized photosensitizer has a positive effect on the yield of nanoparticles.

1.5 Pursuing Greener Advances

The search for new and commercial applications of lignocellulosic materials and lignin valorization reactions is often associated with green chemistry goals. Though lignin is a renewable material and using it as a feedstock substitute to a variety of non-renewable materials is indeed beneficial, there are several other elements from these reactions that can be improved upon so that the resulting

process has a better chance to be accepted into a market increasingly selective towards sustainability.

Solvent selection

Goals for greener solvent selection have been set with different standards depending on the application and volume that is required[8] but general concepts that apply in most cases can be discussed for any type of researching pursuit that involves wet chemistry. Outlined by Fischer[7], finding a green solvent hinges on a critical analysis of its environmental, health and safety aspects, and the second main factor is the energy demand required for its production and end-of-life cycle options, leading to a net cumulative energy demand (CED).

These parameters have been analyzed in multiple conferences and by several entities over the years, leading to the publication of solvent selection guides by GlaxoSmithKline (GSK), AstraZeneca, American Chemical Society's Green Chemistry Institute (ACS GCI), among others. These publications mostly used numerical scoring for key parameters of each solvent, but each group chose different classifications to focus on. An example is the analysis from ACS GCI, which scored classes such as handling safety, health impact, air contamination, water contamination, and waste potential, while GSK, for instance, focused on a global score for environmental impact and divided the handling safety parameter into several categories, generating slightly different conclusions. As the numerical scales generated different results that were difficult to reconcile, and justifying averaging conclusions from different perspectives seemed counterproductive, a more recent attempt at a tool for solvent selection was developed by a consortium gathering contributing scientists from Sanofi, GSK, Pfizer, The University of York, and Charnwood, under the project called CHEM21. This public-private collaboration reviewed the previous three solvent selection systems and adapted their score system into a three-tiered assessment of safety, health and environmental impact,

and solvents were categorized as green (G, or recommended), yellow (Y, or problematic), and red (R, or hazardous).

Table 1.2: Examples from the CHEM21 tool for solvent selection. Some conclusions from previous publications were revised, as shown in the last column, but most were kept. The nomenclature of problematic is not prohibitive but serves as a highlight that even previously tolerated solvents could benefit from the development of more modern substitutes. (Adapted from Prat, D., et. al., 2016)[9]

Family	Solvents	Safety Score	Health Score	Env. Score	Ranking by default	Ranking after discussion
Water	Water	1	1	1	Recommended	Recommended
Alcohols	MeOH	4	7	5	Problematic	Recommended
	EtOH	4	3	3	Recommended	Recommended
	Benzyl Alcohol	1	2	7	Problematic	Problematic
Esters	THF	6	7	5	Problematic	Problematic
	Anisole	4	1	5	Problematic	Recommended
Halogenated	DCM	1	7	7	Hazardous	Hazardous
	Chloroform	2	7	5	Problematic	Highly Hazardous
Aprotic Polar	Acetonitrile	4	3	3	Problematic	Problematic
	DMSO	1	1	5	Recommended	Problematic

Water

If there is ever to be a solvent called the gold standard for green chemistry, it must be water. The solvent with the best safety, health and environmental scores, there is a strong case to recommend it as a solvent in any reaction that does not contain water sensitive components. Problems arise when trying to apply it at large in the field of organic chemistry, where compounds are generally incompatible with it, given mainly to insolubility issues.

Despite the limitations, it remains a goal to transition organic chemistry into aqueous media, to limit current and future environmental impacts, and achieve safer work environments.

Organic solvents

While water stands in a league of its own in terms of green solvents, however limited the current application scenarios may be, organic solvents have the advantage of encompassing a wide range of compounds, providing much needed flexibility for organic chemical reactions.

Alcohols, ketones, ethers, esters, hydrocarbons, halogenated compounds, aprotic polar compounds, amines, acids, the list is extensive and provides compounds with an entire spectrum of polarities, boiling points and freezing points, viscosities, and so on. The examples contained in Table 1.2 show a selection of solvents analyzed by the CHEM21 consortium (Prat, D., et. at., 2016), specifically those that had either a direct or tangential participation on the present work. To classify solvents in the three presented categories, the authors and collaborators first used the score system adopter prior, as shown in Table 1.3.

Table 1.3: Standard rankings of recommendation prior to second analysis. Each solvent is classified by its harshest possible label, based on the conditions set. (Adapted from Prat, D., et. al., 2016)

Scores	Ranking before discussions
One score ≥ 8, or two “red” scores	Hazardous
One score = 7, or two “yellow” scores	Problematic
Any other combination	Recommended

A second assessment was held in the form of special discussions focused on correcting the classification of solvents which presented either a hazard that supersedes the noted classification, or a benefit that raises its recommendation status. Such was the case for acetonitrile, as shown in Table 1.3, due to its health score not fully reflecting the low occupational threshold value. The opposite was true for methanol, which had its classification changed from problematic to recommended, after assessments determined that the occupational threshold value for it was higher than similar solvents.

Catalyst selection

Applying catalysis to existing industrial processes is a part of the tenets of Green Chemistry, and the selection of said catalyst is highly relevant in order to determine not only the efficacy of the reaction in question, but also the economical and scale-up aspects. Stepping back for a moment for more relevant definitions, we may define a catalyst as a material that takes part in a chemical reaction facilitating the reaction by interaction with reactants but is not consumed or is regenerated by the end of the reaction. The main advantage of using a catalyst is to increase the speed of the reaction by lowering the activation energy of one or more steps in the target reaction, which allows it to occur under milder conditions. Though the majority of catalysts work through a thermal mechanism where, after heating, the catalyst uses the thermal energy that is gained to catalyze the reaction toward the desired product, there are alternatives that present better selectivity and energy efficiency.[30]

Heterogeneous *vs* homogeneous catalysis

Catalysts can be divided into homogeneous and heterogeneous. Homogeneous catalysts are named based on their presence in the same phase as the reactant and product, while heterogeneous catalysis tend to have their activity in a yet not fully understood interfacial facet, between multiple phases. Figure 1.8 shows the main difference between the homogeneous and heterogeneous catalysts. In heterogeneous catalysis the reactant interacts with the catalyst usually supported on a solid surface. [31]

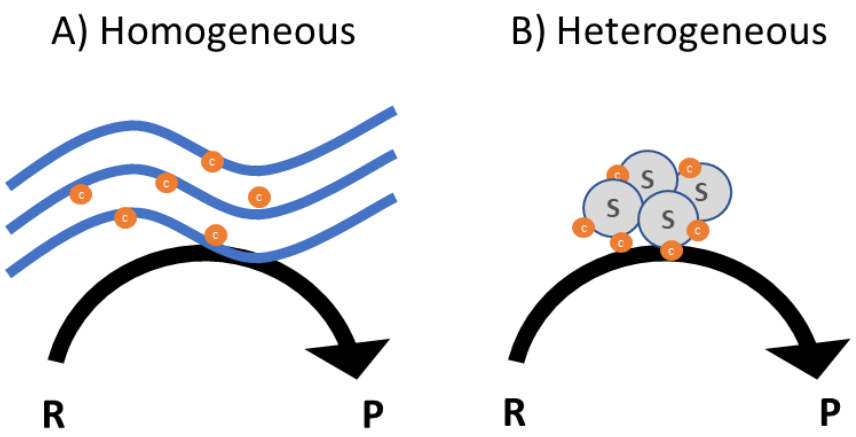

Figure 1.8: Simplified representation of a homogeneous catalytic reaction and a heterogeneous catalytic reaction, as described prior to the works of Scaiano[31] and his contemporaries.

Though this classification is still largely used in the literature, there are aspects that include exchanges between the catalyst and different phases that are simply not taken into account by it. A heterogeneous compound may for instance leach out a homogeneous species, that once in solution fulfills the role of catalyst. In this scenario, was the catalyst the homogeneous species released, or was it the heterogeneous particle that generated it? Scaiano[31] investigated such scenarios, and described three of these particular exchange scenarios as: i) heterogeneous to homogeneous, such as the one previously explained; ii) homogeneous to heterogeneous catalysis, where the homogeneous catalyst forms an insoluble nanostructure complex that possesses the capabilities of a heterogeneous catalyst; and iii) heterogeneous to homogeneous and back, where the heterogeneous catalyst releases the active catalytic species that after the catalysis are deposited back on the surface of the catalyst. Figure 1.9 illustrates these three models.[31]

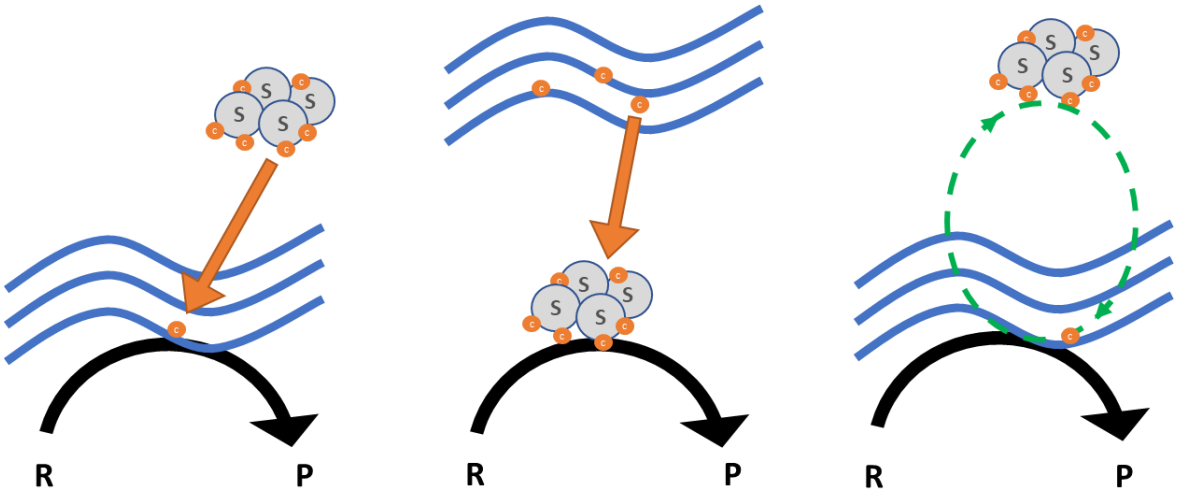

Figure 1.9: Representation of three types of heterogeneous catalysis, with R being a reactant and P representing a product.

One of the greatest advantages of using heterogeneous catalysts is the ability to separate and reuse them, making the process more economically and environmentally friendly, desired attributes of Green Chemistry.

Nanocatalysis and Photocatalysis

For a catalytic process to become industrially viable, and thus advancing the current sustainability agenda, it must be optimized so that the reaction in question may happen in as little time as possible, with high yields and, especially, high selectivity. Through mechanisms previously discussed, NP-based catalysts have become highly sought-after solutions to modern industrial processes, currently being largely employed in the pharmaceutical industry. [32]

To scale up a process, it becomes necessary to employ catalysts with high turnover frequencies, meaning the frequency with which substrates attach, react, and detach from an active site of a catalyst, so that a maximum amount of substrate is being converted in a short amount of time. Nanomaterials, with their high surface areas, have the capacity to reach much higher turnover frequencies than materials in bulk.

Another relevant concept that modifies the properties of a compound reduced to its nanometer dimension is the splitting of its energy bands into discrete

conduction and valence levels. These discreet levels may increase the chance of electronic exchanges to happen, providing nanocatalysts with a unique electronic band structure, and by consequence, unique properties. This electronic band difference is shown in Figure 1.10.[32,33]

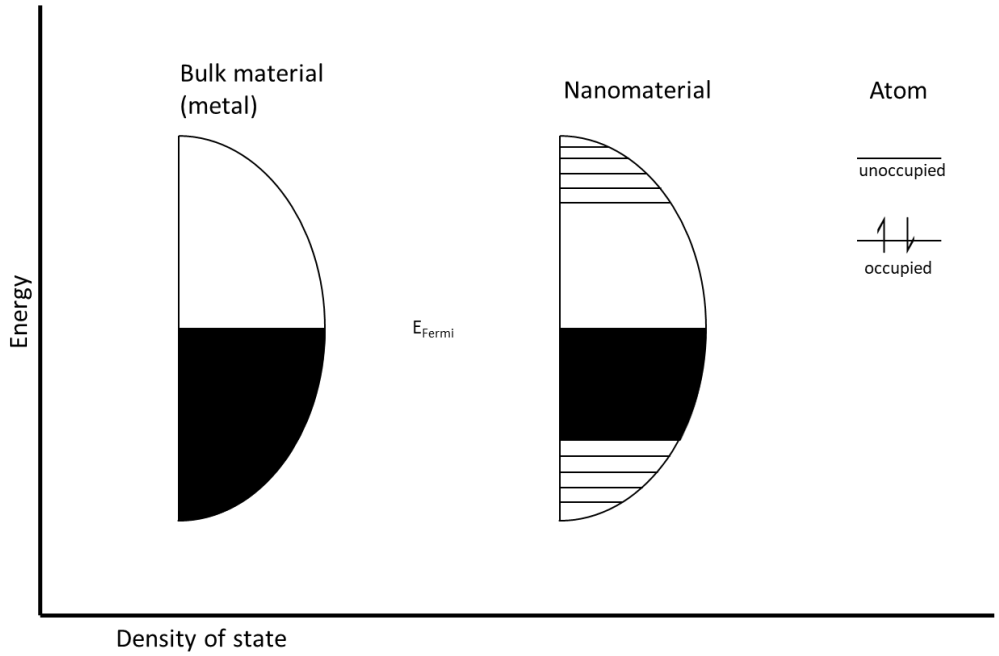

Figure 1.10: Representation of electronic level differences between a bulk material, a nanomaterial, and an atom. Formation of discreet energy levels is represented by vertical lines breaking down single larger energy levels in the nanomaterial.

Photocatalysis is a more specific application of catalysis. As previously mentioned, most catalytic materials have their activity as a response to heat as a source of energy, while photocatalysts function as a response to light irradiation. The typical photocatalytic reaction starts with the absorption of light by the catalyst, incurring in the excitation of the PC, represented by the promotion of an electron from ground energy state into an excited (higher) energy state, and generation of an "electron hole" where it previously occupied.[34-37,]

By understanding the advantages and potential impact that the use of photocatalysis may have on highly energy consuming industrial processes, we may understand the necessity to explore this avenue, even in challenging reaction systems such as lignin valorization.

1.6 Instrumental analytical methodology

From the diverse methodologies available, standouts in the characterization of lignin valorization reactions, for both products and starting materials, include Nuclear Magnetic Resonance (NMR), Gas Chromatography coupled with either Mass Spectroscopy or Flame Ionization Detector (GC-MS/FID), High Performance Liquid Chromatography (HPLC) and UV-Vis Spectroscopy. On the catalyst front, important characterization techniques add to the list both Scanning and Transmission Electron Microscopy (SEM/TEM),

UV-Vis Spectroscopy

UV-Vis spectroscopy is an analytical technique that uses a beam of light with known intensity to measure the absorbance/transmittance of a material at a predetermined wavelength. In short, the beam crosses the sample on its way to a detector, and the difference between the initial emitted light and the detected intensity of the beam are measured. The absorbance is then calculated by the following equation.

$$A = -\log(T) \qquad (1.1)$$

Where T is the transmittance, as described previously as I/I_0, or the quotient between the emitted beam before contact with the sample (commonly in a cuvette) and the beam that reaches the detector after going through the sample.

Since lignin has several light-absorbing functional groups in its structure, and some of the monomeric products of lignin valorization reactions have their own characteristic light absorbance, UV-Vis spectroscopy can be used to great effect for the analysis of these reactions.

UV-Vis spectroscopy is also commonly used as a module of other systems, such as HPLC, which allows for the characterization of different products being separated, in a qualitative and potentially quantitative manner.

To determine the concentration of an analyte in solution, the Beer-Lambert Law can be used, as it describes the relationship between absorbance and the concentration of a sample as shown in the following equation:

$$A = \varepsilon c l \qquad (1.2)$$

Where “A” is the absorbance (optical density), ε (epsilon) is the sample specific constant in $M^{-1}cm^{-1}$, “c” is the sample concentration (in M), “l” is the cuvette’s path length in cm, meaning the distance that the beam of light has to travel through the sample. When analyzing a UV-Vis spectrum, and based on the Beer-Lambert Law, we can positively correlate the height of a particular absorption peak to the concentration of the sample.

Nuclear Magnetic Resonance

NMR interpretation is a key factor in the elucidation of molecular structures and has special importance in lignin studies. In short, NMR is an analytical method through which the spin of the nucleus of an atom is manipulated by an external magnetic field and short radio frequency pulses, and the variation on the applied magnetic field is captured and converted into information on the chemical environment surrounding the spin. We may simplify the concept of spin as being a type of angular momentum, characteristic of subatomic particles, that generates a magnetic dipole moment. Whenever there are no external forces acting upon it, namely a magnetic field, this magnetic dipole is oriented randomly. In the presence of a magnetic field, however, a magnetic dipole moment may align with or against the magnetic field. A lower energy spin will align with the magnetic field as the base energy, while a spin at higher energies will align opposing the direction of the magnetic field. The NMR spectrum is acquired by matching the gap in energy between these two states with the absorption or emittance of a wavelength of a specific radio frequency, and that matched signal/frequency is then measured in terms of intensity and translated to a spectrum. [43-47]

Proton NMR, also referred to as ^{1}H-NMR, has been used to characterize lignin, but by using carbon NMR (^{13}CNMR) one can obtain a greater resolution for quantitative studies[46]. For example, ^{1}H-NMR spectra are generally measured over a spectral width of 10-15 ppm while ^{13}C-NMR is measured with a spectral width of 0-200 ppm. There are certain disadvantages as well with ^{13}C-NMR, such as low isotope sensitivity and low natural presence of the ^{13}C isotope, so obtaining a good spectrum requires longer experimental times. Carbon NMR has been used to characterize lignin since the 1980's, and since model compounds and protolignin studies have been studied extensively at this point, several modern and detailed chemical shift assignment tables are available to characterize lignin. [43-47]

Gas Chromatography

Gas chromatography (GC) is an analytical separation technique used to characterize volatile substances in the gas phase. During experimentation, samples that have been dissolved in a solvent are vaporized without decomposition and are passed through a heated column by an inert carrier gas. The carrier gas serves as a mobile phase and the interior surface of the column is coated with a stationary phase that interacts with the analytes resulting in characteristic elution times. based on their mass and charge.

Gas Chromatography-Mass Spectroscopy (GC-MS)

GC-MS is an analytical method that combines the aspects of gas chromatography with mass spectrometry, acquiring benefits from both. Identification of samples is possible in this equipment by both the retention time, when compared to an internal standard, but also by their mass spectrum. A mass spectrometer ionizes sample molecules, usually to cations, and separates them by external electric and magnetic fields based on their mass and charge. Combining these techniques, it is possible to identify unknown samples, which is a key aspect of the technique when applied to complex systems such as lignin valorization reactions and technical lignin extractions. This equipment also uses a capillary column of around 0.25 mm in diameter, as opposed to a column packed with a stationary phase.[77,78]

Gas Chromatography-Flame Ionization (GC-FID)

Similarly to GC-MS, the gas chromatography section of GC-FIDs works much the same way, with some minor differences in the case of the equipment for the Scaiano Group, though those at this time are not relevant to the present work as they pertain to functionalities not used in the present account's experiments.

An FID is a common detector, especially in quantifications of fine chemicals that are volatile enough for gas-chromatography systems. During the operation this type of equipment, the carrier gas leaving the column is mixed with hydrogen, and the combination of eluting compounds is burned by a flame, surrounded by air and an oxygen-rich environment. One in every 10,000 organic molecules present in the mixture is then converted into a gas-phase ion. Detection is dependent on the formation of these organic ions, as these are detected by a collector electrode positioned just above the flame. Using the mass of carbon delivered to the detector and the magnitude of the current generated, a signal is obtained. This signal is then used for the detection and quantification of organic compounds eluting from the column.[82]

Some of the advantages that can be cited from FID systems is their relative ease of use, as well as being able to be tuned to give little to no signal for common carrier gases, such as He, Ar, or N_2, or typical contaminants in such gases, like O_2 and H_2O. It must be pointed out, however, that FID is a destructive technique, though in applications such as the one from the present work, the volumes of samples available render this point quite irrelevant, but other applications might have a more limiting implementation based on this factor.

High-Performance Liquid Chromatography (HPLC)

Liquid Chromatography is a type of chromatography in which the mobile phase is a liquid, and separation is based on the distribution of chemicals between a liquid mobile phase and a stationary phase, through a variety of mechanisms. HPLC is a more recent addition to the methods derived from Liquid Chromatography (1960s), achieved by innovations on the instrumentation and production of smaller, more stable, and more efficient supports/columns. This analytical technique is

commonly used for routine chemical separations and analysis methods in modern laboratories. Due to its ability to be automated as well as significant advances in the limits of detection and generation of narrower peaks, compared to traditional LC methodology, HPLC became an important and versatile technique over the last 60 years.[82]

Of significant importance for the present work is size-exclusion chromatography (SEC), which is an LC technique that separates chemical compounds based on their size. In short, the stationary phase used is a porous support, possessing an inert surface and a range of pore sizes that are similar to the sizes of the compounds that require separation. As a sample travels through a column that contains this support, smaller components may enter all or most of the pores, while larger components may enter only a few or none of the pores. This results in a longer trajectory for smaller compounds, and a more direct pathway for larger molecules, causing separation, and a comprehensive elution distribution.

In size-exclusion chromatography, the choice of mobile phase is dependent on solubility of the desired analytes in the media, as well as stability of the column's support. Common mobile phases are water, in the case of polar solvents, or tetrahydrofuran, when apolar solvents are necessary. It is also common to have small fractions of the opposite type of solvent in the mobile phase, especially in complex analytes, where not all compounds may be easily carried by the same solvent polarity. The stationary phase on the other hand is solely based on a physical difference in the range and volume of pores available to the solutes. This means that, different from common LC methodologies, there is no weak or strong mobile phase. This makes the choice of the mobile phase more relevant, as this is the main mechanism through which to affect the elution process of the analyte.

When either water or a predominantly aqueous mobile phase is used for SEC (commonly making use of carbohydrate-based supports, polyacrylamide or diol-bonded silica or glass), this particular methodology is often called gel filtration chromatography. In the case of the present work, however, a predominantly organic phase was used as the mobile phase, consisting of tetrahydrofuran and a small

percentage of water, and in this case polystyrene is the most common support, and the size-exclusion method is then referred to as gel permeation chromatography (GPC).[82, 83]

References

1. McCarthy, J. L., & Islam, A. Lignin chemistry, technology, and utilization: A brief history. *ACS Symposium Series*, 1999, *742*, 2–66. https://doi.org/10.1021/bk-2000-0742.ch001

2. Glasser, W. G. About Making Lignin Great Again—Some Lessons From the Past. *Frontiers in Chemistry,* 2019, *7*, 1–17. https://doi.org/10.3389/fchem.2019.00565

3. Britannica, T. Editors of Encyclopaedia (2019, August 7). Macromolecule. Encyclopedia Britannica. https://www.britannica.com/science/macromolecule

4. Hayes, M. H. B., Mylotte, R., & Swift, R. S. Humin: Its Composition and Importance in Soil Organic Matter. In *Advances in Agronomy, 2017,* 1st ed., Vol. 143. Elsevier Inc. https://doi.org/10.1016/bs.agron.2017.01.001

5. Li, S. H., Liu, S., Colmenares, J. C., & Xu, Y. J. A sustainable approach for lignin valorization by heterogeneous photocatalysis. *Green Chemistry*, 2016, *18*(3), 594–607. https://doi.org/10.1039/c5gc02109j

6. Liu, X., Bouxin, F. P., Fan, J., Budarin, V. L., & Hu, C. *Recent Advances in the Catalytic Depolymerization of Lignin towards Phenolic Chemicals: A Review*, 2020, 4296–4317. https://doi.org/10.1002/cssc.202001213

7. Capello, C., Fischer, U., & Hungerbühler, K. What is a green solvent? A comprehensive framework for the environmental assessment of solvents. *Green Chemistry*, 2007, *9*(9), 927–993. https://doi.org/10.1039/b617536h

8. Byrne, F. P., Jin, S., Paggiola, G., Petchey, T. H. M., Clark, J. H., Farmer, T. J., Hunt, A. J., Robert McElroy, C., & Sherwood, J. Tools and techniques for solvent selection: green solvent selection guides. *Sustainable Chemical Processes*, 2016, *4*(1), 1–24. https://doi.org/10.1186/s40508-016-0051-z

9. Prat, D., Wells, A., Hayler, J., Sneddon, H., McElroy, C. R., Abou-Shehada, S., & Dunn, P. J. CHEM21 selection guide of classical- and less classical-solvents. *Green Chemistry*, 2015, *18*(1), 288–296. https://doi.org/10.1039/c5gc01008j

10. Freudenberg, K. Biosynthesis and constitution of lignin. *Nature,* 1959, 183, 1152–1155.

11. Lewis, N. G., & Davin, L. B. *The Nature and Function of Lignins*. Comprehensive Natural Products Chemistry, 1999, v. 3, 617-745.

12. Bevan, E. J., *Cross, C. F*. XVI.—The chemistry of bast fibres. *J. Chem. Soc., Trans.*, 1882, **41**, 90-110

13. Pérez, J., Muñoz-Dorado, Martínez, J. *Biodegradation and biological treatments of cellulose, hemicellulose and lignin: an overview*. International Microbiology, 2002, 5, 53–63. https://doi.org/10.1007/s10123-002-0062-3

14. Kienberger M, Maitz S, Pichler T, Demmelmayer P. Systematic Review on Isolation Processes for Technical Lignin. *Processes*, 2021, 9(5):804. https://doi.org/10.3390/pr9050804

15. Vishtal, A., Andrzej K. Challenges in Industrial Applications of Technical Lignins. Bioresources, 2011, vol. 6, no. 3, North Carolina State University, pp. 3547–68, doi:10.15376/biores.6.3.3547-3568.

16. Huang, J., Ling, L., Sun, D., Chen, H., Yang, D., Li, Q. Bio-inspired synthesis of metal nanomaterials and applications, Chem. Soc. Rev., 2015, vol. 44, 17, 6330–6374.

17. K. J. Klabunde, J. Stark, O. Koper, C. Mohs, D. G. Park, S. Decker, Y. Jiang, I. Lagadic and D. Zhang (1996). Nanocrystals as stoichiometric reagents with unique surface chemistry, J. Phys. Chem., 100, 12142–12153.

18. Nanomaterials definition matters, *Nat. Nanotechnol.*, 2019, **14**, 3, 193.

19. P. N. Sudha, K. Sangeetha, K. Vijayalakshmi, A. Barhoum (2018). Emerging Applications of Nanoparticles and Architectural Nanostructures: Current Prospects and Future Trends, pp. 341–384.

20. M. T. Amin, A. A. Alazba, U. Manzoor (2014). A review of removal of pollutants from water/wastewater using different types of nanomaterials, *Adv. Mater. Sci. Eng.*, 2014, 825910.

21. R. Nagarajan (2008). Nanoparticles: Building blocks for nanotechnology, ACS Symp. Ser., 996, 2–14.

22. C. Buzea, I. Pacheco (2017). EMR/ESR/EPR Spectroscopy for Characterization of Nanomaterials, ed. A. K. Shukla, Springer India, New Delhi, pp. 3–45.

23. T. Prasad Yadav, R. Manohar Yadav and D. Pratap Singh, Mechanical Milling: A Top-Down Approach for the Synthesis of Nanomaterials and Nanocomposites, Nanoscience and Nanotechnology, 2012, 2, 3, 22–48.

24. J. Singh, T. Dutta, K.-H. Kim, M. Rawat, P. Samddar and P. Kumar, 'Green' synthesis of metals and their oxide nanoparticles: applications for environmental remediation, J. Nanobiotechnology, 2018, 16, 1, 84.

25. N. Kumar and S. Kumbhat, in Essentials in Nanoscience and Nanotechnology, 2016, pp. 29–76.

26. J. Polte, Fundamental growth principles of colloidal metal nanoparticles – a new perspective, CrystEngComm, 2015, 17, 36, 6809–6830.

27. N. T. K. Thanh, N. Maclean and S. Mahiddine, Mechanisms of nucleation and growth of nanoparticles in solution, Chem. Rev., 2014, 114, 15, 7610–7630. 23

28. S. Arshadi, J. Moghaddam and M. Eskandarian, LaMer diagram approach to study the nucleation and growth of Cu2O nanoparticles using supersaturation theory, Korean J. Chem. Eng., 2014, 31, 11, 2020–2026.

29. S. Zhu and D. Wang, Photocatalysis: Basic principles, diverse forms of implementations and emerging scientific opportunities, Adv. Energy Mater., 2017, 7, 23, 1700841.

30. J. C. Scaiano and A. E. Lanterna, Is Single-Molecule Fluorescence Spectroscopy Ready to Join the Organic Chemistry Toolkit? A Test Case Involving Click Chemistry, J. Org. Chem., 2017, 82, 10, 5011–5019.

31. K. Zhang, J. Deng, Y. Liu, S. Xie and H. Dai, in Semiconductor Photocatalysis - Materials, Mechanisms and Applications, 2016, pp. 559–561.

32. K. Hashimoto, H. Irie and A. Fujishima, TiO_2 Photocatalysis: A Historical Overview and Future Prospects, Jpn. J. Appl. Phys., 2005, 44, 12, 8269–8285.

33. X. Yan, K. Yuan, N. Lu, H. Xu, S. Zhang, N. Takeuchi, H. Kobayashi and R. Li, The interplay of sulfur doping and surface hydroxyl in band gap engineering: Mesoporous sulfur-doped TiO2 coupled with magnetite as a recyclable, efficient, visible light active photocatalyst for water purification, Appl. Catal. B Environ., 2017, 218, 20–31.

34. P. V. Kamat, Manipulation of charge transfer across semiconductor interface. A criterion that cannot be ignored in photocatalyst design, J. Phys. Chem. Lett., 2012, 3, 5, 663–672.

35. K. G. Stamplecoskie and J. C. Scaiano, Light emitting diode irradiation can control the morphology and optical properties of silver nanoparticles, J. Am. Chem. Soc., 2010, 132, 6, 1825–1827.

36. K. G. Stamplecoskie and J. C. Scaiano, Silver as an example of the applications of photochemistry to the synthesis and uses of nanomaterials, Photochem. Photobiol., 2012, 88, 4, 762–768.

37. Castellote, M.; Bengtsson, N., Principles of TiO_2 Photocatalysis. In Applications of Titanium Dioxide Photocatalysis to Construction Materials: State-of-the-Art Report of the RILEM Technical Committee 194-TDP, Ohama, Y.; Van Gemert, D., Eds. Springer Netherlands: Dordrecht, 2011; pp 5-10.

38. What is Photocatalyst? http://www.greenearthnanoscience.com/what-is-photocatalyst.php (accessed March 11, 2018).

39. Kuvarega, A. T.; Mamba, B. B., TiO_2-based Photocatalysis: Toward Visible Light- Responsive Photocatalysts Through Doping and Fabrication of Carbon-Based Nanocomposites. Crit Rev Solid State Mater Sci 2017, 42 (4), 295-346.

40. Linsebigler, A. L.; Lu, G.; Yates, J. T., Photocatalysis on TiO_2 Surfaces: Principles, Mechanisms, and Selected Results. Chem Rev 1995, 95 (3), 735-758.

41. Schneider, J.; Matsuoka, M.; Takeuchi, M.; Zhang, J.; Horiuchi, Y.; Anpo, M.; Bahnemann, D. W., Understanding TiO_2 photocatalysis: mechanisms and materials. Chem Rev 2014, 114 (19), 9919-86.

42. Ben, H., and Ragauskas, A.J., Heteronuclear Single-Quantum Correlation Nuclear Magnetic Resonance (HSQC-NMR) Fingerprint Analysis of Pyrolysis Oils. Energy Fuels, 2011. 25: p. 5791-5801. (19)

43. Dimitris, S.A., 'Heteronuclear NMR Spectroscopy of Lignins', in Lignin and Lignans, CRC Press, 2010, p. 245-265. (43)

44. Foston, M., Hubbell, C.A., Samuel, R., et al., Chemical, Ultrastructural and Supramolecular Analysis of Tension Wood in Populus Tremula X Alba as a Model

Substrate for Reduced Recalcitrance. Energy Environ. Sci., 2011. 4: p. 4962- 4971. (49)

45. Foston, M., Nunnery, G.A., Meng, X., et al., NMR a Critical Tool to Study the Production of Carbon Fiber from Lignin. Carbon, 2013. 52: p. 65-73. (50)

46. Hu, G., Cateto, C., Pu, Y., et al., Structural Characterization of Switchgrass Lignin after Ethanol Organosolv Pretreatment. Energy Fuels, 2012. 26: p. 740- 745. (68)

47. Ralph J, Lapierre C, Boerjan W. Lignin structure and its engineering. Curr Opin Biotechnol. 2019 Apr;56:240-249. doi: 10.1016/j.copbio.2019.02.019. Epub 2019 Mar 25. PMID: 30921563.

48. G. A. Tuskan, W. Muchero, T. J. Tschaplinski, A. J. Ragaus- kas, Curr. Opin. Biotechnol. 2019, 56, 250–257

49. Y. Pu, S. Cao, A. J. Ragauskas, Energy Environ. Sci. 2011, 4, 3154.

50. S. Wang, G. Dai, H. Yang, Z. Luo, Prog. Energy Combust. Sci. 2017, 62, 33–86.

51. V. Dhyani, T. Bhaskar, Renewable Energy 2018, 129, 695–716.

52. M. M. Rahman, R. Liu, J. Cai, Fuel Process. Technol. 2018, 180, 32–46.

53. K. Lundquist, T. K. Kirk, Acta Chem. Scand. 1971, 25, 889–894.

54. D. M. Miles-Barrett, A. R. Neal, C. Hand, J. R. Montgomery, I. Panovic, O. S. Ojo, C. S. Lancefield, D. B. Cordes, A. M. Slawin, T. Lebl, N. J. Westwood, Org. Biomol. Chem. 2016, 14, 10023–10030.

55. R. Katahira, A. Mittal, K. McKinney, X. Chen, M. P. Tucker, D. K. Johnson, G. T. Beckham, ACS Sustainable Chem. Eng. 2016, 4, 1474– 1486.

56. C. S. Lancefield, I. Panovic, P. J. Deuss, K. Barta, N. J. Westwood, Green Chem. 2017, 19, 202–214.

57. W. Lan, J. S. Luterbacher, Chimia 2019, 73, 591–598.

58. K. H. Kim, C. S. Kim, Front. Energy Res. 2018, 6.

59. S. Ghoreishi, T. Barth, H. Derribsa, Biofuel Res. J. 2019, 6, 937–946

60. F. P. Bouxin, H. Strub, T. Dutta, J. Aguilhon, T. J. Morgan, F. Mingardon, M. Konda, S. Singh, B. Simmons, A. George, Green Chem. 2018, 20, 3566–3580.

61. M. Fache, B. Boutevin, S. Caillol, ACS Sustainable Chem. Eng. 2015, 4, 35–46.

62. S. Backa, M. Andresen, T. Rojahn, in Biomass as Energy Source, CRC Press, 2013, pp. 177–186.

63. J. Mottweiler, T. Rinesch, C. Besson, J. Buendia, C. Bolm, Green Chem. 2015, 17, 5001–5008

64. W. Partenheimer, Adv. Synth. Catal. 2009, 351, 456–466.

65. H. Deng, L. Lin, S. Liu, Energy Fuels 2010, 24, 4797–4802

66. M. Ksibi, S. B. Amor, S. Cherif, E. Elaloui, A. Houas, M. Elaloui, J. Photochem. Photobiol. A 2003, 154, 211–218

67. R. Ma, Y. Xu, X. Zhang, ChemSusChem 2015, 8, 24–51.

68. T. Voitl, P. Rudolf von Rohr, ChemSusChem 2008, 1, 763–769

69. B. Bujanovic, S. Ralph, R. Reiner, K. Hirth, R. Atalla, Materials 2010, 3, 1888–1903.

70. S. K. Badamali, R. Luque, J. H. Clark, S. W. Breeden, Catal. Commun. 2011, 12, 993–995

71. M. Gale, C. M. Cai, K. L. Gilliard-Abdul-Aziz, ChemSusChem 2020, 13, 1947–1966

72. M. Dawange, M. V. Galkin, J. S. M. Samec, ChemCatChem 2015, 7, 401–404

73. P. Maziero, M. d. O. Neto, D. Machado, T. Batista, C. C. S. Cavalheiro, M. G. Neumann, A. F. Craievich, G. J. d. M. Rocha, I. Polikarpov, A. R. Gonçalves, Ind. Crops Prod. 2012, 35, 61–69.

74. C. Cheng, J. Wang, D. Shen, J. Xue, S. Guan, S. Gu, K. H. Luo, Polymer 2017, 9, 240–266.

75. J. M. Ha, K. R. Hwang, Y. M. Kim, J. Jae, K. H. Kim, H. W. Lee, J. Y. Kim, Y. K. Park, Renewable Sustainable Energy Rev. 2019, 111, 422–441.

76. Basheer, S., Kunhi, A., Varadaraj, M., et al., Nuclear Magnetic Resonance Spectroscopic Studies on the Microbial Degradation of Mononitrophenol Isomers. World Journal of Microbiology and Biotechnology, 2007. 23: p. 49-63.

77. Hu, Z., Foston, M.B., and Ragauskas, A.J., Biomass Characterization of Morphological Portions of Alamo Switchgrass. J. Agric. Food Chem., 2011. 59: p. 7765-7772.

78. Gan, H.M., Ibrahim, Z., Shahir, S., et al., Identification of Genes Involved in the 4-Aminobenzenesulfonate Degradation Pathway of Hydrogenophaga Sp. Pbc Via Transposon Mutagenesis. FEMS Microbiol. Lett., 2011. 318: p. 108-114.

79. Jia, Z., Qin, Q., Darvill, A.G., et al., Structure of the Xyloglucan Produced by Suspension-Cultured Tomato Cells. Carbohydr. Res., 2003. 338: p. 1197-1208.

80. Li, D., Yan, Y., Ping, S., et al., Genome-Wide Investigation and Functional Characterization of the Á-Ketoadipate Pathway in the Nitrogen-Fixing and RootAssociated Bacterium Pseudomonas Stutzeri A1501. BMC Microbiol., 2010. 10: p. No pp. given.

81. Hage, D. S. *Chromatography. Principles and Applications of Clinical Mass Spectrometry,* 2018, *1–32.*

82. Majors RE, Carr PW. *Glossary of liquid-phase separation terms*. LC GC (2001). 19, 124-162.

83. H. Ma, H. Li, W. Zhao, L. Li, S. Liu, J. Long, X. Li, Green Chem. 2019, 21, 658–668.

84. W. Zhao, X. Li, H. Li, X. Zheng, H. Ma, J. Long, X. Li, ACS Sustainable Chem. Eng. 2019, 7, 19750–19760.

85. W. Wanmolee, N. Laosiripojana, P. Daorattanachai, L. Moghaddam, J. Rencoret, J. C. del Río, W. O. S. Doherty, ACS Sustainable Chem. Eng. 2018, 6, 3010–3018.

86. L. Jiang, H. Guo, C. Li, P. Zhou, Z. Zhang, Chem. Sci. 2019, 10, 4458–4468.

87. M. V. Galkin, J. S. Samec, ChemSusChem 2014, 7, 2154–2158.

88. X. Ouyang, X. Huang, J. Zhu, M. D. Boot, E. J. M. Hensen, ACS Sustainable Chem. Eng. 2019, 7, 13764–13773.

89. M. V. Galkin, A. T. Smit, E. Subbotina, K. A. Artemenko, J. Bergquist, W. J. Huijgen, J. S. Samec, ChemSusChem 2016, 9, 3280–3287.

90. J. Hu, S. Zhang, R. Xiao, X. Jiang, Y. Wang, Y. Sun, P. Lu, Bioresour. Technol. 2019, 279, 228–233.

91. Prado, N.T.; Oliveira, L.C.A. Nanostructured niobium oxide synthetized by a new route using hydrothermal treatment: High efficiency in oxidation reactions. Appl. Catal. B Environ. 2017, 205, 481–488.

92. Hashemzadeh, F.; Gaffarinejad, A.; Rahimi, R. Porous p-NiO/n-Nb2O5 nanocomposites prepared by an EISA route with enhanced photocatalytic activity in simultaneous Cr(VI) reduction and methyl orange decolorization under visible light irradiation. J. Hazard. Mater. 2015, 286, 64–74.

93. Gibson, C.E.; Kelebek, S.; Aghamirian, M. Niobium oxide mineral flotation: A review of relevant literature and the current state of industrial operations. Int. J. Miner. Process. 2015, 137, 82–97.

94. Xia, Q. et al. Pd/$NbOPO_4$ multifunctional catalyst for the direct production of liquid alkanes from aldol adducts of furans. Angew. Chem. Int. Ed. 53, 9755–9760 (2014).

95. Shao, Y., Xia, Q., Liu, X., Lu, G. & Wang, Y. Pd/Nb_2O_5/SiO_2 catalyst for the direct hydrodeoxygenation of biomass-related compounds to liquid alkanes under mild conditions. ChemSusChem 8, 1761–1767 (2015).

96. Xia, Q. et al. Direct hydrodeoxygenation of raw woody biomass into liquid alkanes. Nat. Commun. 7, 11162 (2016).

97. Okuhara, T. Water-tolerant solid acid catalysts. Chem. Rev. 102, 3641–3666 (2002).

98. Emsley, J. Nature’s Building Blocks: an A-Z Guide to the Elements (Oxford University Press, 2011).

Chapter 2 Valorization Reactions for Technical and Protolignins

2.1 Introduction

Lignin valorization technology and research has evolved over the years in tandem with progress made in the understanding of the structural characteristics of protolignins. Formerly, branched statistical representations were the main existing method to represent lignin's structure, given that only through harsh extraction was analysis of its structure possible.[1-3, 6]

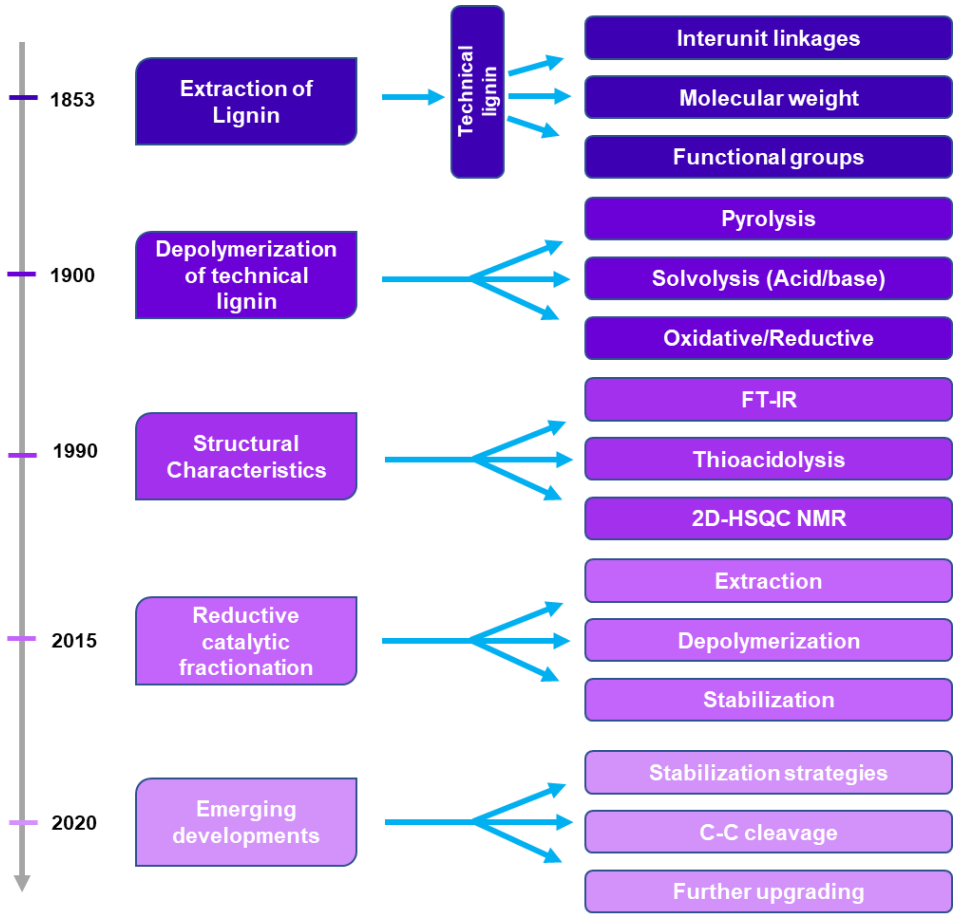

Figure 2.1: Timeline (not to scale in the Y axis) of developments in the lignin characterization field, accompanied by lignin valorization technologies and new strategies that consequently emerged. Adapted from Liu, X. et. al.[7]

Extraction, though, has an inherent bias and produces modified monomers with only hints of how they may have fit together in a larger structure. The development of 2D NMR techniques provided certain leaps in the comprehension of the unaltered structure of lignin, also called protolignins, and provided a pathway to a more linear comprehensive structure of these macromolecules.[1-5]

Biofuel Potential

Conversion of plant biomass into biofuel is a broadly sought-after goal that has the potential to reduce the carbon footprint of fossil fuel usage. Another less discussed benefit is the material availability and its effects on the circular economy. Exploration and refining of fossil fuels has been largely only accessible to a limited number of very large companies due to large upfront costs of remote and deep-sea oil extraction operations, and limited number of viable sources for it, which limit its impact on local economies. Biofuels on the other hand can not only be produced from renewable sources, but the feedstocks for its production are available through agricultural means to a much larger subset of the world's populace. This means that, once the technology evolves to the point of achieving competitive costs to produce biofuels, even smaller communities may have access to biorefining, flattening the pyramid of wealth distribution and directly affecting the entry of communities in the Global Circular Economy.[8, 28]

Going into detail as well as to why the so-called second-generation biofuels, such as the ones produced with lignin, are so important, first we must understand briefly the issue with first generation biofuel. Within the biofuel landscape, one potential hurdle has been the controversial use of food products to produce fuels. Even when the most important food products are not directly being used, such as corn and sugarcane, many farms and plots that once produced food are being converted into soy plantations, for instance, due to the ease of production and high value-added materials that can be extracted, while not easily complementing the local food needs of the populace. Lignin is a strong contender to solve this issue, since its presence in the food and general agricultural waste materials, it makes it

possible to produce biofuels without altering local crops and crop rotations, which are crucial especially for small markets.[19-21,29]

The broadening of lignocellulose applications in the biofuel space, and the optimization of integrated biorefinery processes and reducing the carbon footprint from fossil fuels is of vital importance. [20-23]. Cellulose is a material already present in the bioenergy field and is the most abundant component of lignocellulosic biomass. Despite this, the presence of lignin impedes direct utilization/conversion of these macromolecules into useful biomaterials, due to the recalcitrant nature of the hemicellulose-lignin matrix, with good reason, as this is a structural mechanism that helped plant life thrive and exist in many harsh conditions.[25,26] This is the origin of several pre-treatment methodologies that seek to solubilize and degrade this stable matrix, increasing the access to cellulose and providing better pathways for subsequent chemical processes. As these methods are employed to remove the recalcitrant barrier and obtain cellulose, the recovery of intact structures in the lignin biomass complex has not been a priority, meaning they may be very harsh and destructive. These common methods used include steam explosion, dilute acid and organosolv pre-treatments, among others.[19-24] Regardless, all of these extraction methods produce an aqueous effluent predominantly enriched with degraded hemicellulose and lignin oligomers. In addition, other components such as partially broken units of amorphous cellulose, and other furan-based materials may also be present.[35,36]

As previously discussed, the aforementioned effluent fractions containing residues of cellulose extraction are typically either discarded, burned for energy, or used as animal feedstock, which are all very low value applications of a potentially valuable material. There are also currently little to no commercial uses, save from, as mentioned, an animal feedstock bulking agent.[8] This is where two major new strategies come into play, and the place where a lot of the present research finds its purpose, those being divergent and convergent pathways for lignin biomass valorization.[38] In short, divergent and convergent valorization strategies are characterized by the application of reactions on these complex systems to generate either one or very few major products (convergent strategies), or to generate a

mixture of several products that can either be separated later, or used as a mixture. One simple example of divergent methodology is the complete conversion of lignocellulosic biomass into a mixture of alcohol molecules, that can be used as a bio-sourced combustion fuel.[38] In contrast, an example of convergent strategy for lignin valorization is the use of selective catalysis and photocatalysis for the breaking of β-0-4 lignin bonds to obtain high yields of major lignin monomers. Either way, the chemical or bioconversion of industrial waste into biodiesel and second-generation ethanol as commercial products presents an interesting potential, which may enable the enhancement of the cost-effectiveness for new and existing integrated biorefineries.

Cosmetics Applications

Applications of lignin in cosmetics have gained importance in the last 5 years, as the predominance of inorganic compounds such as TiO_2 and ZnO in sunscreen products grew, due to their high UV light absorbance and limited effect on the biosphere of species, such as coral reefs and other sensitive environments.

2.2 Challenges of Protolignin and Technical Lignin Valorization

For the purposes of this section, the focus will be on specific challenges and limitations faced when attempting a photochemical or photocatalytic method of lignin valorization, based on the nature of the present research account. The present work aimed to achieve protolignin and technical lignin valorization through photocatalytic methods, with the primary intent during its inception to have a heavy focus on the use and experimentation with lignin in the most unaltered or native forms available as an industrial side product. It was our goal to avoid the trappings of a primary focus on molecular models and the expectations that come with high levels of efficiency in reactions of that nature. An environment with real lignin presents a unique combination of challenges that are hard to replicate in a molecular investigation of the photocatalyst's efficacy, such as many pathways for side reactions, radical scavenging, competition for light absorption, adsorption of the catalyst,

repolymerization of products, and inconsistency in quantitative results stemming from lack of homogeneity in lignin structure. [24,25]

These issues were not accounted for in early stages of experimentation from the present work, as specific issues with photochemical reactions in the lignin valorization field were scarcely discussed in the literature reviewed at the time, and only over the course of the last few years did these issues, and with it the strategies to overcome them, became more prominent. Accompanying the results to come will be accounts of strategies that we developed to deal with some of the limitations of photocatalytic lignin valorization and added to those will be other strategies found in recent literature that could supplement future attempts at these experiments, found unfortunately too late to inform our own attempts at it.[24-27]

Much of the early experimentation was also developed as a reaction to the approach often seen in the literature, where lignin is cited in the title of the paper, then never actually experimented on throughout, usually by using molecular model compounds with claims that the representation of a specific bond breakage within lignin on an isolated compound was enough to show the efficiency of a catalyst or method to achieve lignin valorization itself. Upon encountering enough of these examples and observing how much of the advertised efficiency was lost upon experimentation with actual lignin, sometimes showing no activity at all, we decided on a “lignin first” approach, attempting to observe activity by the formation of different products of a select number of photocatalysts, under different light and solvent conditions. The intent was then to bring the results of our findings to the molecular-level investigations afterwards, once one or a few combinations of conditions proved somewhat successful, so that the molecular model approach could elucidate reaction pathways to better optimize lignin conversion.

A core issue that must be highlighted in several lignin extraction/valorization reactions is the stabilization of intermediates for maximizing phenolic monomers. This has been an increasingly studied topic in the past few years, as lignin-first and technical lignin valorization reactions, especially for biofuel applications, have gained significant attention. Both basic and acidic conditions generate opportunities for condensation pathways during extraction and valorization reactions for lignin and

lignin extracts. In both cases, the benzylic position is a key source of condensation, though the processes are slightly different depending on the conditions. Under acidic conditions, the carbocation is favorably generated due to delocalization of the positive charge on the aromatic ring.[13] The difference observed in basic conditions is the generation of quinone methide via delocalization of the negative charge through the aromatic ring up to the elimination of the benzylic hydroxyl. What both conditions have in common is a secondary step where the electrophilic benzylic carbon is attacked by nucleophiles, forming condensed C-C or C-O bonds.[14,15]

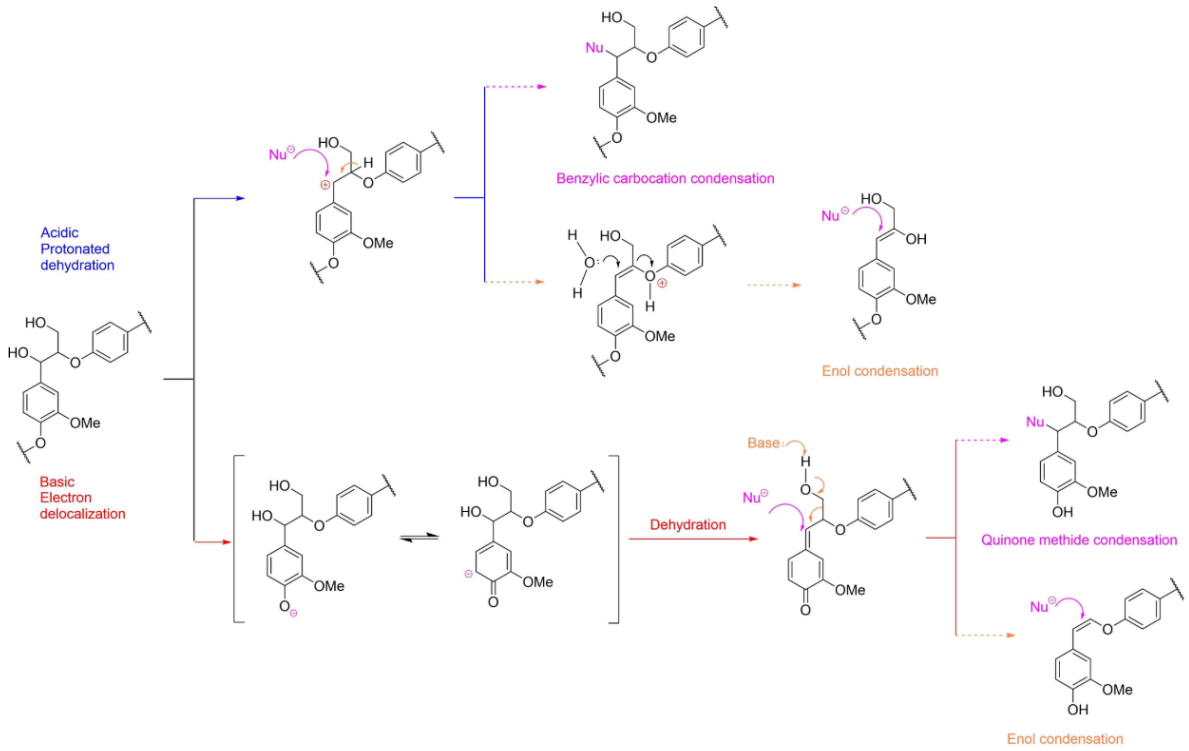

Figure 2.2: Pathways of lignin condensation under acidic and basic conditions. Reproduced from Liu, X., et al. (2020)[7]. Reproduction of material allowed under the Creative Commons license.

2.3 Experimental methodology

Materials and Chemicals

Lignocellulose and lignin samples were a gift from FP Innovations in a single batch to avoid inconsistencies. Unless stated otherwise, all chemicals were

purchased from Sigma-Aldrich and used as received without further purification. Aqueous solutions were prepared using 18.2 MΩ cm^{-1} Milli-Q water obtained from a Millipore System equipped with a 0.22 µm filter.

2.4 Experimental Procedures

Soxhlet extraction of wood and lignocellulose

Sugar maple sawdust has a theoretical chemical composition of 10 to 25% lignins, and 70 to 85% sugars, on a dry weight basis. The dried powder of the different powders of lignocellulose were subjected to Soxhlet extractions in order to concentrate fractions that are more soluble in certain solvents. In short, the Soxhlet extraction was performed by placing the dry powders of different lignin sources, individually, in thimbles, and placed inside a glass apparatus known as a Soxhlet extractor. From a round-bottom flask, a solvent is heated to its boiling point, and recondensed inside the glass section containing the permeable thimble. This section is filled over time, extracting fractions of the powder that are soluble in the solvent used, while the insoluble material is contained inside of the thimble. The solvent eventually is drained back to its original container, where it starts to heat up once more to repeat the process, increasing the concentration of soluble material extracted with each cycle.

Extraction with the Soxhlet apparatus was performed using different solvents such as ethanol, acetonitrile, and chloroform, among others to assess the abundance of different organic compounds that may be obtained in each, and the rate of removal or certain key fractions, be that lignin by-products or otherwise. For the conditions used in these experiments, 200 mL of the solvent were placed in a round-bottom flask, while 2.5 g of the sample material was added to the thimble. The samples were either protolignins obtained from extracts of the lumber industry, or wood powder obtained from sanding the cross-sectional surface of the stump a freshly cut maple wood tree. The extraction thimble used in the first two experiments (noted in the tables as such) were made of paper, and all subsequent experiments were done using thimbles made of glass fiber. The thimble is then placed inside the Soxhlet

apparatus, and the solvent is made to reflux for repeated cycles of extractions. The duration of the experiments was investigated based on the retention of important fractions in the extract, and ranged from 20 to 46 hours, after which these extracts are separated from the solvent by rotary evaporation under vacuum.

Organosolv Extraction

Organosolv pre-treatment was done following previously published methods[16]. This extraction methodology is generally used to obtain mixtures of compounds including lignin structures that are more readily soluble in organic solvents. This is done to facilitate experiments that include catalysts and other conditions that require the absence of water. For this experiment, the crude powdered materials are placed in a round-bottom flask with a reflux apparatus attached above. To the powders in the flask, a mixture containing EtOH at a 65% concentration by volume and 0.76 dry weight percentage of H_2SO_4 is added. The ration of biomass to be extracted to solvent is of 1 to 8 in weight. The mixture obtained is heated to 170 ºC for 1 hour under gentle stirring. This process allowed for the separation of a cellulose-rich fraction, which was kept separate for future experiments that could require such materials, and a lignin-rich and organic solvent-soluble fraction was obtained and safely stored for use in the present work.

Dioxosolv Extraction

Dioxosolv extractions of protolignins and wood extracts was also performed based on adaptations of previously published methodologies.[17] To start, 10 g of lignin-rich powder is dissolved in 120 mL of a 9:1 dioxane/water mixture containing 0.1 M of HCl. The resulting slurry is placed under reflux and gentle stirring for 30 minutes to 1 hour, followed by neutralization of pH to 6-7, and roto-evaporation of the resulting mixture. The solid obtained is then added to 400 mL of cold Milli-Q water and placed in a freezer for 3 h. The resulting precipitate is then collected by centrifugation and dissolved in a minimum amount of 9/1 (v/v) acetone/MeOH mixture. This mixture is added dropwise to 10 equivalent volumes of diethyl ether while being rapidly stirred. Vacuum filtration of the mixture provides a final precipitate, which is then dried under vacuum.

NMR spectroscopy of lignin

NMR analysis of lignin molecular models (BK and BA) as well as precursor compounds and select depolymerization mixtures was carried out in a Bruker Advance II 400 MHz NMR or Bruker AVANCE III HD 600 MHz spectrometer. Experiments were performed at room temperature, solids were dried under vacuum to eliminate prior solvents, then a small sample was combined with one of three deuterated solvents, these being DMSO-d, chloroform-d or D_2O. For higher resolution 1H-NMR and 13C-NMR spectra of protolignin and technical lignin, as well as 2D NMR analysis, 200 mg of each lignin sample was combined with deuterated dimethylsulfoxide (DMSO-d_6, 600 µL) in a sealed vial with a small stir bar and left overnight under gentle stirring and heating at 40°C. NMR data were processed using TopSpin 2.1 software (Bruker BioSpin).[18-22]

GC-MS and GC-FID

Quantification was carried out in a Perkin Elmer, Claurus Gas Chromatograph coupled to a Flame Ionization Detector (FID) and a DB-5 column (30 m length, 0.320 mm diameter, 0.25 µm film) using Helium as a carrier gas and using tert-butyl benzene as an internal standard. A standard curve was prepared with either the components of the molecular model breakage reaction, or in the case of lignin valorization reactions with several molecules chosen as stand-ins for their chemical similarities to obtained compounds. For identification of depolymerization fractions and other quantification processes, mass spectra were collected in an Agilent 6890-N Gas Chromatograph with an Agilent 5973 mass selective detector calibrated with acetophenone, using again t-butyl benzene as an external standard

FT-IR spectroscopy of lignin

FT-IR spectra were obtained using a Thermo Scientific Nicolet 6700 FTIR/ATR spectrophotometer equipped with a Smart iTX diamond/ZnSe universal attenuated-total-reflection (ATR) sampling accessory. Spectra were obtained in the 650‑4000 cm^{-1} range and for each sample 16 scans were taken at a resolution of 4 cm^{-1}

Transmission Electron Microscopy (TEM)

TEM analyses were carried out on a JEM2010F microscope (JEOL, 200 kV, 0.14 nm resolution). Samples were prepared according to established protocol, by dipping carbon-coated copper grids in the sonicated suspension of the material. The digital analysis of the TEM images was done using ImageJ.

TGA analysis of lignin

Thermogravimetric analysis was carried out using a TGA Q5000 from TA instruments, from ambient temperature to 550 ºC, at a heating rate of 10 ºC/minute and under a constant nitrogen flow of 25 mL/min. Data were analyzed with Pyris version 7.

UV-Vis spectroscopy

UV-visible Spectroscopy (UV-VIS) absorption spectra were recorded by a CARY 100 UV-Vis spectrometer and a Cary 7000 UV-Vis spectrometer.

Catalyst preparation

Synthesis of metal nanoparticles supported on TiO_2, Nb_2O_5 and $Nb_3O_{20}P_5$ was done using similar photodeposition methods as previously reported by the Scaiano group[23]. As an example of the methodology used for these, the methodology for the complete synthesis of the Pd@Nb_2O_5 catalyst will be specified, and the differences for the other catalysts will be remarked on when necessary. In short, 500 mg of the support material, in this case Nb_2O_5, is placed in a round-bottom flask. The mass of salt containing the intended supported metal, in this case $PdCl_2$, that needs to be used to obtain the intended loading has been determined in previous experiments, and in this case, 22 mg of the salt was used. A photo-activator in necessary in this case for best coverage and loading results, based on previous findings, so 24 mg Irgacure-2959 were dispersed into a solution of 200 mL of Milli-Q water, added to the flask with the support and the metal salt. The afforded mixture is then purged with Ar for 15 minutes and sonicated in a bath for 10 minutes. The mixture was then placed in a photoreactor equipped with 14 UVA bulbs, where it is irradiated for 5

hours with moderate stirring. The resulting brown slurry was filtered and washed with Milli-Q water and EtOH three times to remove any unreacted PdCl2. In the case of catalysts supported onto TiO2, washing of the catalyst was done usually by centrifugation, since the support (P95 TiO2) may have partial losses seeping through regular laboratory filter papers. In all cases, the following step was placing the washed catalyst in a desiccator under vacuum overnight to dry. Characterization of nanoparticles obtained by this method has been previously done in the Scaiano group by TEM, XPS, ICP-EOS and DRS. The loading of Pd onto TiO_2 supports was found to be 2% metal loading (w/w) and particles were ~1.6 nm in size, and a comparable loading was found for Pd loading onto Nb-based supports with this method.

2.5 Results and Discussion

Unless specified, the terms “water” and “H_2O” used throughout refer to 18.2 MΩ cm^{-1} Milli-Q water obtained from a Millipore System equipped with a 0.22 μm filter. Hinton A lignin and FP lignin both refer to the same source and batch of protolignin, donated to us by FP Innovations from pine lignocellulosic extractions. The term “small molecules” is used in the context of this work to refer to materials in the range observable through our GC-MS equipment, and examples of such can be found in Figures 2-12 to 2-17. This is used in contrast to larger compounds outside of this range, which can be comprised of dimers and trimers of benzylic compounds, and polymeric materials, such as lignin and sugars.

Selection of starting materials

A selection process was used on the available technical and protolignin samples obtained from Sigma, and Hinton A lignin samples gifted from FP Innovations to determine the best fit for the experiments and type of valorization reaction that the present work focuses on. The main methodology chosen for this selection was the use of HSQC 2D NMR spectroscopy, as described in the previous section.

The results from the selection process were based on the observations shown in Figure 2.3, where in the region corresponding with the resonances of C-H bonds from β-O-4 carbons was the determining factor. Higher concentrations of both α and β resonances were seen in red and azure blue, placed closer to the expected signal locations.[44,45]

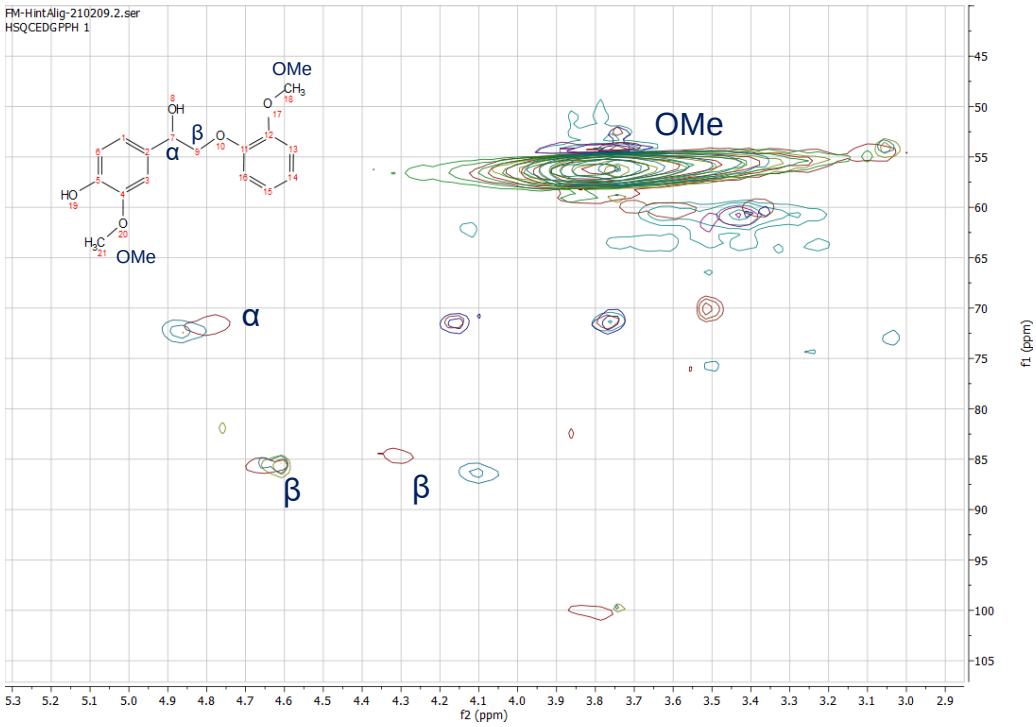

Figure 2.3: HSQC NMR spectra of the four protolignin samples in contention as the subject for our experiments. The red/light blue spectra correspond to Hinton A lignin, the dark green/navy spectra are from HW lignin, the light green/purple spectra are from K31 lignin, and finally the azure blue/brown spectra are from ZHL lignin.

Stronger signals in the labelled regions indicate higher concentrations of β-O-4 containing moieties, which is ideal for the type of breakage intended with the current host of catalysts and photochemical procedure planned for the present work. With that, the two candidates were Hinton A lignin and ZHL lignin, and the deciding factor was the solubility of both in organic/aqueous solutions, which made Hinton A the preferable choice.

Technical Lignin Extraction

Following the extraction methods previously discussed, analysis of the samples post-extraction consisted of GC-MS of the soluble components, HPLC with a size exclusion (GPC) column to estimate size distribution of the compounds, and UV-Vis spectroscopy of each sample to compare the absorption spectra of the obtained material to that of known spectra from organosolv lignin samples found in the literature.

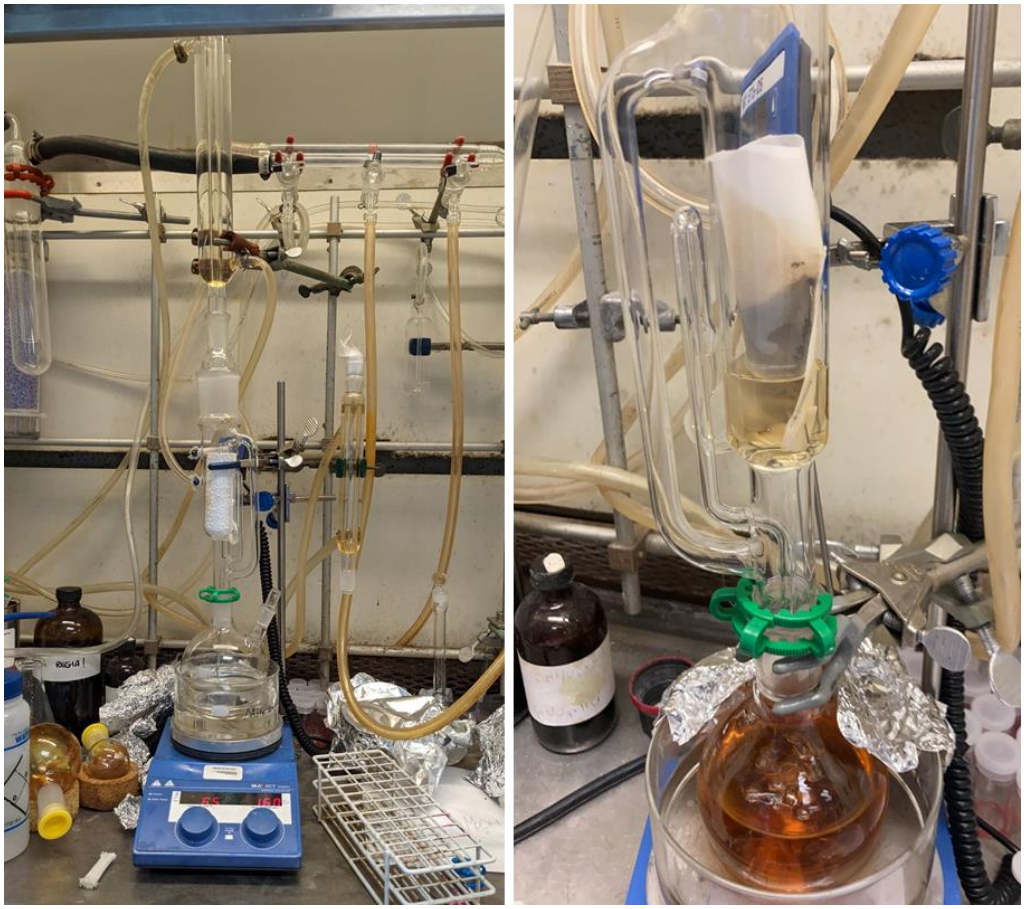

Figure 2.4: Soxhlet extraction setup for lignin and raw wood samples. A paper thimble is shown on the right-side picture, as this was an early extraction example, while on the left the setup is equipped with a glass fiber thimble.

First extractions were done using 200 mL of ethanol as the solvent, as it is very commonly used to obtain organosolv fractionations of lignin, with 2.504 g of Hinton A lignin inside of a paper thimble. The extracting solvent cycled through the sample every hour, and extraction was done initially for 25 hours, though an aliquot

was taken at 20 h for analysis. The UV-Vis spectra of the sample obtained is shown in Figure 2.5.

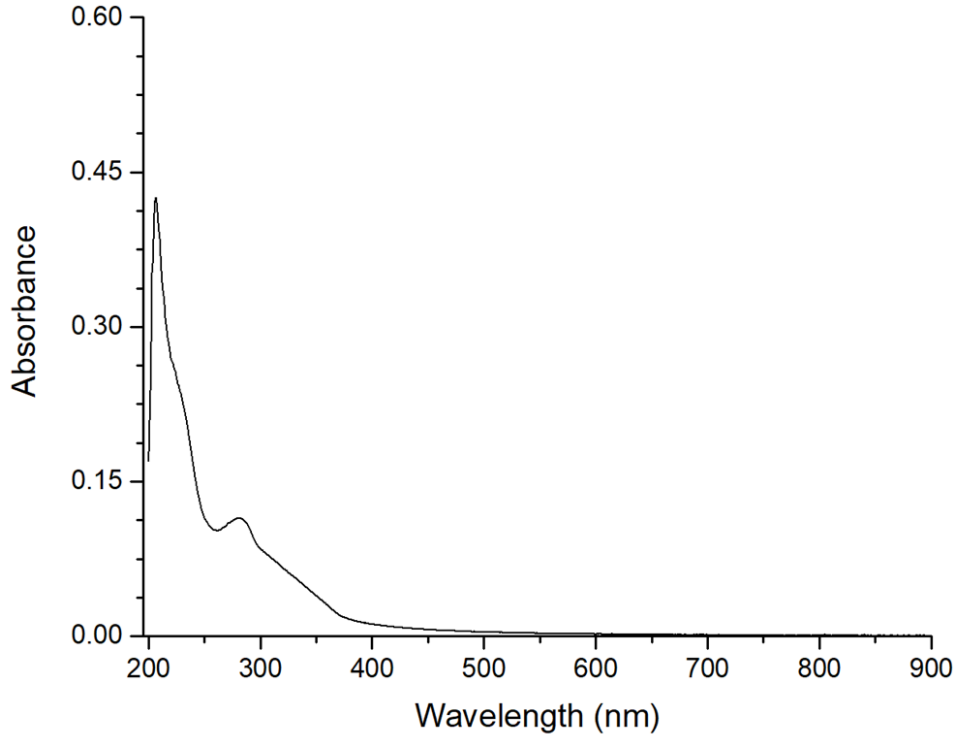

Figure 2.5: Absorbance spectra from aliquot of technical lignin extract, from a Hinton A sample, after 20 h under Soxhlet reflux with EtOH. Absorption band at 280 nm is common for lignin fractionation samples.

The first sample obtained showed no small molecules when analyzed by GC-MS, and the yield of organosolv lignin was approximately 30%, with a final mass of 0.830 g of dry lignin obtained from this initial extraction.

After Soxhlet extraction and prior to analysis, this sample was evaporated with a rotary evaporator at room temperature and separated into three portions. The first one third of the sample was analyzed unaltered while the second was dissolved in 15 mL of HPLC-grade AcN, though some precipitate remained in the vial. This second portion was then filtered, and the filtrate set aside. The solids that remained in the filter paper were then washed with MeOH. Each fraction was analyzed by UV-Vis, as shown in Figure 2.6. The difference between samples is lower in terms of absorption than the figure may imply, given that the separation in the baseline is most likely due to experimental differences. Though subtle changes in the

absorbance around 240 nm might still indicate a populational difference in chromophores, the absorbing groups are largely similar.

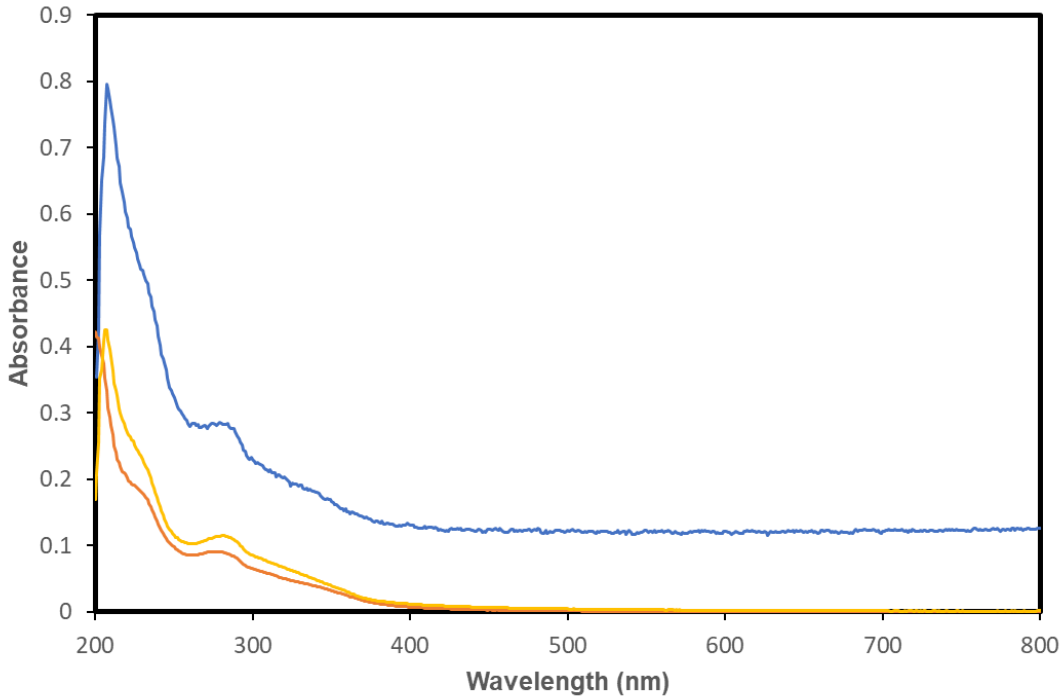

Figure 2.6: Soxhlet extraction of Hinton A lignin, in three different fractions. Yellow represents the unaltered extract from ethanol when resolubilized in EtOH. The red line indicates acetonitrile-soluble compounds from the obtained solid mixture, while the blue line indicates methanol-soluble compounds.

The nomenclature that will be used for each extract from this point forward, including all of its subdivisions, will be based on the extraction method and instance, meaning a sequential numbering starting with the very first extraction, while specifying which fraction if refers to when necessary. This extract thus far discussed shall then be referred to as “Soxhlet1”, or “Sox1” if an abbreviation is necessary.

Following this result, an extraction using 100 mL of acetonitrile with 2.515 g of Hinton A lignin in the Soxhlet system was performed, followed by another with 100 mL of chloroform and 2.504 g of Hinton A lignin. The results for all three extractions are shown in the Table 2.1.

Table 2.1. Summary of initial Soxhlet extractions using paper thimble and different organic solvents

Solvent	Name	Lignin	Initial mass	Final mass	Yield

EtOH (200 mL)	Soxhlet1	Hinton A	2.504 g	0.830 g	30%
AcN (100 mL)	Soxhlet2	Hinton A	2.515 g	0.179 g	7%
$CHCl_3$ (100 mL)	Soxhlet3	Hinton A	2.504 g	0.447 g	18%

Based on our analysis of the literature, and results from this section, we addressed unextracted Hinton A lignin to be a protolignin, based on the profile obtained from the extractions, which will be further explained in this section, but in short, this material's extract yield was equivalent to one done with protolignins, while technical lignins would be expected to have slightly higher yields, based on their already selective structures.

One issue that was identified with these early extractions was the possibility that the paper thimble could be leaching compounds that could easily be mistaken for lignin extracts, given the cellulosic nature of paper. Other issues could be the adsorption of small molecules onto the thimble paper, based on chemical affinity, which could generate inconsistent results for the extractions. To address this issue, we acquired glass fiber extraction thimbles (30 mm x 100 mm, N086R from Advantec), which also allowed us to use a larger mass of lignin to start the extraction. Out of the three solvents used for extractions thus far, AcN was the one with the most selective profile of products, as well as having other desirable characteristics, which will be discussed further into the present work. Hence, AcN extractions were used for follow-up batches with the new glass fibre thimbles.

Table 2.2: Follow-up extractions using acetonitrile and glass fiber extraction thimbles

Solvent	Name	Lignin	Initial mass	Final mass	Yield
AcN (200 mL)	Soxhlet4	Hinton A	10.0 g	0.60 g	6%
AcN (200 mL)	Soxhlet5	Hinton A	10.0 g	0.61 g	6%

Technical lignin samples obtained by this method are a dark brown color, as opposed to the light brown of the original protolignin used. Figure 2.7 shows the color difference between the two lignin samples.

Figure 2.7: On the left: Hinton A protolignin obtained from FP Innovations; on the right: extracted technical lignin via Soxhlet4, with AcN.

Another technical lignin extraction performed was the dioxosolv-lignin extraction process, which is widely used in the literature since it is known to generate more water-tolerable fractions of lignin, and also to carry the least number of small molecules through the extraction procedure, facilitating the quantification of products. Upon analysis of the dioxosolv lignin extract by GC-MS, more thorough washing steps were taken since many reactants from the extraction itself were observed.

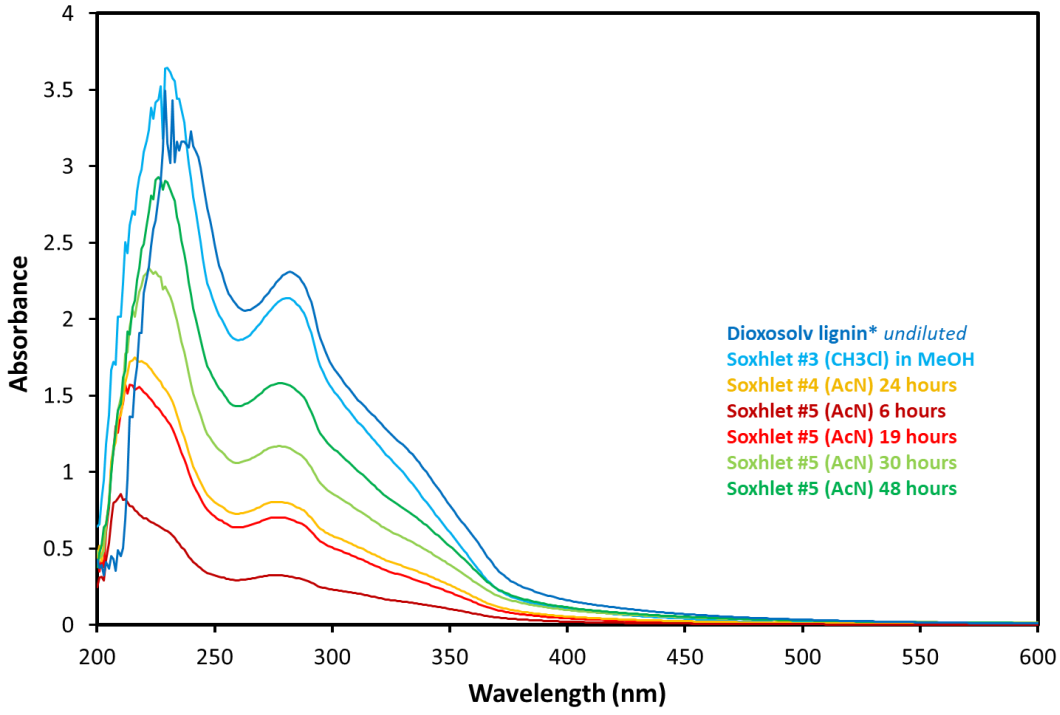

Figure 2.8: Absorbance spectra from technical lignin extracts of different batches and dioxosolv lignin

In an attempt to achieve a similar result as the dioxosolv lignin extraction, but using the Soxhlet extraction methodology, an extraction by Soxhlet with water as the solvent was conducted. The results demonstrated a much lower yield of technical lignin, comparatively to both the dioxosolv method and the organic solvent based Soxhlet extractions, as can be seen by the UV-Vis spectra in Figure 2.9.

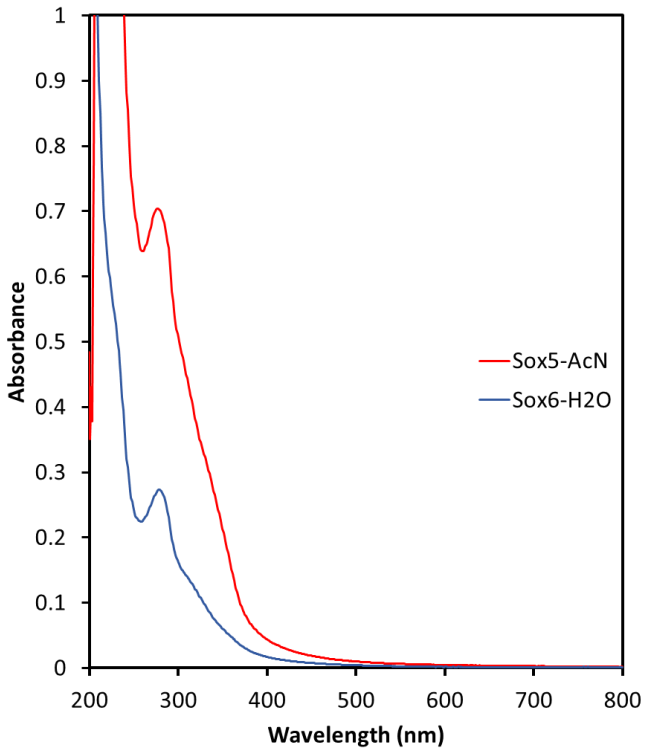

Figure 2.9: Absorbance of samples obtained from Soxhlet extraction of Hinton A lignin. Both extractions were done under the same amount of time, with the same volume of solvent and initial mass of lignin. Spectra were taken with the same dilution for both samples, meaning differences in band intensity are due solely to lignin solubility in different solvents.

The last material used for obtaining technical lignins was a washed sawdust, obtained by using a belt-sander on a stump of freshly cut sugar maple tree (*Acer saccharum*). The homogeneous fine and light-brown powder was used both as a secondary protolignin source, and extracted for the production of technical lignins, through the same processes shown previously, including dioxosolv and Soxhlet extractions. Figure 2.10 shows the source of the sugar maple sawdust and the large batch of powder obtained, for continuity purposes.

Figure 2.10: Top left image shows maple tree stump, minutes after cutting. Bottom picture shows belt sander being used to obtain the sugar maple protolignin powder: Top-right:

Technical Lignin Valorization

Starting with the technical lignin obtained from Soxhlet1 (EtOH, 200 mL), an initial test into the effects of a known photocatalyst with the mixture was attempted to observe the changes in the composition of lignin. Prior to the reaction, in order to minimize unwanted solids and adjust concentration, 0.25 g of the Soxhlet1 lignin was dissolved in 95 mL of AcN, filtered and analyzed by HPLC. Reaction was carried out in a test tube using 2 mL of the extract with a 3 mg/mL concentration of lignin, and 22 mg of TiO_2 as the photocatalyst, under air. The light source used for this and many subsequent reactions was an array of 7 concentrated UVA LEDs, which will be referred as UVA LEDi (LED illuminator) as per the manufacturer's nomenclature (LuzChem). The reaction was cooled using a small fan connected to the LEDi, which kept the majority of the solution from heating past 30 °C, but the exact site of irradiation is expected to be a hot spot in every one of these reactions. Temperatures

were taken using an Etekcity 800 infrared thermometer. Results from the HPLC-MS from before and after the reaction are shown in Figure 2.11.

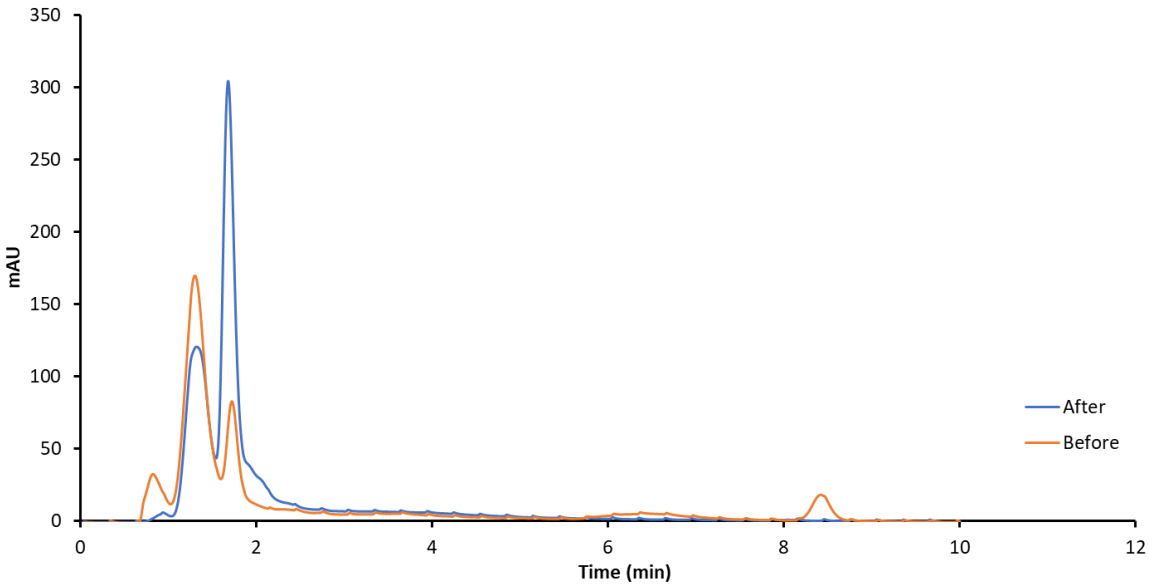

Figure 2.11: HPLC-MS spectra of valorization reaction using acetonitrile-soluble compounds from Soxhlet1 mixture, using 99% THF and 1% H_2O. Shown in orange is the extract prior to reaction, and in blue is the product mixture after 2 hours under UVA LEDi irradiation in the presence of TiO_2, under air.

The column used in this case is a normal phase column, instead of the size exclusion column used in certain analysis from this work. In order to interpret this data, a few considerations based on the mass spectra obtained must be made. Firstly, the mass of the compounds released by the column increases in direct proportion to the time elapsed. Secondly, is that compounds released within up to the two-and-a-half-minute mark are largely small molecules including monomers of lignin and other side products, while compound populations observed afterwards have much higher molecular masses, being compound mixtures of heavy dimers and trimers of lignans. Based on these parameters and comparing the spectra from before and after the valorization reaction, we may infer the possibility of complete conversion of compounds of higher molecular weight, observed from the disappearance of the peak found between 6 and 9 minutes of elution through the column. This is expected, as the tendency is that extracted trimers of lignans and

other structures of even higher molecular weight tend to break down into monomers and lighter dimers, though since repolymerization pathways do exist, it is a positive result to observe that compounds within those molecular weights are no longer present. We do observe, however, that compounds of the smallest molecular weight previously present tend to become scarcer, and that can be due to a large number of things, but repolymerization and condensation mechanism come to mind as possible causes for such loss, as well as the photosensitivity innate to certain small molecular fractions of lignin generating compounds with lower molecular weight than this analysis is capable of detecting, possibly eluding within the solvent window.

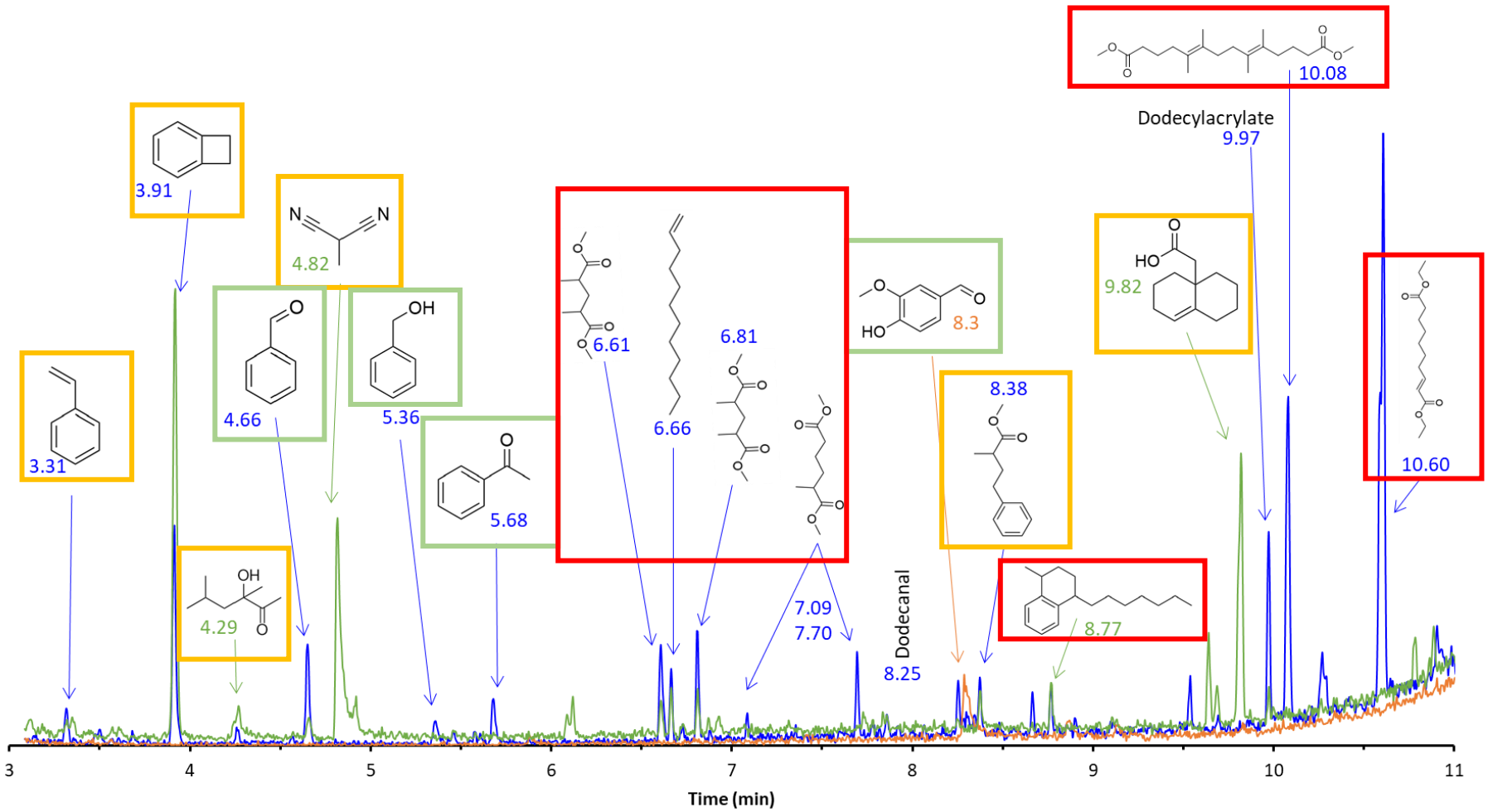

Figure 2.12: GC-MS analysis of products from valorization reaction of Soxhlet1 lignin with TiO_2 under UV irradiation using a multi-headed LED illuminator (5 simultaneous UV LEDs). Compound structures estimated by mass spectra using MS library. Orange line represents post extraction mixture, blue line represents valorization reaction after 2 hours, and green line shows products after 19 hours.

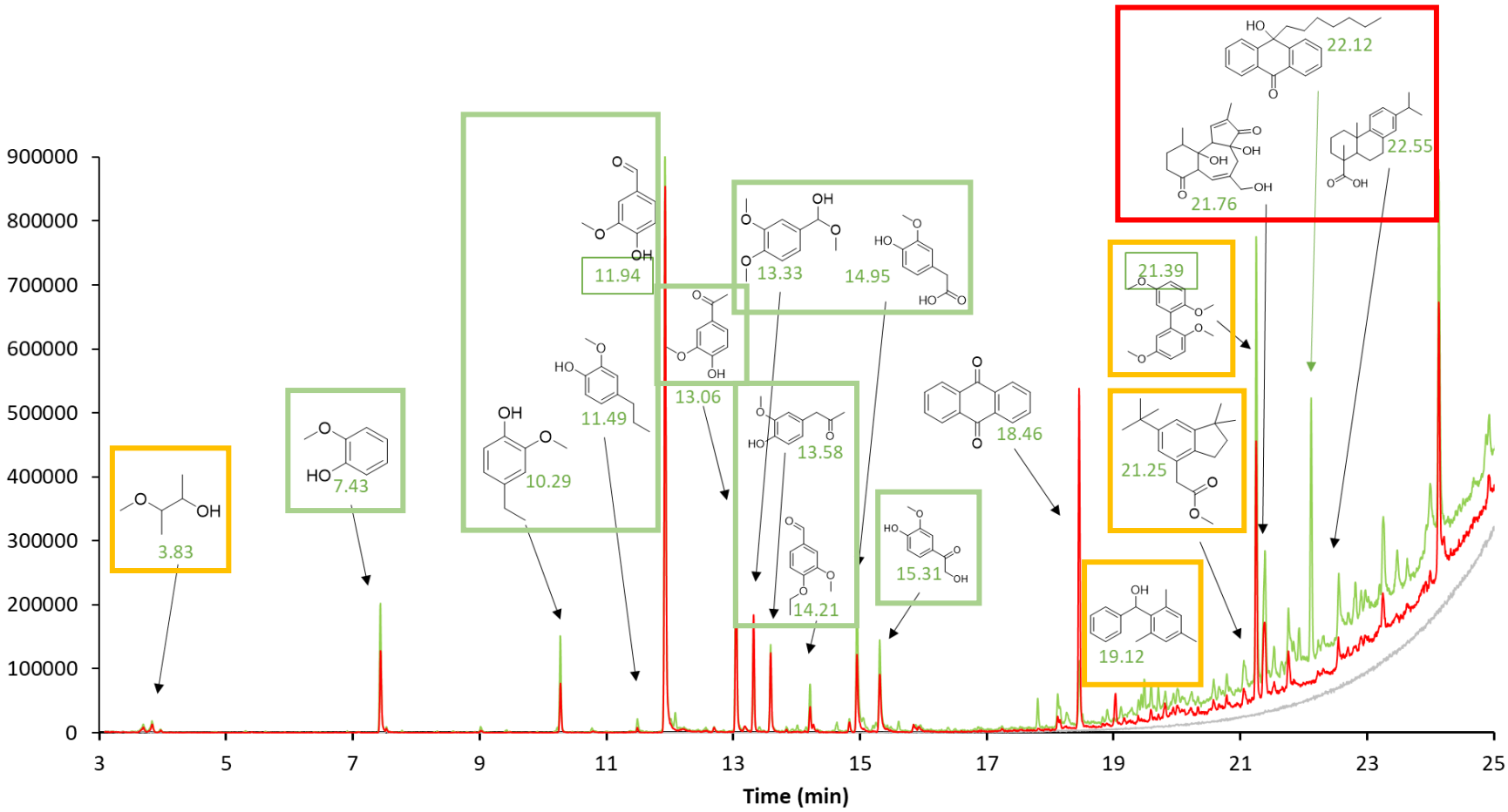

Figure 2.13: GC-MS analysis of products from valorization reaction of Soxhlet3 lignin with Pd@TiO_2 under UV irradiation using a multi-headed LED illuminator (5 simultaneous UV LEDs). Compound structures estimated by mass spectra using MS library.

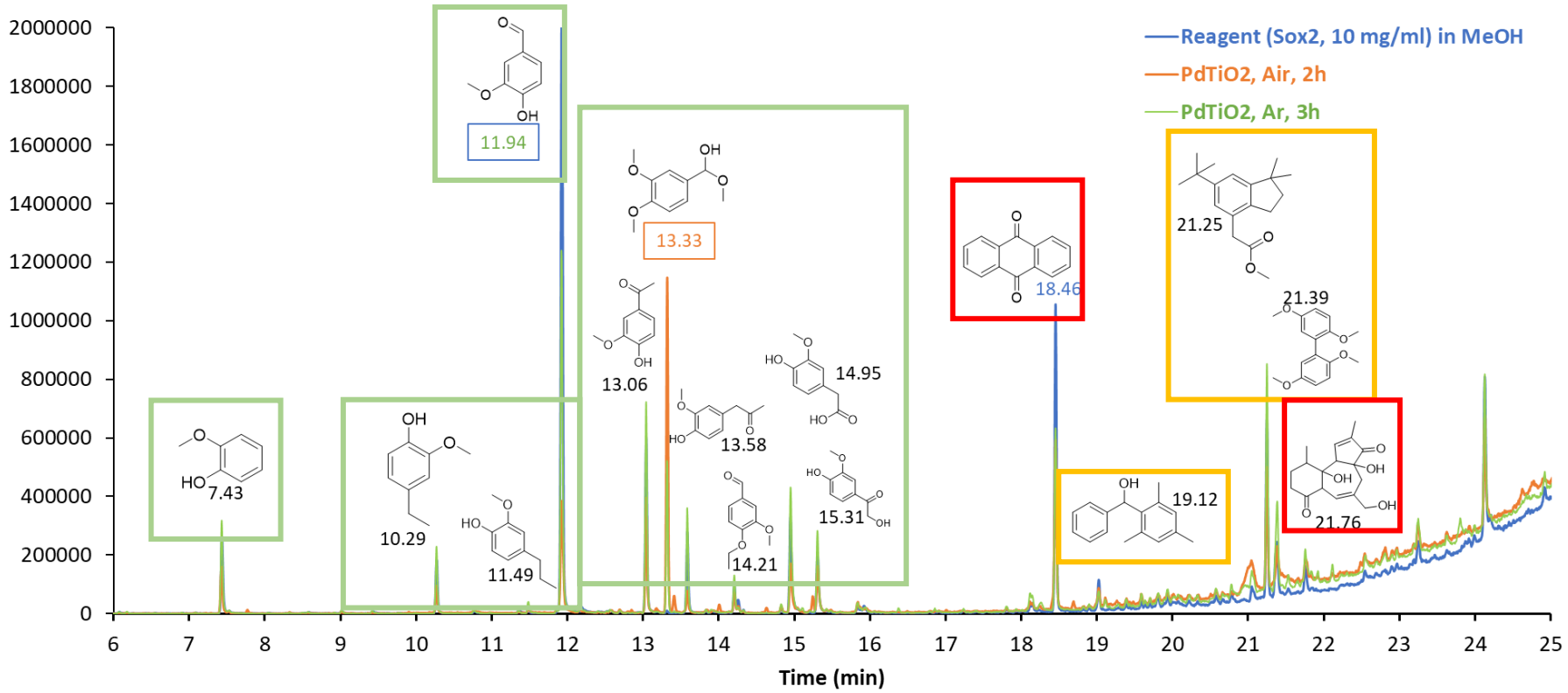

Figure 2.14: GC-MS analysis of products from valorization reaction of Soxhlet2 lignin with Pd@TiO_2 under UV irradiation using a multi-headed LED illuminator (5 simultaneous UV LEDs). Compound structures estimated by mass spectra using MS library.

For the purpose of analyzing the contents of Figures 2.11-2.13, we turned to a thorough look at common lignin monomer structures, linkages, and overall structure. Our analysis of basic linkages and building blocks, as well as the use of available commercial compounds, allowed us to either determine or infer a confidence level to the structures estimated by the GC-MS library of results. Known lignin products, monomer, monomer derivatives, and confirmed structures by comparison with commercial standards were highlighted in a green box, and this was seen more commonly within lower molecular weights, most likely due to instrumental affinity of the column and detector used to the structures within those intervals. Molecular structures that were not confirmed but bear resemblance in either molecular mass or structure to compounds observed within the same range of elution from the column assessed are highlighted in orange boxes and were mostly used for estimates of total extraction yields, and not for their individual values. Molecular structures that were either highly unlikely to be found among lignin extracts, as well as known additives to wood and lignocellulose processing, meaning they did not originate from the natural wood extract, are highlighted in red. This last category included anthraquinone, which was found to be added as a bleaching agent during wood processing by the company that gifted us with these samples and extracts from early paper thimbles that were used in lignin extraction.

Based on this initial result and comparison with similar results in the literature, a calibration curve was devised to calculate yields for the products observed, and the use of commercial compounds was also employed to verify the estimated results obtained from the mass-spectrometry library. Based on structures and elution time of commercial compounds and contrasting them with products from the library of results, we may access the veracity or at least impart a confidence level to the structures seen in Figure 2.15 and other associated results.

We chose to focus on a few key molecules to follow in terms of yield and as a measure to evaluate the success of each catalytic system and extraction. Determining which compounds to include in said shortlist started with one of the major compounds to be produced from lignin, 4-hydroxy-3-methoxybenzaldehyde (vanillin), since it is a compound that is already commercial, and it retains functional

groups which can be used in platform chemical studies after further processing. In addition to vanillin, other major products were quantified for most reactions, those being 2-methoxyphenol (guaiacol), 4-methoxyacetophenone (acetanisole), and 4-hydroxy-3-methoxyacetophenone (acetovanillone). Acetanisole and guaiacol are also important since they can be related to one mechanism for the valorization of lignin commonly studied, which is the β-0-4 bond breaking. This mechanism was further investigated using of molecular model compound reactions, as will be discussed in Chapter 4.

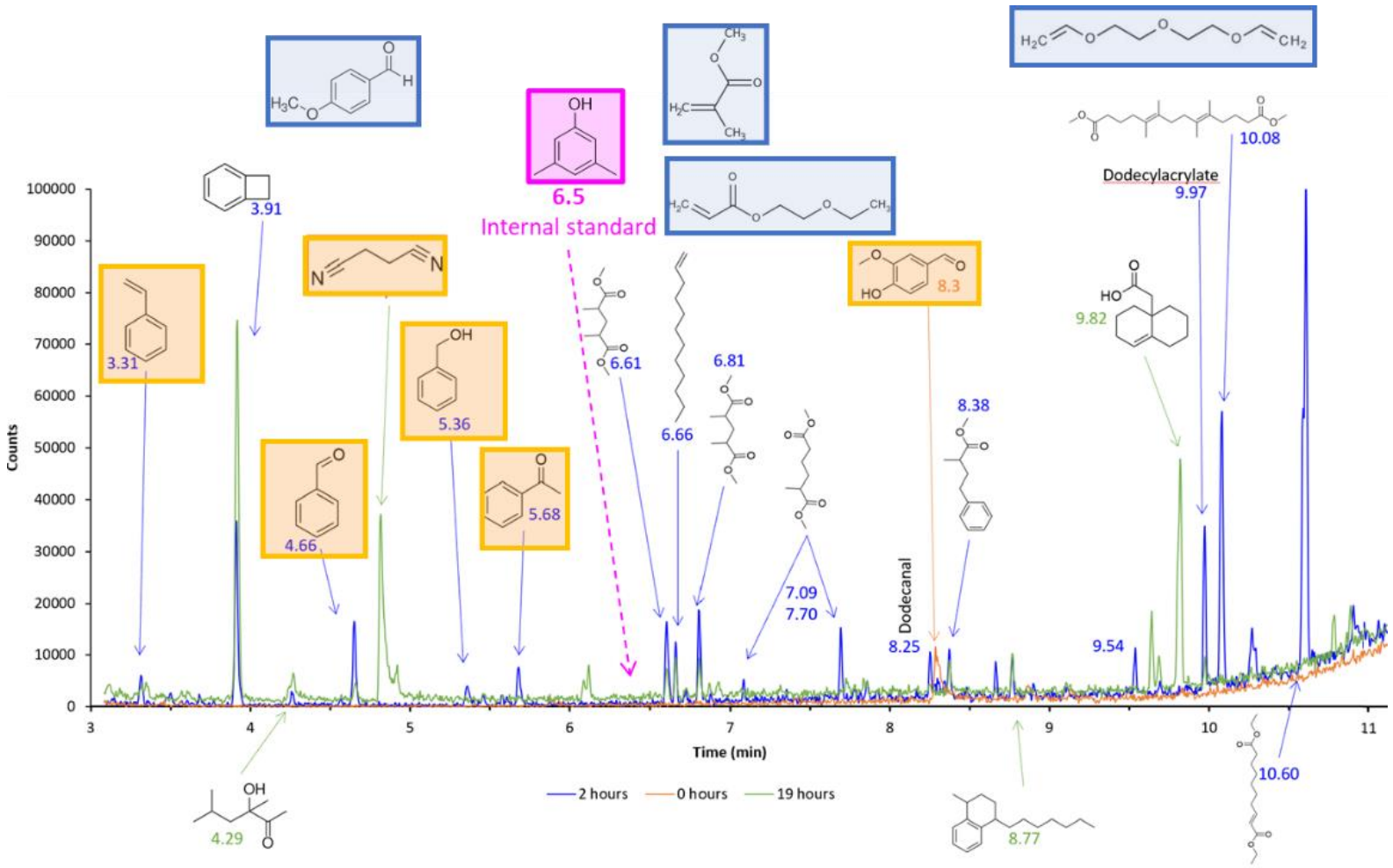

Figure 2.15: GC-MS spectra of Soxhlet1 post reaction sample, highlighting in orange compounds that were commercially available, in blue compounds used as comparable standards, and in pink the chosen internal standard. Orange spectra obtained after lignin extraction, blue spectra obtained after 2 hours of valorization reaction, and green spectra obtained after 19 hours of valorization reaction.

The next step was to experiment with a few different photocatalysts and observe which showed better production of small molecule products from lignin valorization reactions. It was determined as well that experimentation should revolve around the extract from Soxhlet4 (200 mL of AcN, 10 g of starting lignin for 24 hours) and from the dioxosolv extraction product, as the former showed the highest yields of lignin during early experiments, and the latter showed no small molecules in the extract before valorization reactions. This approach could give important information on the effects of an expected mixture of small molecules during valorization reactions with real lignin samples, as well as facilitate yield calculations. Catalysts that were tested at this time included TiO_2, $Pd@TiO_2$, $Pd@Nb_2O_5$, Nb_2O_5, and $NbOPO_4$.

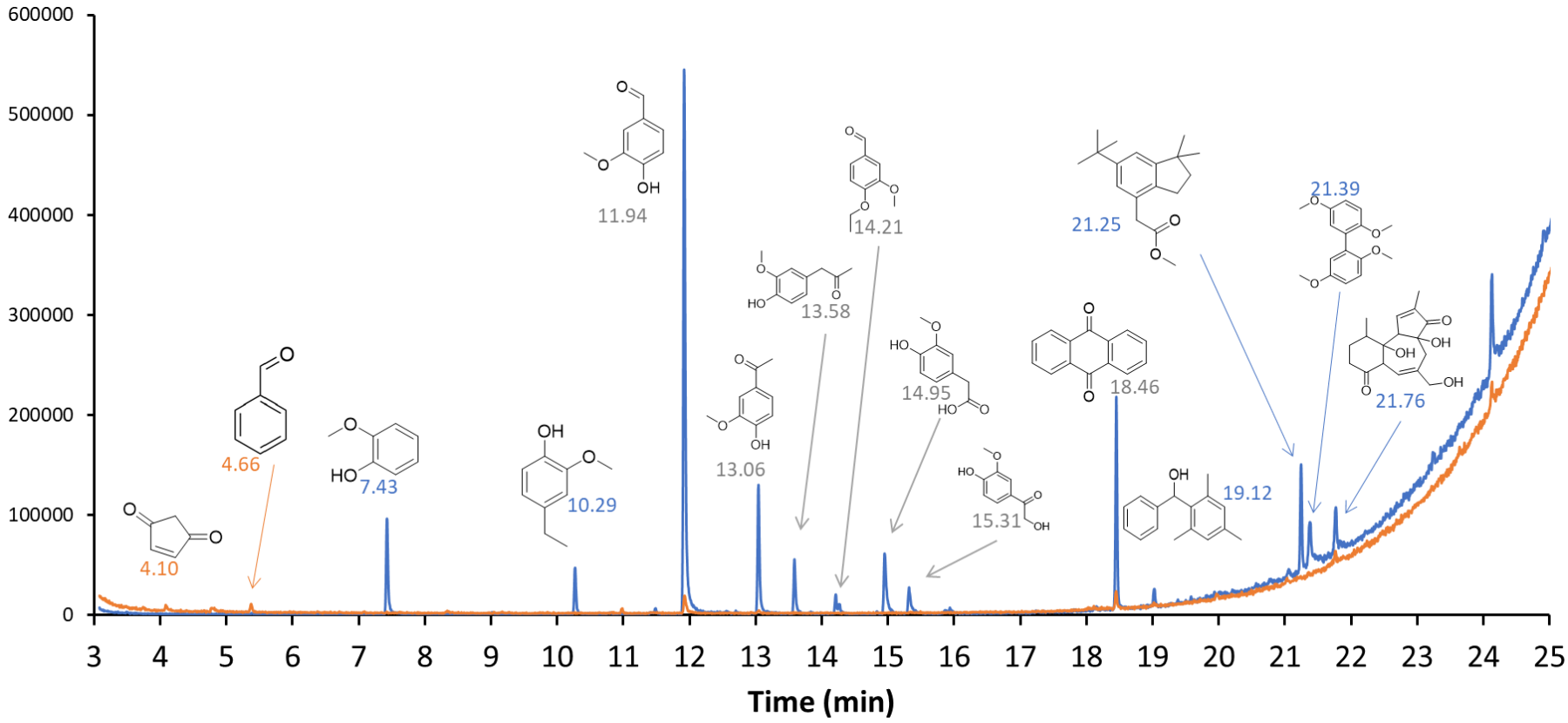

Figure 2.16: GC-MS analysis of products from valorization reaction of Soxhlet4 lignin with TiO_2. Time zero represented by blue line, while orange line represents spectra after 2 h reaction. Compound structures estimated by mass spectra using MS library.

Arranged in Table 2.3 are the calculated yields for the monomeric compounds found on the Soxhlet4 extraction. This example illustrates the limitation in overall mass of products obtained based on the initial dry mass of starting material utilized.

Table 2.3: Yield of small molecules observed after Soxhlet extraction without further reactions.

Extraction	Product	Concentration (mg/ml)	Yield (%)
Soxhlet extraction 4 200 ml AcN 24 hours 10 mg Hinton A Lignin *Yield ≈ 6% wt (3 mg/ ml)*	Vanillin	0.037	1.22
	Guaiacol	0.006	0.20
	4-Hydroxy-3-methoxyacetophenone	0.011	0.36

Though some yield of vanillin was achieved from early technical lignin valorization reactions, a tendency was observed that longer reactions seem to produce lower yields, and upon closer inspection we observed that phenolic products obtained were being lost over time during UV irradiation, with or without the presence of the catalyst.

Experiments were also conducted to determine if the catalyst could cause loss of small molecular products without irradiation. When run under dark conditions, the same technical lignin valorization reactions with each catalyst showed small yields, but also no loss of said products over time. Figure 3.17 shows the loss of major products from the extracted mixture in Soxhlet4 by light irradiation over time, without the presence of a catalyst. When the same experiment was done with visible light, no product loss was observed, which led us to two possible solutions for this hurdle. The first solution attempted was adapting our reaction system to accommodate UV irradiation of the catalyst and lignin, while protecting the products from its damaging effects. This was done through the use of a biphasic reaction system, in which the catalyst and the lignin would be in a denser solvent, being irradiated, while an upper phase containing a second solvent would harbor the products of the reaction.

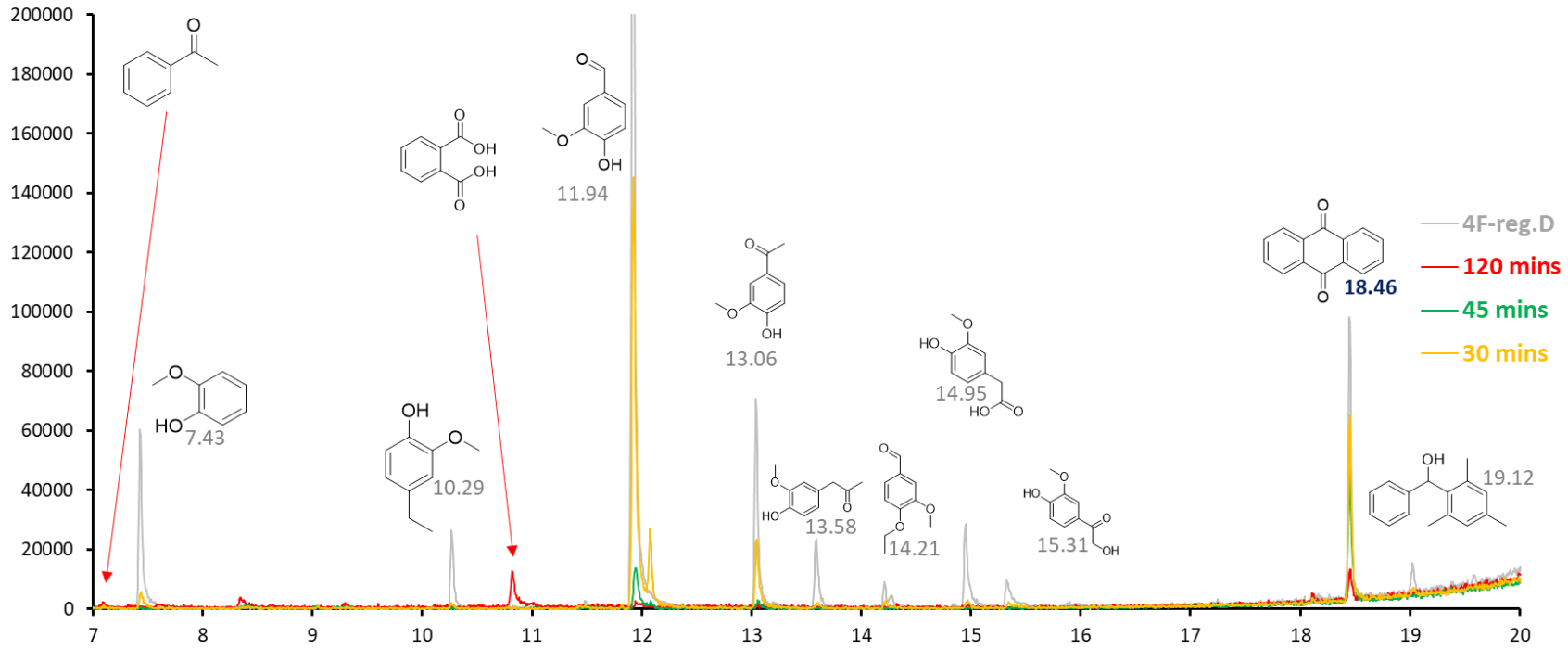

Figure 2.17: GC-MS analysis of lignin extracts exposed to high-powered UV irradiation using an LEDi (7 LED array). Grey spectrum indicates compounds prior to irradiation, yellow represents compounds after 30 minutes of irradiation, green and red show remaining compounds after 45 and 120 minutes respectively.

The loss of Guaiacol and other chromophores contained in the product mixture can also be observed by the difference in the color of valorization reaction under different conditions. This effect can be observed in Figure 2.18, every vial shown started with the same lignin extract, from Soxhlet4, and reactions were conducted in acetonitrile, using 22 milligrams of catalyst (with the exception of the no catalyst control, of course), under air and at room temperature, with the same UVA LEDi light source referenced thus far.

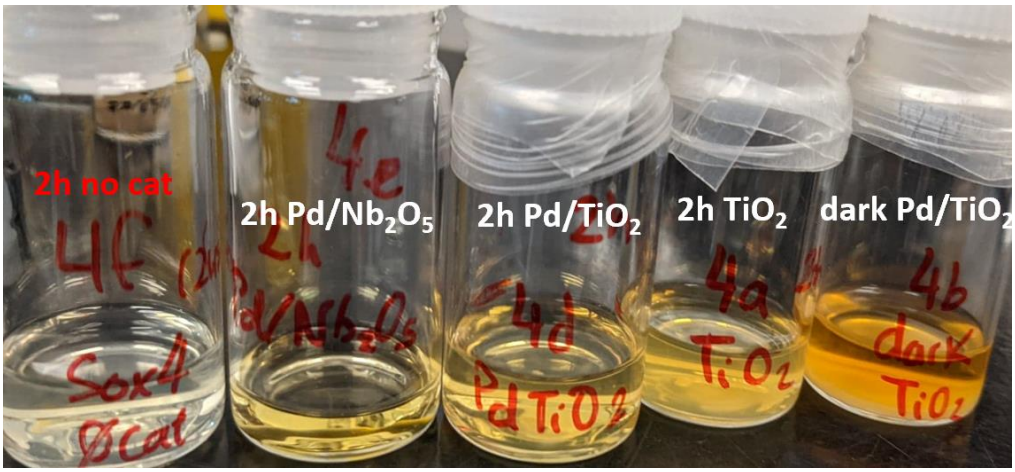

Figure 2.18: Color difference from irradiation tests under different catalytic conditions, including controls for no light, and light with no irradiation. See picture for labels.

Visible-Light Reactions for Technical Lignins

Under UV light irradiation, it was observed that several products are lost over time. Beyond the systems shown previously, attempts at visible-light irradiation photocatalysis were made as a means to obtain higher yields of products, as it was observed that under visible light there was little to no loss of major products from the technical lignin extractions and valorization reactions. For the first battery of experiments with visible light we turned to heterogeneous photocatalysts with a semiconductor as a support, and a visible light-absorbing nanoparticulate metal as the principal catalytic agent, followed by the synthesis and experimentation with two visible light-absorbing quantum dot species, CdS and CdSe QDs.

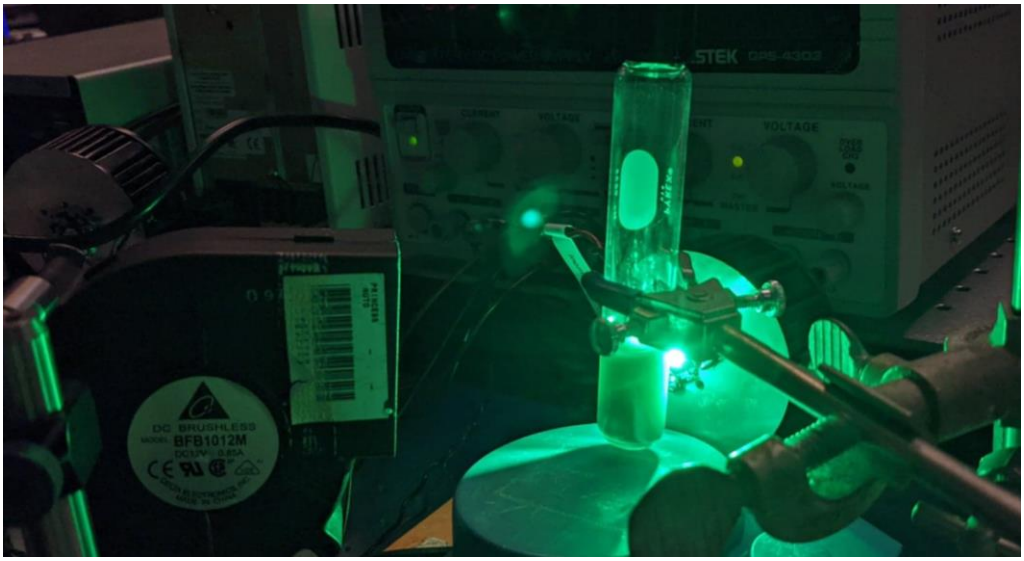

Figure 2.19: Reaction setup for visible light irradiation for technical lignin valorization. Single LED light at 525 nm, air cooling, using Au@TiO_2 as the catalyst, in AcN.

Technical lignin yield considerations and results

Besides the already mentioned limitation of light irradiation interacting with products from the valorization reaction, and side reactions of condensation lowering the detected final yield by GC-MS, we also identified that much of the vanillin production from the technical lignins extracted through the Soxhlet methodology can also be achieved with only the light. Thus, we began adjusting the yield by subtracting the vanillin yield of the light only reactions from ones achieved with photocatalysis.

A summary of notable yields and catalysts is shown in Figure 2.20. It does bear mention as well that these yields will always appear as deceitfully small, but this is since only a single product is being analyzed, as well as the fraction of the total mass that can generate quantifiable products is also far lower than the total mass of lignin used in any given reaction. For context, yields achieved from lignin experiments in the literature that low percentiles, anywhere from 0.1% to 9% of the total mass of lignin used, is often considered a good result that, if anything, has potential to be expanded upon.[7,45] This is often placed in the context of the thousands of tons of lignin produced yearly and that go either unused or burned for energy, from which the production of 0.1% of valuable products is very significant.

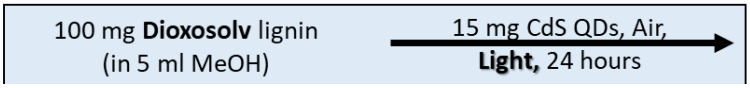

Exp nº	Light	Changes	Vanillin yield (%)	Corrected vanillin yield (%)
1	Visible (400-600nm) - parking lot light	No catalyst	0.0015	
2	Visible (400-600nm) - parking lot light	---	0.0060	**0.0045**
3	Visible (400-600nm) - parking lot light	Under N_2	0.0015	**0.0000**
4	Blue LED (465 nm)	No catalyst, MeOH/H_2O (1:1), under N_2	0.0000	
5	Blue LED (465 nm)	MeOH/H_2O (1:1), under N_2	0.0025	**0.0025**
6	Blue LED (465 nm)	Under N_2	0.0037	**0.0033**
7	Blue LED (465 nm)	---	0.0202	**0.0198**
8	Blue LED (465 nm)	AcN (5 ml)	0.1117	**0.0803**
9	Blue LED (465 nm)	No catalyst, AcN	0.0314	
10	Blue LED (465 nm)	No catalyst	0.0004	

Scheme 2.1: Visible light reactions with CdS quantum dots as well as controls, under both blue LED light, and also using a powerful parking lot light.

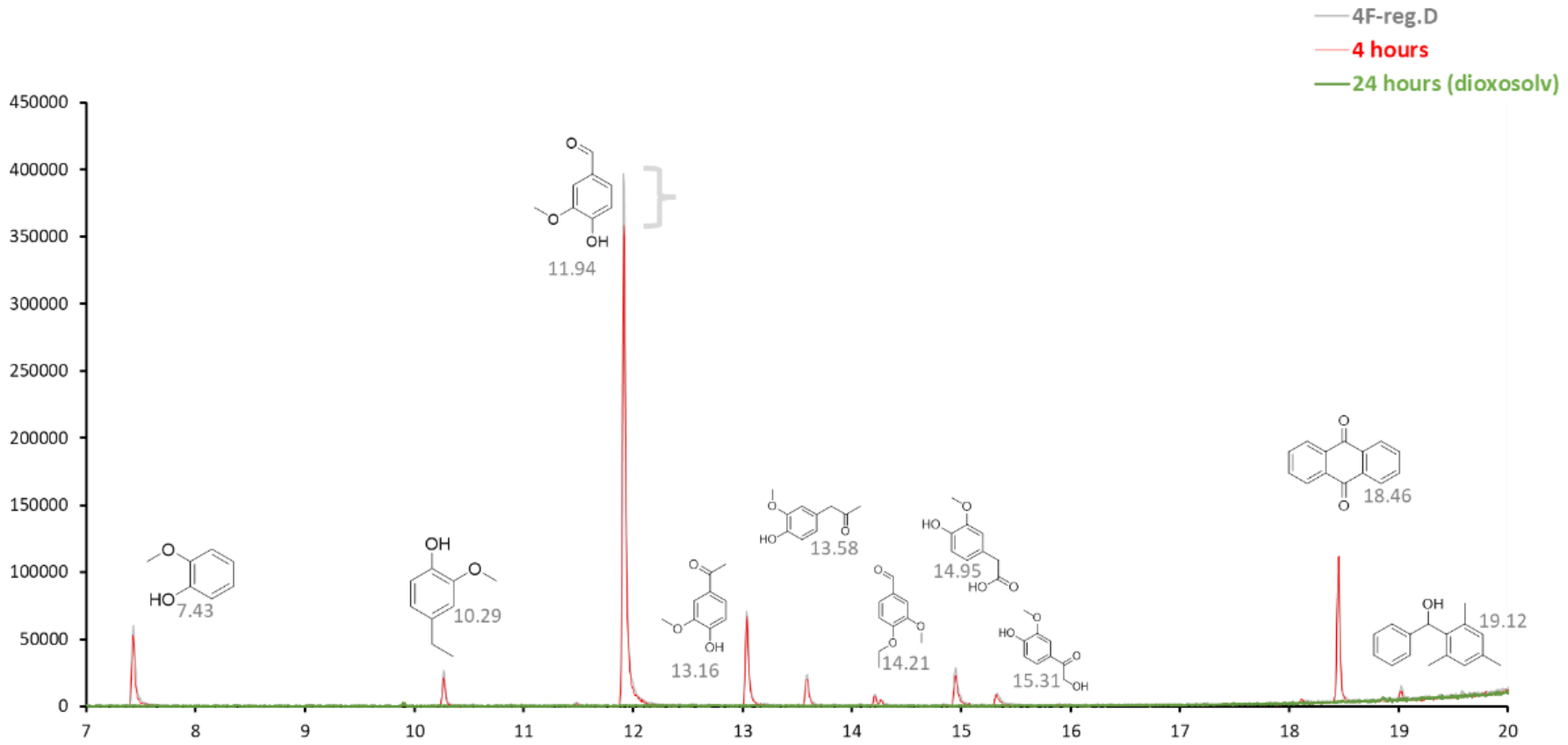

Figure 2.20: GC-MS spectra of Au@TiO_2 photocatalyzed reaction of dioxosolv technical lignin.

Protolignin Valorization Strategies

Developed in parallel to the technical lignin experiments shown in the previous 2 sections, protolignin valorization reactions were conducted, both to contrast the results obtained from the technical lignins, and also to observe new avenues to add value to lignin that are not necessarily just in the production of small molecules.

Early experimentation involved the use of water as a solvent, and the use of surfactants combined with niobium-based photocatalysts in an attempt to develop cleaner and greener lignin valorization systems. Reactions were done using 8 milligrams of Hinton A lignin with no further modifications, with 6 mL of solvent. Unless otherwise indicated, surfactants were used just under their calculated critical micellar concentration (CMC). Two surfactants of opposite micelle polarity were tested early on, centrimonium bromide (CTAB, or $C_{19}H_{42}BrN$) and sodium dodecyl sulfate (SDS, or $CH_3(CH_2)_{11}SO_4Na$), in order to observe which one had the best contribution to lignin suspension stability in aqueous solution for the betterment of valorization reactions in water. To assess their effectiveness, two test tubes were charged with SDS and CTAB separately, while remaining about 1% below their respective CMCs, then 6 mL of water was added to both, followed by 8 mg of Hinton A lignin and a magnetic stir bar. The mixtures were then stirred for 30 minutes, and subsequently observed for another 10 minutes. The mixture containing CTAB presented the longer lasting suspension and was thus chosen initially as the target surfactant to be tested.

Figure 2.21: LED irradiation setup for protolignin valorization reactions.

In a standard reaction, 2.5 mg of CTAB were mixed with 6 mL of Milli-Q H_2O, 8 mg of Hinton A lignin, 20 mg of the catalyst and a magnetic stir bar. UV irradiation was used with a standard single-headed LED. Reaction vessel, colour and irradiation setup can be seen in Figure 2.21. Following each reaction, the mixture was centrifuged, and a sample of the aqueous phase was set aside for HPLC-GPC analysis, to ascertain the size difference of the remaining soluble fraction of lignin. Following that, to the tube containing the solids and remaining aqueous phase after the reaction, 2 mL of EtOAc was added, and the mixture was left stirring for 30 minutes, after which the organic phase was removed and analyzed using GC-MS and HPLC-MS. Catalysts tested included $NbOPO_4$, Nb_2O_5, and TiO_2. From the organic extractions analyzed by GC-MS, no small organic molecules were detected.

Reactions including $NbOPO_4$ showed a significant visual difference in the lignin and solution post reaction, where the previously dark brown solid turned to a light tan, almost white colour, which seemed interesting and prompted additional

investigations of the conditions used, even though no small organic molecules had been extracted successfully. The GPC results from the aqueous phase showed a significant decrease in the size of soluble compounds present after the reaction when compared to the initial protolignin sample.

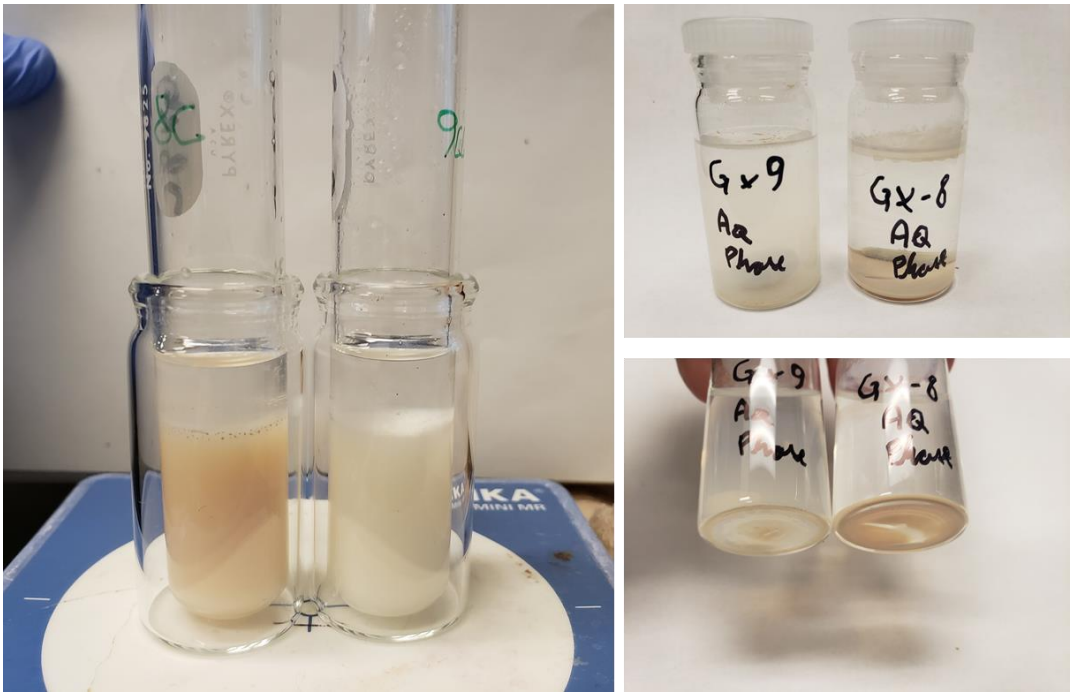

Figure 2.22: Post-reaction mixtures during extractive procedures for protolignin valorization. Depicted are standard samples with TiO_2 as the catalyst in sample 8, and $NbOPO_4$ as the catalyst in sample 9. Panel to the left shows the extraction procedure intended for small molecular compounds, with organic solvent added as a top layer and stirring. Panels to the right depict aqueous phase after extraction and settling of the solids.

For these results with little to no detected monomeric or smaller products, characterization and measure of the success and degree of transformation of lignin becomes challenging. The confirmation of lignin modification was possible with the analysis of the remaining solid content of the reaction by FT-IR, shown in Figure 2.23. The contents of the whitened lignin shown in Figure 2.24 are compared to the original lignin sample (Hinton A), and with the pure catalyst used in the same reaction. The predominant vibrations in the post reaction sample between 1040-1050 represent deformation vibrations of C-H bonds in guaiacyl rings, while the one between 1220-1265 are the vibrations of guaiacyl rings and stretching vibrations of C-O bonds.[46] This confirms the conversion of lignin into guaiacyl-rich samples, which made the lack of small molecular products all the more puzzling. Our initial theory

was that they remained attached to a larger polymeric structure through the aliphatic tail of the monomer, keeping them from being extracted and observed in GC-MS and FID analysis. This theory may have been subsequently disproven based on the observation that bands representing syringyl and aromatic ring vibrations, which should be abundant if the main polymeric structure remained, were significantly lower in the post reaction sample, showing only C=O bonds at the α and β locations. This may signify that the monomers produced have a very strong attachment to the catalyst, and release from the niobium phosphate particles' surface would require further experimentation.

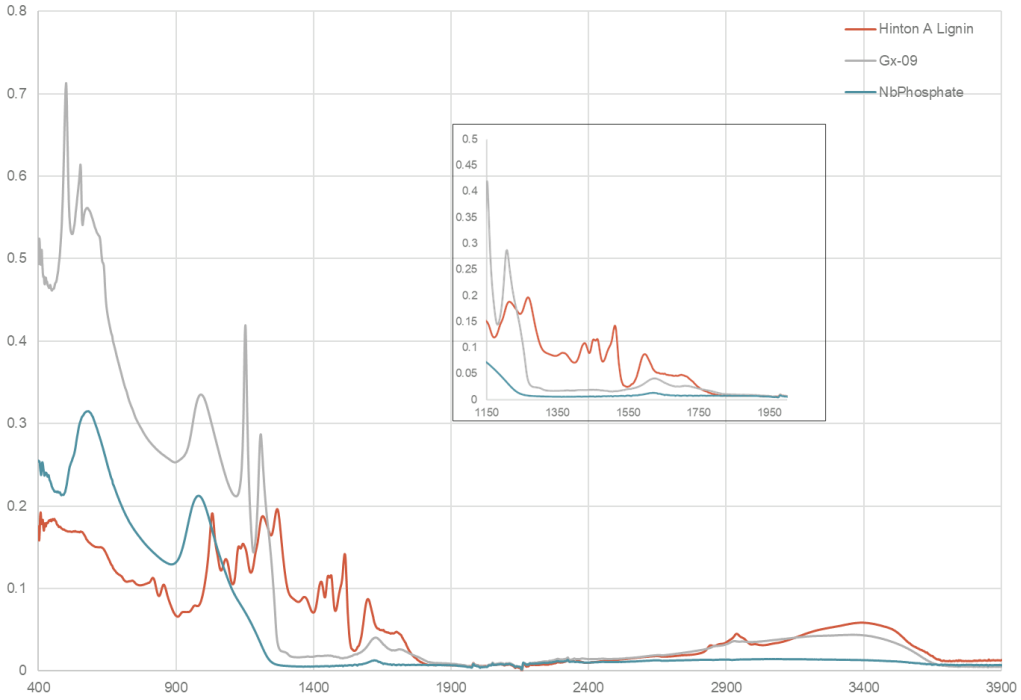

Figure 2.23: FT-IR analysis of solid content post valorization reaction of protolignin sample (grey). Original protolignin is shown in orange, while the catalyst on its own is shown in green. Inset shows an expanded view of highly modified region between samples, including

In table 2.4 some results from the protolignin valorization reaction are shown. For these, vanillin is used as a standard product for quantification purposes, while the corrected yield refers to the yield of vanillin in the reaction subtracted from the yield of the same system, but in the absence of the catalyst. Estimated total yield is the approximate yield of small molecules observed, and it serves only as a rough estimative of total lignin conversion.

Table 2.4: Protolignin valorization reaction results. Vanillin yield calculated using GC-MS and GC-FID data. Estimated total yield is here used as a term for the sum of the yields for products detected by GC-MS and GC-FID based on calibrated curves with standards shown in Figure 2.15. Percentage is based on total initial mass of material.

Exp nº	Catalyst	Solvent	Time	Vanillin yield	Corrected yield	Estimated total yield
1	$NbOPO_4$	3 mL AcN	20 h	-	-	3%
2	$Pd@Nb_2O_5$	3 mL AcN	20 h	2%-	1.5%	4%
3	$PtAu@TiO_2$	3 mL AcN	20 h	1.5%-	0.5%	2.5%
4	$Pd@TiO_2$	3 mL AcN	20 h	1%	0.25%-	1.5%

To validate the results observed, 2D NMR analysis was performed to obtain the for the spectra of the Hinton A lignin used in these reactions. More specifically, HSQC analysis allowed for the observation of resonances attributed to the C-H bonds in the β-0-4 region, those being quite characteristic within a certain range, depending on variations in the moieties structures.

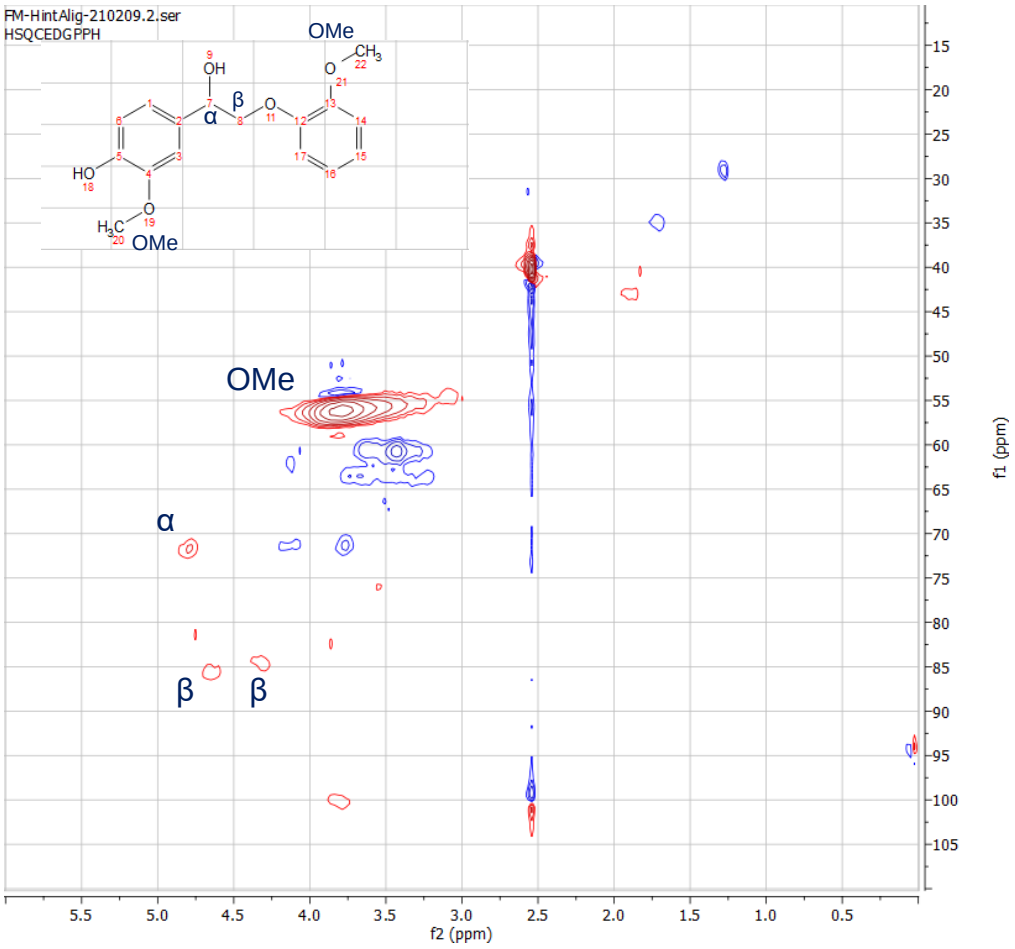

Figure 2.24: HSQC NMR of Hinton A lignin sample, dissolved in DMSO-d.

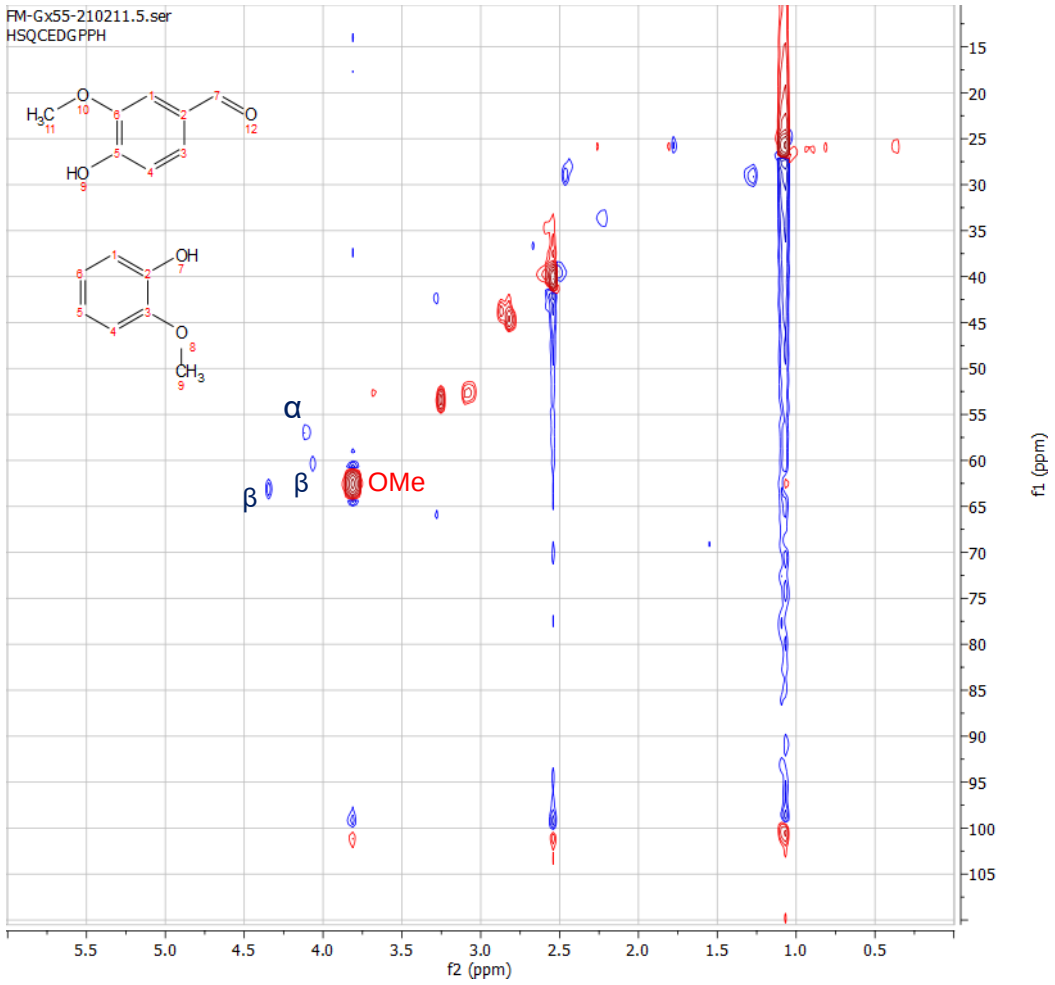

Figure 2.25: HSQC NMR of the reaction mixture for a lignin valorization reaction, dissolved in DMSO-d. The conditions for the reaction were UV irradiation for 20h, using 15mg of $Pd@Nb_2O_5$ as the sole catalyst, in 3mL of AcN, and 5 mg of Hinton A lignin.

The result of this characterization was then contrasted with the HSQC NMR of the remaining solid from the depolymerization reactions, as shown in Figure 2.25, which elucidates the shift of C-H resonances corresponding to α and β carbons observed in β-0-4 segments. The shift to the methoxy resonance could be attributed to the fact that in the polymeric chain of lignin, the terminal carbons are often further bound to the next monomer in the chain, whilst in the new spectra, those are now comprised of R-O-CH_3 resonances. This led to the conclusion that, despite the limitations in concentration that made the analysis more limited in scope, it is sufficient to indicate that the polymer chain was broken, and vanillic compounds were formed.

Biphasic Reaction Setups for Lignin Valorization

One strategy used to promote lignin valorization under UV light irradiation, while attempting to limit or even eliminate the loss of vital products was the use of biphasic solvent systems. Inspired by the extraction procedures used in certain aqueous protolignin valorization experiments, a first setup was conceived by placing a heavier solvent on a test tube and charged with the lignin sample, the catalyst, and a magnetic stir bar. Following that, a second solvent, chosen for being less dense than the first one, while being also sufficiently immiscible and in which the monomeric and other small molecular products are highly soluble in, is carefully poured on top of the first one. A sheet of aluminum foil is wrapped around the area containing the upper solvent, and the resulting mixture is placed in between the light source and the stir plate. An example of this setup is shown in Figure 2.26.

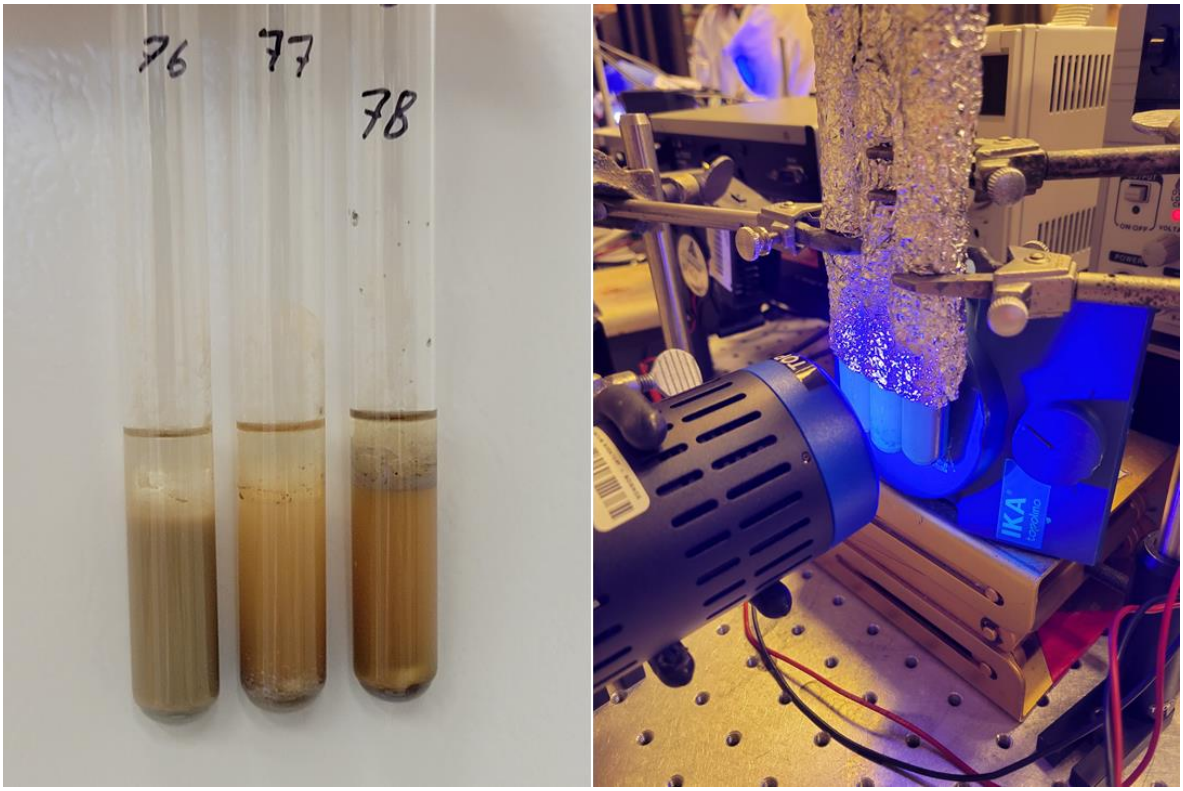

Figure 2.26: Biphasic reaction setup used for valorization reaction of protolignin samples using Kessil's PR160L 370 nm UV LED.

The solvent mixture chosen for most of the experiments conducted, which presented the best results, was a combination of 5 mL of Milli-Q H_2O as the denser

solvent, and 2 mL of EtOAc as the top layer solvent. Ethyl acetate was the solvent used for extractions during previous aqueous reactions, and is poorly soluble in water, thus presenting an ideal second phase to the setup. This experiment showed a higher yield of lignin valorization products for both catalytic and catalyst-free systems, when irradiated.

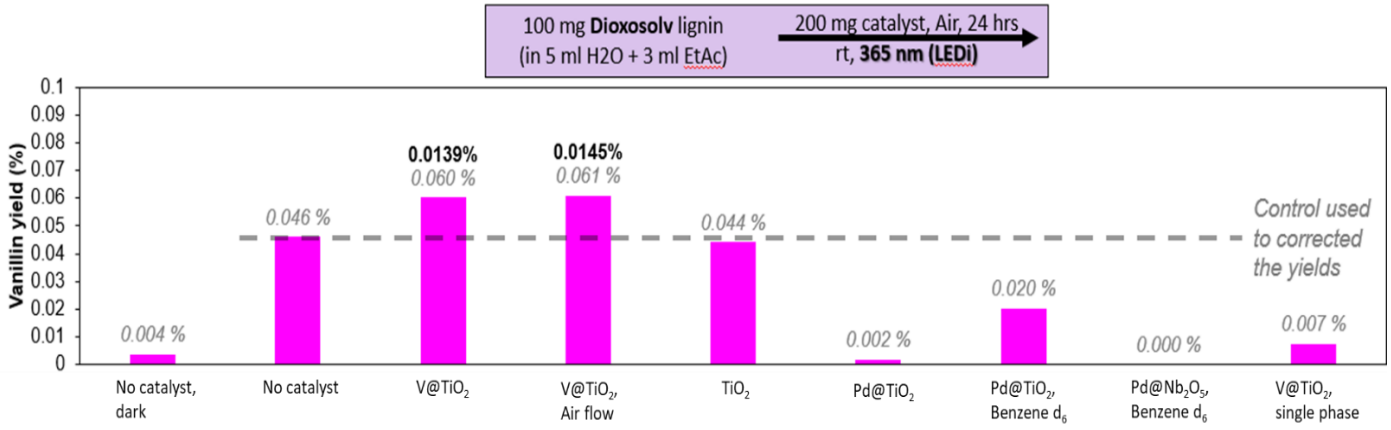

Scheme 2.2: Summary of biphasic conditions with dioxosolv lignin. Reaction conditions shown in box above graph, and exceptions shown after catalyst below each bar.

Achieving lignin valorization without catalyst doesn't detract on its own the possibilities opened by photocatalysis of lignocellulosic biomass. As we can observe in the examples contained in Scheme 2.2, vanadium-based catalysts were capable of producing more than double the single-product yield of light in our non-flow biphasic setup. This opens the way for several improvements, from optimizations in the synthesis of the catalyst, to different approaches to extracting lignin and increasing the single-target yield achieved.

Protolignins were also experimented on using the biphasic approach, and a summary of results is shown in Table 2.5. The difference in yields observed from technical lignin reactions and protolignin reactions is expected, as the extractions themselves tend to release some amount of vanillin, but have the added limitation of releasing a lot more side products, which hinders the analysis of each product mixture after valorization reactions

.

Table 2.5: Summary of protolignin valorization results using biphasic system

Exp nº	Catalyst	Solvent	Time	Vanillin yield	Corrected vanillin yield
1	$NbOPO_4$	5 mL H_2O + 2 mL EtOAc	20 h	0.3%	-
2	$Pd@Nb_2O_5$	5 mL H_2O + 2 mL EtOAc	20 h	2.2%	2.0%-
3	$Pd@TiO_2$	5 mL H_2O + 2 mL EtOAc	20 h	1.3%	0.9%-
4	AuPd@TiO2	5 mL H_2O + 2 mL EtOAc	20 h	2.6%	2.3%

A second biphasic system was assembled, and early experimentation seems promising, though at this point, certain variables and time constraints prevented these from making it into the current version of this research. This system can be seen in Figure 2.27, with a picture of the assembled flow system on the left, and a scheme explaining each element on the right.

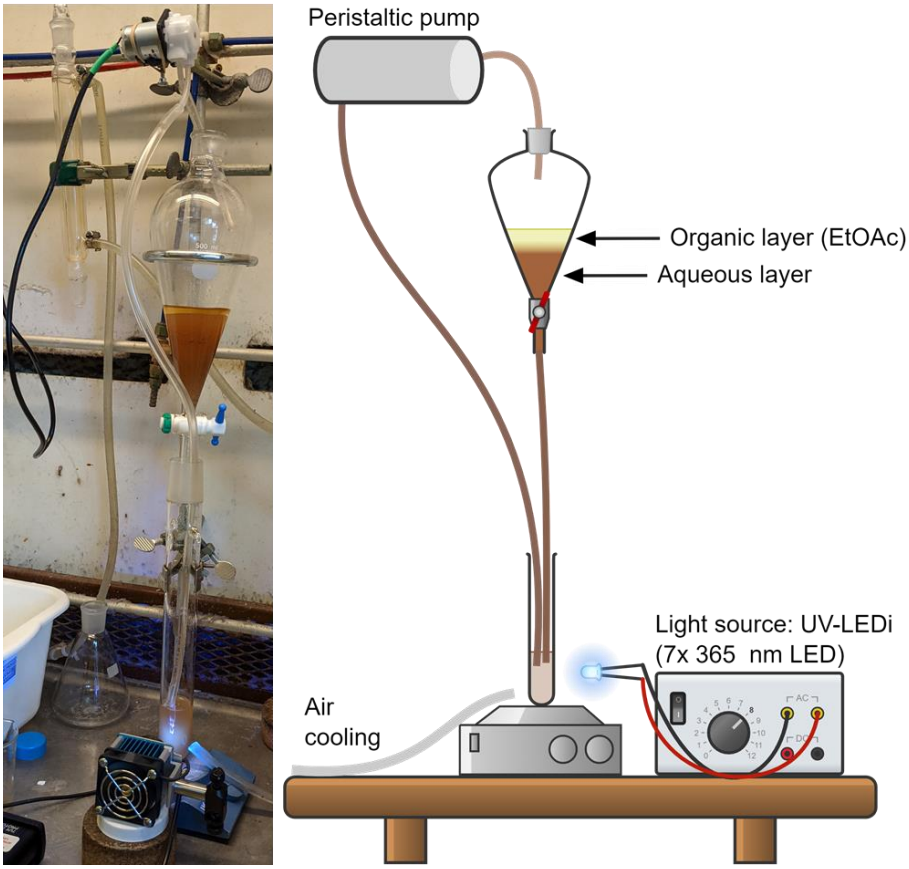

Figure 2.27: (Left) Picture of second biphasic system. (Right) Scheme drawn to elaborate on key elements of second biphasic system. See legend in scheme for component breakdown.

2.6 Future Work

One of the issues identified is the competition between the condensation reactions and breaking of lignin in the reactions tested. Though recent experimentation has attempted to steer valorization reactions with acid and basic character into catalyst-free systems, minimizing lignin condensation while retaining the benefits of a catalytic reaction is still desirable. Some recent experiments have indicated that the presence of formic acid can be a strong stabilizing agent, by supplying hydrogen to both products and intermediates. It has also been shown to have some catalytic capabilities on it's own, though our interests would be in the combination of formic acid and photocatalysts.[13, 14] Carbon monoxide generated from acid decomposition of the formic acid, incidental during solvolysis processes of technical lignins, has also been shown to have an important role in this reaction.[15]

Further experimentation with the flow biphasic system is necessary. A few changes to the materials used in the tubing is advised so that it minimizes retention of material inside of the tube, and also to stop the release of plastic derivatives into the reaction mixture. Optimizing the control of the flow from the separation funnel into the reaction vial is desirable, as well as improvements to the irradiation system. These changes may enable this reaction setup to produce consistently higher yields than stationary biphasic reactions.

Substantial improvements to the way lignin conversion and product detection and yield calculations are necessary. So far, the most straightforward way to assess the success of a reaction is through calculation of the vanillin yield, but this is a poor representation of the wider possibilities achievable using photocatalysis in lignin valorization. A better standardized way of calculating total product yield should be procured and applied to the reactions here discussed, as our methodology may have overlooked largely successful reactions based on a single-minded approach to product characterization.

References

1. Yue, F., Lu, F., Regner, M., Sun, R., & Ralph, J. Lignin-Derived Thioacidolysis Dimers: Reevaluation, New Products, Authentication, and Quantification. *ChemSusChem*, 2017, *10*(5), 830–835.

2. Harman-Ware, Anne E., et al. “A Thioacidolysis Method Tailored for Higher-Throughput Quantitative Analysis of Lignin Monomers.” Biotechnology Journal, vol. 11, no. 10, WILEY-VCH Verlag, 2016, pp. 1268–73,

3. Harman-Ware, A. E., Foster, C., Happs, R. M., Doeppke, C., Meunier, K., Gehan, J., Yue, F., Lu, F., & Davis, M. F. A thioacidolysis method tailored for higher-throughput quantitative analysis of lignin monomers. *Biotechnology Journal*, 2016, 11(10), 1268–1273.

4. Ralph, J., Lapierre, C., Marita, J. M., Kim, H., Lu, F., Hatfield, R. D., Ralph, S., Chapple, C., Franke, R., Hemm, M. R., Van Doorsselaere, J., Sederoff, R. R., O’Malley, D. M., Scott, J. T., MacKay, J. J., Yahiaoui, N., Boudet, A. M., Pean, M., Pilate, G., … Boerjan, W. (2001). Elucidation of new structures in lignins of CAD- and COMT-deficient plants by NMR. *Phytochemistry*, *57*(6), 993–1003.

5. Ralph, J., Hatfield, R. D., Quideau, S., Helm, R. F., Grabber, J. H., & Jung, H. J. G. Pathway of p-Coumaric Acid Incorporation into Maize Lignin As Revealed by NMR. *Journal of the American Chemical Society*, 1994, *116*(21), 9448–9456.

6. Chen, X., Li, H., Sun, S., Cao, X., & Sun, R. Effect of hydrothermal pretreatment on the structural changes of alkaline ethanol lignin from wheat straw. *Scientific Reports*, 2016, vol. *6*, 1–9.

7. Liu, X., Bouxin, F. P., Fan, J., Budarin, V. L., & Hu, C. *Recent Advances in the Catalytic Depolymerization of Lignin towards Phenolic Chemicals: A Review*. 2020, 4296–4317.

8. Kumar, V., Chandel, A. K., Kumar, S. P. J., Sharma, S., Sevda, S., Ingle, A. P., & Pant, D. Circular economy aspects of lignin: Towards a lignocellulose biorefinery. Renewable and Sustainable Energy Reviews, 2020, 130 (January), 109977. https://doi.org/10.1016/j.rser.2020.109977

9. Liao Y, Koelewijn SF, Bossche GVD, Aelst JV, Bosch SVD, Renders T, Navare K, Nicolaï T, Aelst KV, Maesen M, Matsushima H, Thevelein J, Acker KV, Lagrain B, Verboekend D, Sels BF. A sustainable wood biorefinery for low–carbon footprint chemicals production. Science, 2020, 367(6484), 1385–90.

10. Obydenkova SV, Kouris PD, Hensen EJM, Heeres HJ, Boot MD. Environmental economics of lignin derived transport fuels. Bioresource Technologies, 2017, 243, 589–99.

11. Vangeel T, Schutyser W, Renders T, Sels BF. Perspective on lignin oxidation: advances, challenges, and future directions. Top Current Chemistry, 2018, 376(4), 30.

12. Zakzeski J, Bruijnincx PC, Jongerius AL, Weckhuysen BM. The catalytic valorization of lignin for the production of renewable chemicals. Chem. Rev., 2010, 110, 3552–99.

13. C. S. Lancefield, I. Panovic, P. J. Deuss, K. Barta, N. J. Westwood, Green Chem. 2017, 19, 202–214.

14. W. Lan, J. S. Luterbacher, Chimia, 2019, 73, 591–598.

15. K. H. Kim, C. S. Kim, Front. Energy Res. 2018, 6.

16. Pan, X., Xie, D., Yu, R.W., et al., *The Bioconversion of Mountain Pine Beetle-Killed Lodgepole Pine to Fuel Ethanol Using the Organosolv Process.* Biotechnol. Bioeng.*,* 2008. 101: p. 39-48.

17. de Vries, J.G., *Catalytic Conversion of Renewable Resources into Bulk and Fine Chemicals*. The Chemical Record, 2016, 16: 2787-2800.

18. Ben, H., and Ragauskas, A.J., *Heteronuclear Single-Quantum Correlation-Nuclear Magnetic Resonance (HSQC-NMR) Fingerprint Analysis of Pyrolysis Oils*. Energy Fuels, 2011. 25: p. 5791-5801.

19. *In Situ NMR Characterization of Pyrolysis Oil During Accelerated Aging*. ChemSusChem, 2012. 5: p. 1687-1693.

20. Dimitris, S.A., '*Heteronuclear NMR Spectroscopy of Lignins'*, in Lignin and Lignans, CRC Press, 2010), p. 245-265.

21. John, R., and Larry, L.L., *'NMR of Lignins'*, in Lignin and Lignans, CRC Press, 2010), p. 137-243.

22. Elhage, A.; Lanterna, A. E.; Scaiano, J. C. Tunable Photocatalytic Activity of Palladium-Decorated TiO_2: Non-Hydrogen-Mediated Hydrogenation or Isomerization of Benzyl-Substituted Alkenes. ACS Catal. 2017, 7, 1, 250–255.

23. Tran, M. H., Phan, D. P., & Lee, E. Y. (2021). Review on lignin modifications toward natural UV protection ingredient for lignin-based sunscreens. *Green Chemistry*, *23*(13), 4633–4646.

24. Widsten, P. (2020). *Lignin-Based Sunscreens—State-of-the-Art, Prospects and Challenges*.

25. Lee, S. C., Tran, T. M. T., Choi, J. W., & Won, K. Lignin for white natural sunscreens. *International Journal of Biological Macromolecules*, 2019, *122*, 549–554.

26. Bianchi, D., Franzosi, G., and Romano, A.M., 'Process for the Production of Lipids from Biomass', Eni S.p.A., Italy . 2012, p. 41pp.

27. Huang, D., and Qian, J., 'Method for Producing High-Purity Mannooligosaccharide Via Enzymic Hydrolysis of Manna-Containing Hemicellulose', Peop. Rep. China . 2013), p. 11pp.; Chemical Indexing Equivalent to 156:388287 (CN).

28. Gong, Z., Shen, H., Wang, Q., et al., Efficient Conversion of Biomass into Lipids by Using the Simultaneous Saccharification and Enhanced Lipid Production Process. Biotechnol. Biofuels, 2013. 6: p. 36.

29. Liang, M.-H., and Jiang, J.-G., Advancing Oleaginous Microorganisms to Produce Lipid Via Metabolic Engineering Technology. Prog Lipid Res, 2013. 52: p. 395-408.

30. Yu, X., Zeng, J., Zheng, Y., et al., 'Simultaneous Saccharification and Fermentation of Lignocellulosic Biomass for Single Cell Oil Production by Oleaginous Microorganisms', Washington State University Research Foundation, USA . 2013, p. 34pp.

31. Pu, Y., Kosa, M., Kalluri, U.C., et al., Challenges of the Utilization of Wood Polymers: How Can They Be Overcome? Appl. Microbiol. Biotechnol., 2011. 91: p. 1525-1536.

32. Ragauskas, A.J., Beckham, G.T., Biddy, M.J., et al., Lignin Valorization: Improving Lignin Processing in the Biorefinery. Science (Washington, DC, U. S.), 2014. 344: p. 709

33. Ragauskas, A.J., and Huang, F., 'Chemical Pretreatment Techniques for Biofuels and Biorefineries from Softwood', in Pretreatment Techniques for Biofuels and Biorefineries, Springer, 2013, p. 151-179.

34. Ramires, E.C., Megiatto, J.D., Gardrat, C., et al., Valorization of an Industrial Organosolv–Sugarcane Bagasse Lignin: Characterization and Use as a Matrix in Biobased Composites Reinforced with Sisal Fibers. Biotechnology and bioengineering, 2010. 107: p. 612-621.

35. Supanchaiyamat N, Jetsrisuparb K, Knijnenburg JTN, Tsang DCW, Hunt AJ. Lignin materials for adsorption: current trend, perspectives and opportunities. Bioresour Technol 2019;272:570–81.

36. Wang H, Pu Y, Ragauskas A, Yang B. From lignin to valuable products–strategies, challenges, and prospects. Bioresour Technol 2019, 271:449–61.

37. T. Renders, G. Van den Bossche, T. Vangeel, K. Van Aelst, B. Sels, Curr. Opin. Biotechnol. 2019, 56, 193–201

38. H. Deng, L. Lin, S. Liu, Energy Fuels, 2010, 24, 4797–4802

39. M. Ksibi, S. B. Amor, S. Cherif, E. Elaloui, A. Houas, M. Elaloui, J. Photochem. Photobiol. A, 2003, 154, 211–218

40. Z. Dong, H. Yang, P. Chen, Z. Liu, Y. Chen, L. Wang, X. Wang, H. Chen, Energy Fuels 2019, 33, 9934–9941

41. L. Kong, C. Liu, J. Gao, Y. Wang, L. Dai, Bioresour. Technol. 2019, 276, 310–317.

42. Saadia, A., Ashfaq, A., and Khursheed, A., Pollution Control Trends in Pulp and Paper Industry. Environ. Pollut. Control J., 2010. 13: p. 43-46.

43. Duan, Y., Wan, J., Wang, Y., et al., Study on Saccharification of Eucalyptus Lignocelluloses Hydrolysis and Reaction Kinetics in Supercritical Water. Taiyangneng Xuebao, 2013. 34: p. 689-695.

44. Sun, Z., Bottari, G., Afanasenko, A., Stuart, M. C. A., Deuss, P. J., Fridrich, B., & Barta, K. (2018). Complete lignocellulose conversion with integrated catalyst recycling yielding valuable aromatics and fuels. *Nature Catalysis*, *1*(1), 82–92.

45. Shao, Y., Xia, Q., Dong, L., Liu, X., Han, X., Parker, S. F., Cheng, Y., Daemen, L. L., Ramirez-Cuesta, A. J., Yang, S., & Wang, Y. (2017). Selective production of arenes via direct lignin upgrading over a niobium-based catalyst. Nature Communications, 8(May), 1–9.

46. El, R., Brosse, N., Chrusciel, L., Sanchez, C., Sannigrahi, P., & Ragauskas, A. Characterization of milled wood lignin and ethanol organosolv lignin from miscanthus. Polymer Degradation and Stability, 2009, 94(10), 1632–1638.

Chapter 3 Molecular Model Studies

3.1 Introduction

Lignin, as previously defined, is primarily a network of guaiacyl, p-hydroxyphenyl, and syringyl units connected by an assortment of ether linkages. This constitutes an alkyl aryl ether backbone, which is heterogeneously functionalized with methoxyl, benzyl alcohol, and phenolic hydroxyl species.

The catalytic conversion of lignin through selectively cleaving ether linkages results in lower molecular weight compounds, such as aromatic acids and phenols, some of which may eventually replace certain equivalent petroleum-derived commodities and fine chemicals.

A few factors complicate the efficient conversion of lignin into value-added chemicals and wide-spread adoption of lignin as a valuable feedstock. Notable among those are the variability of ether linkages between monomers, the reactivity of associated hydroxyl groups, and finally the instability of resulting monomeric products under reaction conditions. A simplified lignin structure in Figure 3.1, a schematic representation not to scale, also includes a condensed monolignol building blocks that represents guaiacyl, p-hydroxyphenyl, and syringyl units.[1]

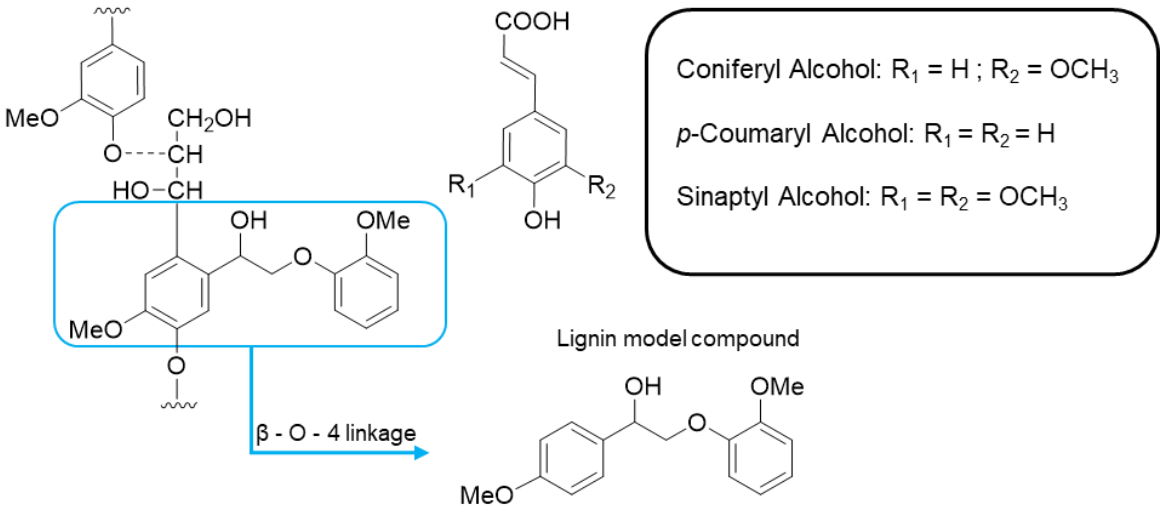

Figure 3.1: Lignin structure highlighting β-O-4 ether linkage, as well as generic monolignol structural diagram, and 2-(2-Methoxyphenoxy)-1-(4-methoxyphenyl)ethanol model compound (commonly referred to as “BA”)

The molecular model of choice for the present study was a β-O-4 representative model called 2-(2-methoxyphenoxy)-1-(4-methoxyphenyl)ethanol. Since part of the mechanism studied may have an interplay between its alcohol group possibly being converted into a ketone, the model as shown is referred to as BA, while the ketone equivalent is referred to as BK. The reason for this choice has to do with the inter-unit linkage abundance in common wood samples, where the predominant linkage is β-O-4, being present in 45 to 50% of linkages in softwoods, around 60% in hardwoods, and up to 84% in grasses. The complete relationship between each linkage, represented by a lignin model compound, and their respective abundance is shown in Table 3.1.

Another reason that makes the choice of BA as a model compound an interesting one are the very challenges of using it in a photochemical system. One of the major issues discussed about the acquisition of small molecules from lignin is the instability of certain produced monomeric units, and this model (BA) is an example that produces such unstable structures, especially under light. Understanding such a crucial limitation and studying strategies and systems that may overcome said limitations is essential in the pursuit of methodologies that may eventually be applied to the complex protolignin valorization challenge.[2,3]

There are many theories regarding different mechanisms for the breakage of each linkage binding lignin together, and much has been done to study them using molecular models. In the context of catalytically and photocatalytically cleaving β-O-4 linkages we may assume the interplay between three mechanisms, though more may certainly exist: one-pot C_α-C_β bond cleavage via formation of C_β or O_α radical and proton-coupled electron transfer (PCET) process; one-step C-O bond cleavage via C_α radical intermediate; and a two-step approach that uses separate conditions to enact benzylic oxidation on the model and only then promotes C-O breaking. A simplified version of these reactions has been represented in Figures 3.2 and 3.3.

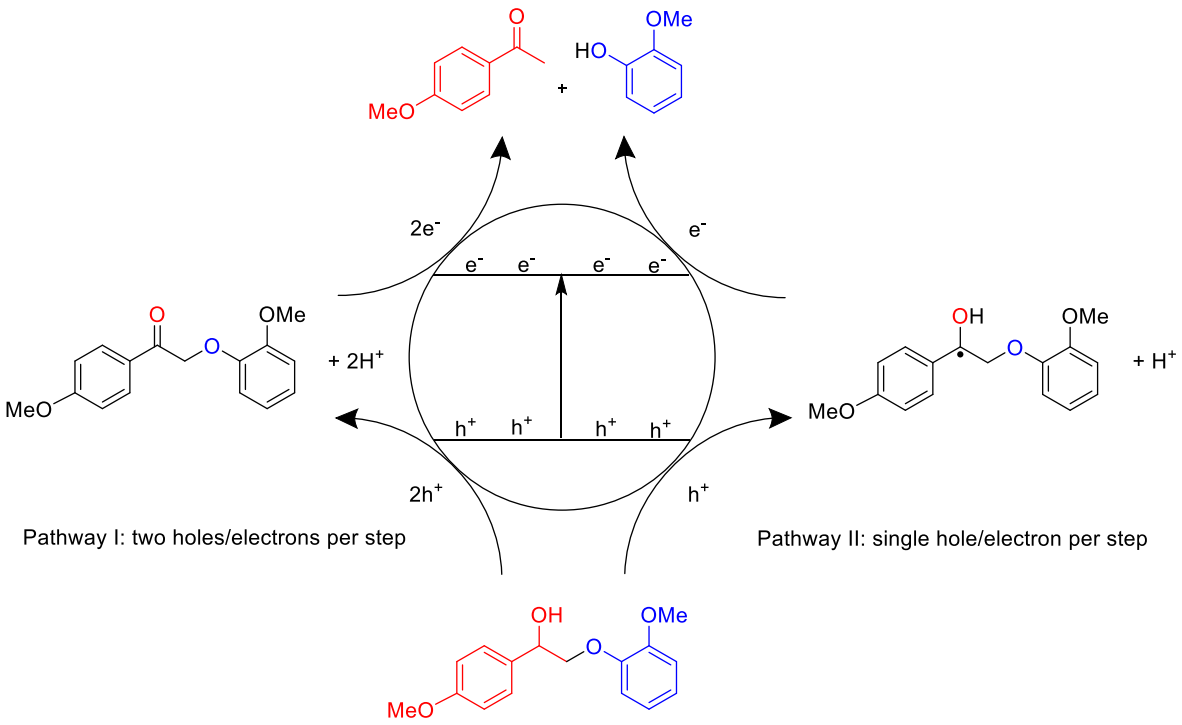

Figure 3.2: Two theorized pathways for the β-O-4 linkage molecular model breaking for lignin valorization reactions. Adapted from Chen, H., et al. (2021).

The representation of Pathway I in Figure 3.2 omits the formation of the radical in the process, since this is highly dependent on the conditions and catalyst used, and for the specific cases in the present study, we do not have enough evidence to confirm the identity of the radical formed. Complementary, and perhaps addressing more directly the format adopted to represent these reactions in the present work, Figure 3.3 shows three pathways for the formation of β-O-4 products from BA. The third pathway shown represents a two-step reaction in which different conditions produce the ketone form of the molecular model and the final products. The differentiating factor is the ability to detect reasonable amounts of BK in the reaction mixture prior to the introduction of the new light or catalyst, for instance. An example of this mechanism will be present in our experiments as will be shown later.

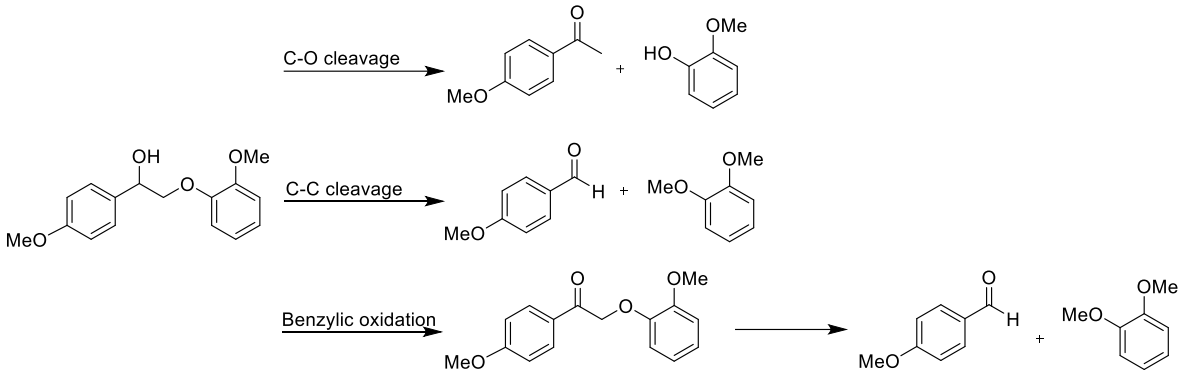

Figure 3.3: Three pathways known and applicable for our experiments using β-O-4 alcohol models. First two cleavages involve a single set of conditions and radical intermediates leading to a “single step” conversion into products, while benzylic oxidation requires a different catalyst or conditions to produce ketone in the structure.

Table 3.1: Linkage structure and distribution of occurrence in major certain plant groups. Adapted from Rinaldi (et. al, 2016)[1].

Name	β-aryl ether	Resinol	Phenylcoumaran	Biphenyl + Dibenzodioxocin	Spirodienone	Diaryl ether
Linkage structure from model compound	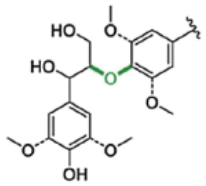	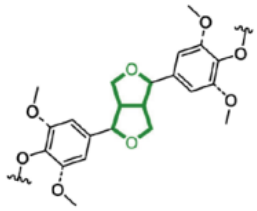	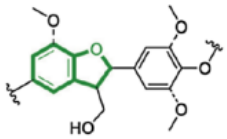	a 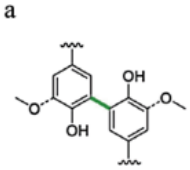 b 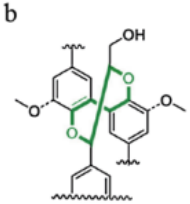	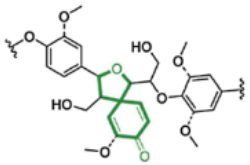	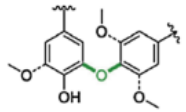
Inter-unit linkage	β-O-4	(β- β) + (y-O-α)	(β–5)+(α–O–4)	5–5[a] (5–5)+(α–O–4)+(β–O–4)[b]	β–1+(α–O–α)	4–O–5
Softwood (%)	45-50	2-6	9-12	5-7	1-9	2
Hardwood (%)	60-62	3-16	3-11	<1	1-7	2
Grasses (%)	74-84	5-11	5-11	--	-	-

With these factors in mind, the goal of this section was to explore some of the challenges and opportunities presented by different photochemical systems in the lignin valorization space. Through the investigation of β-O-4 linkage breaking reactions with different photocatalysts, solvents, and light sources, we aimed to better understand observations from the protolignin and technical lignin valorization reactions from the previous chapter, as well as identifying new directions for them.

3.2 Experimental Methodology

Molecular model synthesis

The process of synthesizing this model was accomplished similarly to previous literature on the subject[16]. A 125 mL round bottom flask was charged with 2-bromo-4′-methoxyacetophenone (2.5 g, 10.9 mmol), guaiacol (1.49 g, 12.0 mmol), potassium carbonate (2.27 g, 16.4 mmol), and acetone (75 mL). The round bottom flask was then attached to a reflux system after receiving a magnetic stir bar and was heated in an oil bath to reflux (76 °C) and stirred for 3 hours. The resulting mixture was observed to turn from a light yellow to a darker orange colour.

At the end of the reflux, the mixture was left to cool down to room temperature, after which it was filtered through a 2 cm layer of silica and concentrated using a rotary evaporator at room temperature. The crude product had a mixture of white and yellow powders, signaling impurities, and two methods were used to purify them. The first was using chromatography on SiO_2, with a 4/1 mixture of hexanes and ethyl acetate, which presented lower yields than expected, being only around 55% of the initial 0.5 g of crude product.

A second methodology used for purification of the final product was recrystallization, using two different solvents, first with ethanol (EtOH), and then with ethyl acetate (EtOAc). Recrystallization with EtOH gave a yellow/white mixed product even after several cycles with filtration, but ethyl acetate was able to give a fully white solid after just two cycles, with higher yields than the column chromatography (>85%).

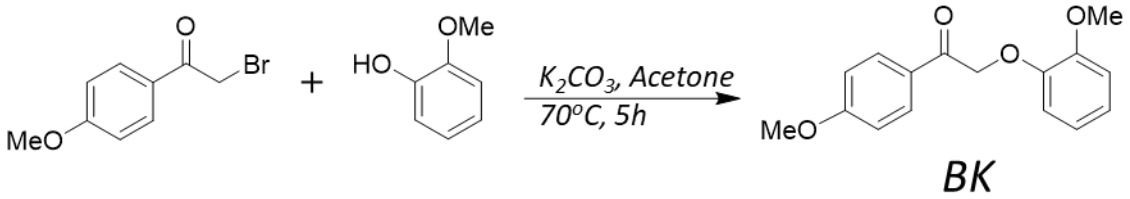

Figure 3.4: Reaction summary for the synthesis of the molecular model compound "BK"

Synthesis of the benzylic alcohol model 2-(2-methoxyphenoxy)-1-(4-methoxyphenyl) ethanol, also referred to here as "BA", was done in a similar fashion as to prior reports as well. To a 100 mL round bottom flask were added 1.2 g of BK, 20 mL of tetrahydrofuran (THF), 5 mL of Milli-Q water, and 0.329 g of sodium borohydride ($NaBH_4$) added in three equal portions to maximize the bubbling time of the mixture. After bubbling of gas ceased, the mixture was stirred at room temperature for 3 hours. After mixing, the resulting solution was quenched with 35 mL of saturated aqueous ammonium chloride (NH_4Cl) and diluted with an equal volume of water. The mixture was then extracted using EtOAc (4 x 25 mL), and the combined organic extracts were washed with brine, dried over magnesium sulfate ($MgSO_4$), filtered, and then concentrated in the rotary evaporator to give a slightly yellow oil.

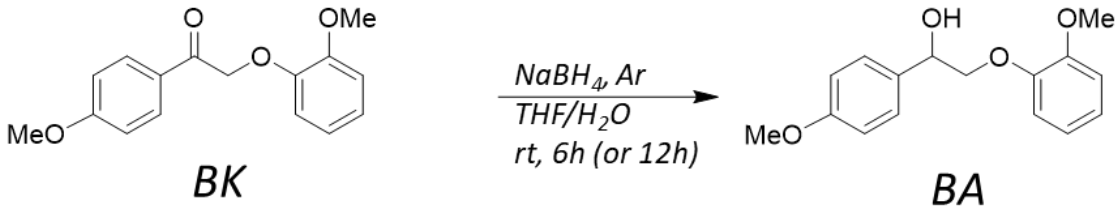

Figure 3.5: Simplified reaction for the conversion of molecular model BK into molecular model BA

(75:25, hexanes/EtOAc). Purified BA was also obtained via recrystallization in a minimum amount of 75:25, hexanes/EtOAc in yields of up to 90%. Purified crystals obtained in the recrystallization method are shown in Figure 3.6.

Figure 3.6: Purified BA crystals after recrystallization with hexanes/EtOAc.

3.3 Results and Discussion

Many of the experiments in this section were developed in conjunction, or at least in response, to experiments done with results and observations from the technical and protolignin investigations done in Chapter 3. This is due to the “lignin first” type of approach adopted so that real results and effects observed when complex lignin systems were present would then be further investigated on the molecular level, since the other way around tends to provide false expectations. Most schemes in this results section will contain the three main target compounds from the lignin valorization reaction attempted in our experiments, those being BK as a product of benzylic oxidation, and the pairing of guaiacol and acetanisole from the C-O breaking of the model. The representation of BK does not necessarily equate to a reasonable yield of BK being found in the process, as the pathway achieved for that particular reaction may bypass the formation of the ketone in its own step. Thus, if no yield of BK is shown in the table or discussed after it, it is assumed that no detectable yield of BK was present.

Oxidation of Dimeric Model Compound in Water

As discussed in Chapter 1, transitioning organic reactions from typical organic solvents to aqueous media is highly desirable, since the solvent may be reused after separation of organic compounds, and the safety and environmental benefits of using water as a solvent cannot be overstated.[4,5] Thus, the first conditions tested in this work for the breaking of molecular models were done in Milli-Q water, assisted by surfactants. The choice of using surfactants as a part of these reactions was, firstly, for consistency with similar reactions done with technical lignins in which the surfactant often stabilizes the lignin suspension in water, and second, in order to assist in the contact between the heterogeneous catalyst and the organic molecules in the aqueous media.[4] Select results from these experiments are shown in Scheme 4.1, accompanied by the yields of the two expected products and the ketone-substituted form of the starting material.

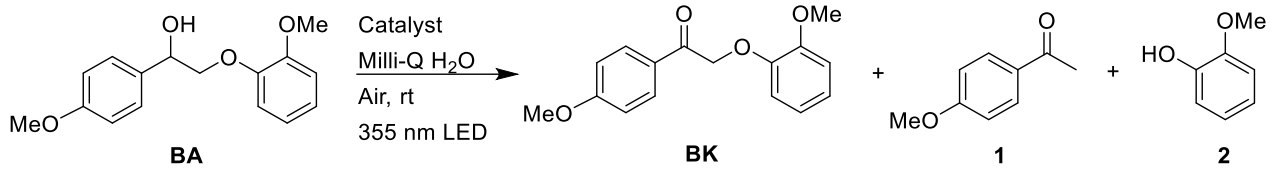

BA **BK** **1** **2**

Exp nº	Catalyst	Surfactant	Time	Conversion	Yield BK	Yield 1	Yield 2
1	$NbOPO_4$ (1.3 μmol)	CTAB	3 h	20%	-	-	-
2	$NbOPO_4$ (1.3 μmol)	CTAB	15 h	60%	10%-	5%	2%
3	$NbOPO_4$ (1.3 μmol)	-	15 h	40%	6%-	3%	1%
4	TiO_2 (1.2 μmol)	CTAB	15 h	10%	-	-	-

Scheme 3.1: Breaking of molecular model BA in aqueous media using niobium phosphate and TiO_2 as catalysts. Yield based on maximum yield from starting material, acquired by GC-FID analysis.

Upon examining the results contained in Scheme 3.1, niobium phosphate showed some reactivity under aqueous conditions, though the yields of the individual molecular models were often close to or below our limits of detection. It is possible that most of the losses were due to the extraction and drying process associated with the aqueous phase reactions, and that those are either inflating the estimated conversion numbers or masking the real yields. It is possible that much of the organic compounds added to the mixture is either in hydrophobic pockets of the surfactant

or attached to the surface of the catalyst. Titanium dioxide showed poor activity in water and was also unable to remain as a stable solid suspension for very long, forming large agglomerates which are bound to show lower catalytic activity. This was partly the purpose of the experiment, as this contrast demonstrates the need for further studies of niobium-based compounds as primary catalysts or as supports in aqueous reactions as the primary catalyst.

Some concerns with the use of CTAB as a surfactant for these reactions arose from the stirring and observation of foaming atop the solution, which can cause some issues with the mixing of the components and is generally undesirable for these reactions. Furthermore, as CTAB could be a contributing factor in the poor extraction observed in the first few reactions, a designer surfactant was sought after, since they are tuned specifically to accommodate organic chemical reactions in water, are non foaming, and are said to have good stability and are said to facilitate the extraction of organic components after the reaction. We chose TPGS-750M as the surfactant of choice, due to its versatility as an amphiphile surfactant developed for metal-catalyzed organic reactions in water, such as Heck reactions, Suzuki-Miyaura, olefin metathesis, among others.

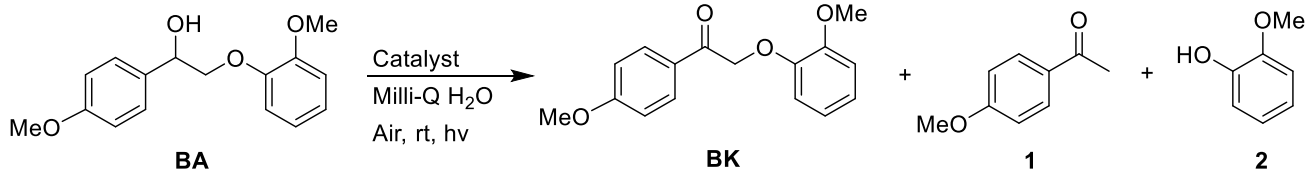

BA **BK** **1** **2**

Exp nº	Catalyst (1.3 µmol)	Surfactant	Time	Conversion	Yield BK	Yield 1	Yield 2
5	$NbOPO_4$	2% TPGS-750M	15 h	20%	-	-	-
6	$Pd@Nb_2O_5$	2% TPGS-750M	15 h	100%	10%-	5%	2%
7	$Pd@TiO_2$	2% TPGS-750M	15 h	40%	6%-	3%	1%
8	$NbOPO_4$ + $Pd@TiO_2$	2% TPGS-750M	15 h	10%	-	-	-

Scheme 3.2: Breaking of molecular model BA in aqueous media using niobium phosphate and TiO_2 as catalysts. Yield based on maximum yield from starting material, acquired by GC-FID analysis.

The use of a novel designer surfactant, especially one made with renewable materials such as TPGS-750M, is highly desirable, and its presence seemed to enhance the conversion of BA into products greatly compared to CTAB. Even so, there is not an extensive amount of research done with photochemical stability of this designer surfactant, only thermal and chemical, and what was observed from the GC-MS and GC-FID results hampered the use of these in a meaningful way. Different from the valorization reactions of lignin, where a multitude of products is expected, only a handful of products is expected at most from the molecular model breaking reactions, but instead, in the presence of TPGS-750M over a dozen unidentified compounds can be detected. This may be from a photochemical instability of the surfactant that had not been previously discussed in literature.

Oxidation of molecular model compounds in organic solvents

Our research then pivoted into simplifying the systems used, as the introduction of aqueous media and subsequent extractions was leading to inconclusive results with lignin valorization and to molecular model breaking inconsistencies. In order to still abide by the ideas expressed in Chapter 1 on the use of greener and less dangerous solvents, MeOH and AcN were used for the majority of experiments, as the former is a recommended solvent according to most classifications, and the latter is only problematic in the safety standards by a small margin and may yet be used under the right conditions. For reactions using organic solvents, analysis was conducted by centrifuging the sample to separate the catalyst and the solution containing organic products and starting material. The organic phase is then passed through a syringe filter to ensure no solids enter the columns of either chromatography instruments.

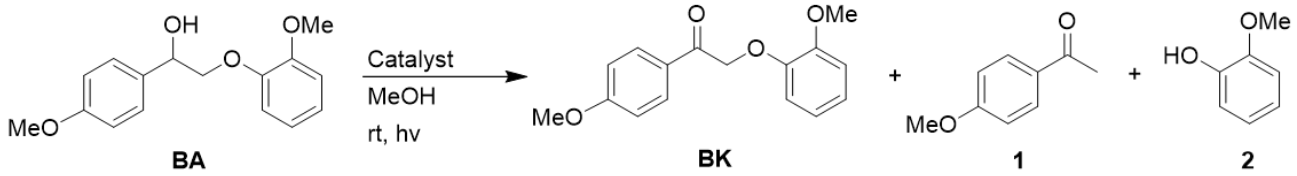

BA **BK** **1** **2**

Exp nº	Catalyst	Atmosphere	Time	Light	Conversion	Yield 1	Yield 2
9	2 mg $NbOPO_4$	Air	15 h	365 nm	13%	1%	-
10	2 mg $NbOPO_4$	Argon	15 h	365 nm	9%	-	-
11	2 mg $Pd@TiO_2$	Air	15 h	465 nm	20%-	3%	-
12	2 mg $Pd@TiO_2$	Argon	15 h	465 nm	34%-	4%	-
13	1 mg $NbOPO_4$ + 1 mg $Pd@TiO_2$	Air	15 h	465 nm + 365 nm	27%-	2%	-
14	1 mg $NbOPO_4$ + 1 mg $Pd@TiO_2$	Argon	15 h	465 nm + 365 nm	32%-	2%	-

Scheme 3.3: Reactions with 0.9 mM of BA lignin model in 1.5 mL of MeOH, using niobium phosphate and $Pd@TiO_2$ as catalysts. Yield based on maximum yield from starting material, acquired by GC-FID analysis.

The initial goal of these experiments was to test the ability of niobium phosphate to convert the molecular model into the two major products under UV-light irradiation. Parallel to those, we chose a visible light catalyst to contrast these reactions, and $Pd@TiO_2$ was chosen given past experiences of our research group with it, and thus it was similarly tested also under both an inert atmosphere and under argon, using a 465 nm single-head LED as the light source. Lastly, a combination of both catalysts and light sources was done, to see if any complementary effects could be observed.

The results shown in Scheme 3.3 under both light sources, as well as both under argon and air, were shown to be below expectations. The yields achieved from these reactions were not too dissimilar to the ones observed for aqueous reactions, which we acknowledge need several further optimizations to reach its true potential. Oxidation of the molecular model into the ketone equivalent was at its best under blue light irradiation in the presence of the palladium catalyst, especially under argon, with a total conversion of 34% in reaction **12**, although one can make a case for the system shown in both **13** and **14**, as only half of the mass of the palladium catalyst was present in both, and a similar conversion value was achieved, and in **13** we observed an improvement of this reaction under air which may be significant.

Given the underwhelming results in MeOH, we decided to experiment with similar conditions under acetonitrile, switching to this solvent for the reasons previously discussed. In order to isolate individual conditions to a better degree, the following battery of experiments were conducted exclusively under UV light, which can be seen in Scheme 3.4.

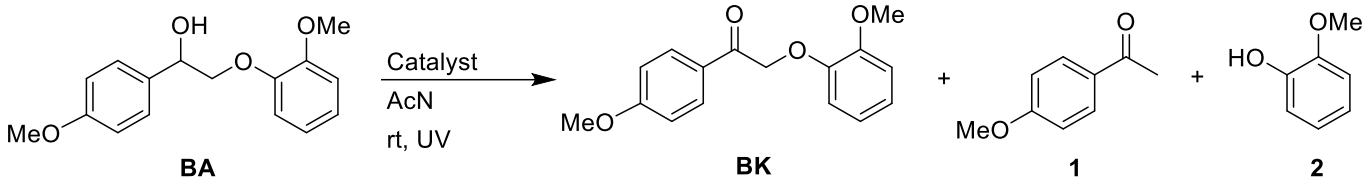

BA **BK** **1** **2**

Exp n°	Catalyst	Reactant	Time	Light	Conversion	Yield 1	Yield 2
15	14 mg $Pd@TiO_2$	5 mM BA	20 h	365 nm	37%	26%	20%
16	14 mg TiO_2	5 mM BA	20 h	365 nm	40%	38%	38%
17	14 mg $Au@TiO_2$	5 mM BA	20 h	365 nm	24%	10%	3%
18	14 mg $NbOPO_4$	5 mM BA	20 h	365 nm	64%	3%	31%
19*	-	5 mM of **1** and **2**	20 h	365 nm	-	0 (88%)	80%

Scheme 3.4: Reactions with 5 mM of BA lignin model in 2 mL of AcN, using niobium phosphate, TiO_2, $Pd@TiO_2$, and $Au@TiO_2$ as catalysts. Yield based on maximum yield from starting material, acquired by GC-FID analysis.

Due to new observations, finds in the literature reports, and difficulties associated with detections limits of our instruments, it was decided that the starting material should be at a higher concentration for these new experiments. While maintaining the proportion of catalyst to starting material was important, it was relevant to our interests to make full use of the irradiating light in the specific volume used. We determined that a normalized amount of about 7 mg of catalyst per mL of solvent was an ideal start. It was also included a control vial in this setup, where acetanisole and guaiacol were placed under similar concentrations to the starting material, without the presence of a catalyst, and were subjected to the same UV-light irradiation and workup as the rest of the samples, in order to observe if full recovery of the products would be possible, as can be seen in reaction **19** of scheme 3.4.

Comparing the results obtained, still on Scheme 3.4, with recent work done with a photochemical approach to molecular model studies[13-15], some of these

present quite the upside. The conditions used were simple, with no need for a high pressure of inert or reductive gases, there was no base present, and no optimizations for the stabilization of products were known at the time, meaning the yields of 30% and above achieved under these circumstances have many avenues to be improved.

Following the success of the previous experiments, a screening of heterogeneous catalysts was planned, using different metals and semiconductive supports. A higher concentration of the reactant was chosen so that we could better observe conversion issues and compensate for some of the light limitations of this reaction. Since we ascertained that some product is lost to light, the lower the concentration of product, the higher the margin on error introduced by said difference, making it harder to evaluate these results. Scheme 3.5 shows the results of this next battery of experiments, with 10 mM of starting molecular model, under UV irradiation, for 20 h in sealed vials without purging.

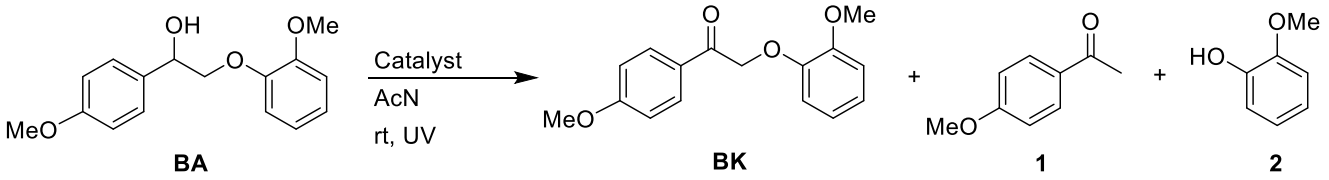

BA **BK** **1** **2**

Exp n°	Catalyst	Reactant	Time	Light	Conversion	Yield 1	Yield 2
20	14 mg $Pt@TiO_2$	10 mM BA	20h	365 nm	71%	36%	27%
21	14 mg $Au@TiO_2$	10 mM BA	20h	365 nm	66%	45%	30%
22	14 mg $AuPd@TiO_2$	10 mM BA	20h	365 nm	97%	48%	32%
23	14 mg $Au@ZnO_2$	10 mM BA	20h	365 nm	89%	37%	5.0%
24	14 mg $Pd@Nb_2O_5$	10 mM BA	20h	365 nm	100%	12%	3.8%

Scheme 3.5: Reactions with 10 mM of BA lignin model in 2.0 mL of AcN, under air, with a host of different photocatalysts. Yield based on maximum yield from starting material, acquired by GC-FID analysis.

The results shown in Scheme 3.5 show great promise, since the high conversion values, and reasonable yields, especially for **20**, **21** and **22**, indicate that with the right techniques to improve product stability, complete conversion of this β-O-4 lignin model is attainable under photocatalytic conditions. Reaction condition **22** in particular, which used a AuNP decorated onto a $Pd@TiO_2$ catalyst, shows particular promise, since it has the highest yield and conversion of the starting material.

Despite the complete conversion of starting material, reaction condition **24** shows very little yield of acetanisole and guaiacol detected under the available conditions. One explanation for this occurrence is that either the products from the reaction or the starting material itself are strongly attaching to the surface of the catalyst, justifying to some extent why they are not present in the chromatograms after a simple separation process. Another possibility is that there may be a formation of different products involved, which would align with observed peaks at very low elution times in these sample's chromatograms. There is data in the literature that indicates that niobium-based catalysts may facilitate the demethoxylation of benzylic molecular models, which may be followed by hydrogenation of benzyl rings with the right conditions, such as a co-catalyst that may assist this process and low pressures of H_2.[11] Further thoughts on some of the improvements that can be made to these reactions will be shared in Chapter 4, for future work on this topic.

Several of the photocatalysts shown on Scheme 3.5 have been shown to be photocatalytically active under visible light conditions, and thus, following the success of the catalysts used under UV-irradiation, as attempt was made to observe if a similar result could be achieved under visible light irradiation. The target wavelength was decided based on the absorption of the metal decorating the support.

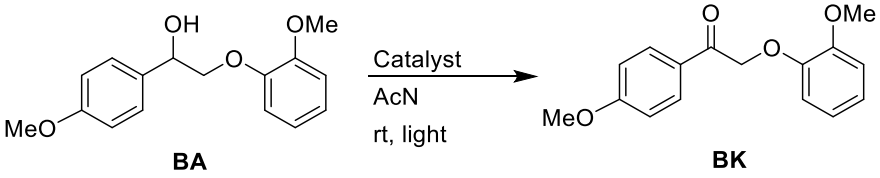

BA **BK**

Exp n°	Catalyst	Solvent	Reactant	Light Source	Time	Yield	Conversion
25	14 mg $AuPd@TiO_2$	2 mL AcN	10 mM **BA**	Green LED	20h	2%	10%
26	**14 mg $Pd@Nb_2O_5$**	**2 mL AcN**	**10 mM BA**	**Blue LEDi**	**20h**	**15%**	**65%**
27	14 mg $Pt@TiO_2$	2 mL AcN	10 mM **BA**	Blue LED	20h	5%	40%
28	14 mg $AuPd@TiO_2$	2 mL AcN	10 mM **BA**	RGB LEDi	20h	5%	15%

Scheme 3.6: Screening of visible-light irradiation conditions, using 10 mM of BA lignin model in 2.0 mL of AcN, under air. Yield based on maximum yield from starting material, acquired by GC-FID analysis.

Nanoparticles of noble metals of palladium, gold, and platinum were decorated onto common semiconductive supports, and the yields at first seemed to indicate that these conditions were not optimal in any of the light conditions and combinations assessed. Though the highest yield achieved was only 15% using $Pd@Nb_2O_5$ catalyst, lower than previous results but still notable, the most important achievement of these experiments was in the conversion observed.

What set apart conditions **26** and **27** from previous experiments is that we were able to produce and quantify the formation of BK after the reaction. Previous experiments may have shown low percentages of BK being formed, as a probable side product of the oxidative breakage of the model compound under ultraviolet irradiation conditions, but in this case, it was produced under visible light in considerate amounts by both **26** and **27**. In the case of 26, 45% of the starting material was converted into BK, while in 27 the yield of BK was around 30%.

In order to put these results into perspective, using a comparison with similar literature, we may be interested in the work of Corey R.J. Stephenson and his research associates. His group has done numerous experiments attempting to merge visible-light photoredox and transition metal catalysis in order to enhance lignin valorization, with a focus on molecular model studies, and in one such case, Kärkäs (M. D., et. al, 2016)[13] performed experiments involving an Iridium photoredox catalyst and several palladium catalysts, to separately but concurrently perform benzylic oxidation followed by C-O bond cleavage of a β-O-4 lignin model compound. Although their work reached higher yields for the benzylic oxidation step, upwards of 85%, their methodology required a much more expensive homogeneous catalyst ($[Ir\{dF(CF_3)ppy\}_2$- (dtbbpy)]PF_6), in addition to Pd(OAc), as well as sodium persulfate as a base, in a comparable amount of time (15 hours), under blue light and room temperature. Also relevant is their use of DMF as the solvent of choice, which as previously shown, is considered a dangerous solvent recommended to be substituted whenever possible. Our experiment in MeCN achieved 65% conversion with an easily recyclable catalyst, while their experiment with the same solvent resulted in only 11% yield of ketone yield. Further experimentation with optimization

of this benzylic oxidation step, as well as the continuation of our work on the second step (to follow) could result in greener overall conditions for the same lignin valorization reactions.

While reactions that use UV irradiation in lignin valorization reactions have to contend with the loss of key products caused by their photosensitivity, visible light reactions have to compensate for longer reaction times and, more often than not, additional components such as bases, higher temperatures, or pressurized reductive environments. Certain strategies have begun to arise[2] that combine the capabilities of both approaches, in dual-light irradiation systems, that sequentially irradiate the sample with visible light until a maximum of a precursor such as BK is formed, and then UV light is introduced causing a rapid conversion of BK into products, and further converting BA through the chain until an optimal yield of acetanisole and guaiacol is achieved. This approach shortens the necessary time of irradiation under both conditions, making it possible for an optimization of the system until a condition with higher maximum yields is achieved.

Using this as a basis, we sought to find an optimal co-catalytic system that could take maximum advantage of the produced BK once UV irradiation starts, so a battery of experiments was planned to determine a catalyst that would not compete or cause side-reactions during the visible light phase, and at the same time, that could quickly obtain high yields of acetanisole and guaiacol.

Table 3.2: Conditions for ketone model conversion into products using 370 nm UV light irradiation, using 2 mL of AcN as the solvent. Yields calculated using GC-FID and GC-MS.

Exp n°	Catalyst	Reactant	Time	Light	Conversion	Yield 1	Yield 2
29	10 mg TiO_2	5 mM BK	3 h	dark	-	-	-
30	No catalyst	5 mM BK	3 h	370 nm	90%*	4%	2%
31	10 mg TiO_2	5 mM BK	3 h	370 nm	99%	75%	55%
32	10 mg $NbOPO_4$	5 mM BK	3 h	370 nm	100%*	10%	5%

*Conversion under these conditions may be the product of mishandling of sample or experimental missteps.

Before discussing the complete results in Table 3.2, it bears mention based on the observed results in condition **30**, that in repeated experiments in the early

stages of this work it was theorized that BK was not photostable, appearing to be converted into unidentified products when irradiated by UV light without the presence of a catalyst. This was found to contradict a report by Lanzalunga and Bietti (2000)[13] showing that for photoconversion of this type of compound, a hydrogen atom transfer is necessary. This is possible either through an intramolecular hydrogen donor, such as a phenolic neighbouring group, or an extra-molecular donor, like a hydrogen-rich polar solvent. It is then possible that for the observed conditions, BK was not fully purified in that instance, leading to photoreactions by hydrogen transfer from guaiacol, for instance.

The remaining results in Table 3.2 were later corroborated with a sample of BK confirmed to be pure based on multiple analysis, although no further investigations on the observations for condition **30** were made. The best candidate for the co-catalyst under the current goals is TiO_2, given that it selectively converted BK into products with 75% yield for acetanisole, and 55% for guaiacol. The reaction with niobium phosphate showed the selective formation of a compound with a much lower molecular mass than the targets of the reaction, implying that successive oxidation reactions of the benzyl ring from the products may occur, generating a product with lost aromaticity. The same, to a lesser extent, can be seen with the experiment with no catalyst, although the compounds generated were not identified, nor particularly selective.

The near complete conversion of BK in 3 h as shown in **31** is a promising result, and further studies should optimize this value, in case lower times may achieve higher yields, even if with less conversion, due to the photosensitivity of the products.

Another experiment was devised to assess if the mechanism observed under blue light irradiation in reactions 25 to 28 for the formation of products 1 and 2 was possible starting from BK, or if the formation of BK was a side reaction, independent of the conversion of BA into products 1 and 2.

We moved to use blue light irradiation and BK as a starting material to observe if any conversion into the two main products was possible with several photocatalysts. The reactions shown in Scheme 3.6 were done using a well plate illuminator with blue 465 nm LEDs, and the vials containing the mixtures were placed on top of the well plate such that each vial was directly irradiated from the bottom by at least one LED, and some light from neighbouring LEDs also irradiated them from the sides. The well plate illuminator itself was then placed on top of a large magnetic stir plate, so that small magnetic stir bars placed on each of the vials provided the mixture with reasonable stirring. The setup as described can be seen in Figure 3.4.

This experiment was conducted in this way in order to facilitate future optimization reactions that would benefit from blue light irradiation, seeing as dozens of conditions can be placed over the well plate and tested at the same time.

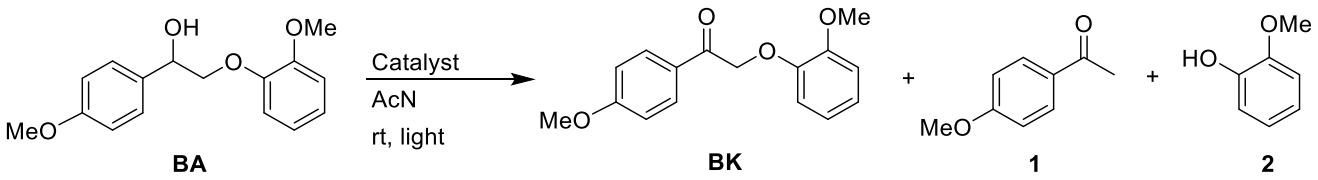

BA **BK** **1** **2**

Exp n°	Catalyst	Reactant	Time	Light	Conversion	Yield 1	Yield 2
33	No Cat	10 mM BK	20 h	Blue WPI	0%	0%	0%
34	14 mg $Pt@TiO_2$	10 mM BK	20 h	Blue WPI	0%	0%	0%
35	14 mg $Pt/Au@TiO_2$	10 mM BK	20 h	Blue WPI	0%	0%	0%
36	14 mg $AuPd@TiO_2$	10 mM BK	20 h	Blue WPI	2%	2%	0%
37	14 mg $Pd@Nb_2O_5$	10 mM BK	20 h	Blue WPI	0%	0%	0%
38	14 mg NbPhosph	10 mM BK	20 h	Blue WPI	5%	0%	0%

Scheme 3.7: Reaction conditions for ketone model conversion into products using 465 nm blue light irradiation from a well-plate illuminator. Yields calculated using GC-FID and GC-MS

These reactions confirmed our suspicions that the mechanism converting BA into acetanisole and guaiacol is separate from the mechanism that converts BA into BK. This can be seen from the presence of two catalysts that were able to achieve reasonable yields of acetanisole and guaiacol from BA, as well as formation of high amounts of BK, those being $Pd@Nb_2O_5$ and $Pt@TiO_2$. Neither catalyst was able to show any detectable conversion of BK.

Figure 3.7: Setup for rapid screening of conditions for the photocatalytic cleavage of lignin molecular models using blue light irradiation of a well plate illuminator.

A final set of experiments was conducted in parallel with results and experiments from Chapter 3, using CdS quantum dots to attempt visible light breaking of the β-O-4 lignin model compound, as shown in table 3.3. CdS quantum dots are known to have good photocatalytic activity under visible light irradiation, and have been shown to cleave molecular models of similar composition.[8,9] Two experiments were set up using the same CdS QD batch as shown previously, and they were placed in a vial with 10 mM of the BA model compound, under air, and irradiated with the blue well-plate illuminator. Two different solvent conditions were tested, based on literature on the subject, one being a 2:1 mixture of AcN and EtOH, and the second a 1:1 mixture of H_2O and EtOH.

Table 3.3: Conditions and results from photochemical cleavage reaction of 10 mM of BA lignin model, using CdS quantum dots as catalyst. Yield estimated based on GC-MS and GC-FID analysis.

Exp n°	Catalyst	Solvent	Time	Light	Conversion	Yield 1	Yield 2
1	5 mg CdS QDs	2:1 AcN/EtOH	20h	Blue WPI (465 nm)	>2%	>1%	>1%
2	5 mg CdS QDs	1:1 H_2O/EtOH	20h	Blue WPI (465 nm)	>2%	>1%	>1%

Estimation of the yields was necessary since results were very close to the error limits of the technique used. This indicated that these catalysts did not seem suitable for the set of conditions and the overall system we were experimenting on. Further analysis revealed that several by-products and compounds from the synthesis of que QDs still remained in the mixture, making further purifications needed. Considering that better visible light results had been previously achieved with catalysts that were much easier to synthesize, this section of our research was put on the backburner in terms of molecular model experimentation, while we attempted to explore other alternatives with real lignin.

References

1. Rinaldi, R., Jastrzebski, R., Clough, M. T., Ralph, J., Kennema, M., Bruijnincx, P. C. A., & Weckhuysen, B. M. Paving the Way for Lignin Valorisation: Recent Advances in Bioengineering, Biorefining and Catalysis Angewandte., 2016, 8164–8215.

2. Luo, N., Wang, M., Li, H., Zhang, J., Liu, H., & Wang, F. Photocatalytic Oxidation-Hydrogenolysis of Lignin β-O-4 Models via a Dual Light Wavelength Switching Strategy. ACS Catalysis, 2016, 6(11), 7716–7721.

3. Chen, H., Wan, K., Zheng, F., Zhang, Z., Zhang, Y., & Long, D. Mechanism insight into photocatalytic conversion of lignin for valuable chemicals and fuels production : A state-of-the-art review. Renewable and Sustainable Energy Reviews, 2021, 147(May), 111217.

4. Liu, X., Bouxin, F. P., Fan, J., Budarin, V. L., & Hu, C. Recent Advances in the Catalytic Depolymerization of Lignin towards Phenolic Chemicals : A Review, 2020, 4296–4317. https://doi.org/10.1002/cssc.202001213

5. Ramamurthy, V. Micellar control of photochemical reactions. Proceedings of the Indian Academy of Sciences - Chemical Sciences, 1984, 93(4), 635–646.

6. Kitanosono, T., Masuda, K., Xu, P., & Kobayashi, S. Catalytic Organic Reactions in Water toward Sustainable Society. Chemical Reviews, 2018, 118(2), 679–746.

7. Liu, X., Bouxin, F. P., Fan, J., Budarin, V. L., & Hu, C. Recent Advances in the Catalytic Depolymerization of Lignin towards Phenolic Chemicals: A Review. 2020, 4296–4317.

8. Nguyen, S. T., Murray, P. R. D., & Knowles, R. R. Light-driven depolymerization of native lignin enabled by proton-coupled electron transfer. ACS Catalysis, 2020, 10(1), 800–805.

9. Enright, M. J., Gilbert-Bass, K., Sarsito, H., & Cossairt, B. M. Photolytic C-O Bond Cleavage with Quantum Dots. Chemistry of Materials, 2019, 31(7), 2677–2682.

10. Han, G., Yan, T., Zhang, W., Zhang, Y. C., Lee, D. Y., Cao, Z., & Sun, Y. Highly Selective Photocatalytic Valorization of Lignin Model Compounds Using Ultrathin Metal/CdS. ACS Catalysis, 2019, 9(12), 11341–11349.

11. Zhao, H., Hu, X., Hao, J., Li, N., Zhi, K., He, R., Wang, Y., Zhou, H., & Liu, Q. An efficient bifunctional Ru-$NbOPO_4$ catalyst for the hydrodeoxygenation of aromatic ethers, phenols and real bio-oil. Applied Catalysis A: General, 2020, 591.

12. Lanzalunga, O., & Bietti, M. Photo- and radiation chemical induced degradation of lignin model compounds. 2000, 56, 85–108.

13. Bosque, I., Matsuura, B. S., & Stephenson, C. R. J. Photocatalytic Oxidation of Lignin Model Systems by Merging Visible-Light Photoredox and Palladium Catalysis. 2016, 2, 8–11.

14. Bosque, I., Magallanes, G., Rigoulet, M., & Ka, M. D. Redox Catalysis Facilitates Lignin Depolymerization. 2017, 1–8.

15. Kärkäs, M. D., Matsuura, B. S., Monos, T. M., Magallanes, G., & Stephenson, C. R. J. Biomolecular Chemistry the key to a sustainable carbon-neutral future. 2016, 1853–1914.

16. Enright, M. J., Gilbert-Bass, K., Sarsito, H., & Cossairt, B. M. Photolytic C-O Bond Cleavage with Quantum Dots. *Chemistry of Materials*, 2019, *31*(7), 2677–2682. https://doi.org/10.1021/acs.chemmater.9b00943

Chapter 4 Suggestions for Future Work

Upon first reading through the present body of work, one may be excused to think that it speaks against the use of photocatalysis for the advancement of lignin valorization reactions, for we have seemingly found somewhat as many reasons for it as we did against it. It is my conviction, however, that this is the ideal space for new ideas within science to grow: not too perfect otherwise anyone else can achieve it, and probably has, and not impossible so that future attempts can feasibly use what was learned to bring these ideas to new heights. It is with that in mind that we provide some pathways for future work, using what was learned throughout both the experimental journey of this work, as well as the one to write the present account.

Starting with future improvements to the molecular model results achieved, an investigation of the many strategies being used to improve product stability currently in the literature could be applied to great effect to further optimize the results shown in Chapter 4. Further investigation on the applicability of a biphasic setup should be done, this time including the use of molecular model compounds, to evaluate its impact on final yields. Of particular note, the use of AuPd@TiO_2 as a photocatalyst in the production of acetanisole and guaiacol from the molecular model BA showed very promising results that, given the right product-stabilizing strategy, could be a viable pathway that should be investigated further.

During our experimentation on the production of BK with photocatalysis using visible light irradiation, followed by UV irradiation to convert it into the desired products, we found conditions that presented very promising results. The use of Pd@Nb_2O_5 with TiO_2 as a co-catalyst has the potential to achieve high yields under mild conditions, according to the isolated experiments conducted. Unfortunately, due to time constraints and delays due to experimental mishaps, initial testing failed to

fully represent the capability of this system, thus leaving further testing to determine the future of this approach.[1]

Further testing of the best conditions found with the molecular model studies should be done with both protolignins and technical lignins.[2] The addition of formaldehyde to lignin valorization reactions has been linked to a protective pathway that may avoid repolymerization or dimerization side reactions and provide higher yields of monomeric units.[3] The addition of ethylene glycol has also been shown to promote a similar protective pathway, through acetal formation on the reactive phenolic aldehyde site of extracted monomeric units. It is also important to note that these stabilized products may also possess different photostability than the unprotected variants, and therefore an investigation of the presence of formaldehyde and ethylene glycol in the molecular model breakage reactions may serve to quantify that factor. [4-7]

Future work should thus explore the successful reactions for lignin transformation discussed in Chapter 3, in an application-focused approach for photochemical reactions. Since obtaining monomers has several challenges in batch, from the degradation of products to the competing light absorption of certain lignin moieties, flow photocatalysis is highly recommended.

The two-phase photochemical flow system assembled for the study of extracted lignin can be further improved upon by designing a system with a better pump or that has the two containers at the same level, by using a second pump to control the flow into each receptacle. This reactor can have further applications on other reactions with photosensitive products, and thus may have an impact that extends beyond lignin valorization reactions.

Since obtaining small molecules is not the only pathway to lignin valorization, it is important to note that lignin decolorization was achieved under mild aqueous conditions, and thus the production of decolorized lignin using niobium phosphate as a photocatalyst, for sunscreen applications should be investigated. Expanding upon

our findings, thorough colorimetric studies should be conducted, correlating the time of the reaction to different bleaching intensities, to achieve desirable coloration. Incorporation of this material into a base cream for stability testing is also necessary.[2,3]

The observed formation of a film in conditions shown in Chapter 3 indicates a possible pathway to new organized polymers produced from repolymerization of selective monomer units from lignin. This could be a pathway into the production of value added, petroleum-free thin films and polymers, although much remains to be tested to expand these findings.

Another strategy that may benefit the evolution of lignin as a resource is the continued experimentation of direct lignocellulosic-bound protolignin valorization, rather than technical lignin alternatives. Though the use of technical lignin limits the variability and unpredictability of certain results, these lignin-first processes allow for a more seamless coupling of the lignin valorization industry with existing industries that value the lignin-free extract containing cellulose and hemicellulose, such as pulp and paper, first generation ethanol facilities, and many others.[2]

A thorough techno-economic analysis of all different lignin applications stemming from photochemical and photocatalytic systems is necessary, as there is a common saying among industry-related publications in the subject that reads "…one can make anything out of lignin except money…" (Kumar, 2020).[2] The infrastructure necessary for advanced biorefineries that would be capable of producing some of the so called "low-cost" products made from lignin has been shown to appear quite prohibitive, given that the return is not assured when considering a new class of materials entering a space with existing products of high quality and lower costs. It must be said that the viability of some of these applications hinges on Governmental incentives and policies that stimulate the growth and wide-spread adoption of renewable resources, over existing petroleum-derived products.

By expanding our knowledge of protolignin valorization, through a sea of uncertainty and inconsistent results, we may see the emergence of a better and more economically viable lignin valorization industry.

References

1. Luo, N., Wang, M., Li, H., Zhang, J., Liu, H., & Wang, F. (2016). Photocatalytic Oxidation-Hydrogenolysis of Lignin β-O-4 Models via a Dual Light Wavelength Switching Strategy. ACS Catalysis, 6(11), 7716–7721.

2. Kumar, V., Chandel, A. K., Kumar, S. P. J., Sharma, S., Sevda, S., Ingle, A. P., & Pant, D. (2020). Circular economy aspects of lignin : Towards a lignocellulose biorefinery. Renewable and Sustainable Energy Reviews, 130 (January), 109977. https://doi.org/10.1016/j.rser.2020.109977

3. Liu, X., Bouxin, F. P., Fan, J., Budarin, V. L., & Hu, C. (2020). Recent Advances in the Catalytic Depolymerization of Lignin towards Phenolic Chemicals : A Review. 4296–4317.

4. Shuai, Li, et al. “Formaldehyde Stabilization Facilitates Lignin Monomer Production During Biomass Depolymerization.” Science (American Association for the Advancement of Science), vol. 354, no. 6310, AMER ASSOC ADVANCEMENT SCIENCE, 2016, pp. 329–33, https://doi.org/10.1126/science.aaf7810.

5. Deuss, Peter J., et al. “Aromatic Monomers by in Situ Conversion of Reactive Intermediates in the Acid-Catalyzed Depolymerization of Lignin.” Journal of the American Chemical Society, vol. 137, no. 23, American Chemical Society, 1900, pp. 7456–67, https://doi.org/10.1021/jacs.5b03693.

6. Lahive, Ciaran W., et al. “Advanced Model Compounds for Understanding Acid-Catalyzed Lignin Depolymerization: Identification of Renewable Aromatics and a Lignin-Derived Solvent.” Journal of the American Chemical Society, vol. 138, no. 28, American Chemical Society, 2016, pp. 8900–11, https://doi.org/10.1021/jacs.6b04144.

7. Deuss, Peter J., et al. “Metal Triflates for the Production of Aromatics from Lignin.” ChemSusChem, P. J. Deuss, C. W. Lahive, C. S. Lancefield, N. J. Westwood, P. C. J. Kamer, K. Barta, J. G. de Vries, ChemSusChem 2016, 9, 2974., vol. 9, no. 20, Blackwell Publishing Ltd, 2016, pp. 2974–81, https://doi.org/10.1002/cssc.201600831.

8. de Vries, Johannes G. “Catalytic Conversion of Renewable Resources into Bulk and Fine Chemicals.” Chemical Record, vol. 16, no. 6, Blackwell Publishing Ltd, 2016, pp. 2787–800, https://doi.org/10.1002/tcr.201600102.

Appendix A: Reprint Permissions

Figure 1 Permission Documentation

Figure 2 Permission documentation

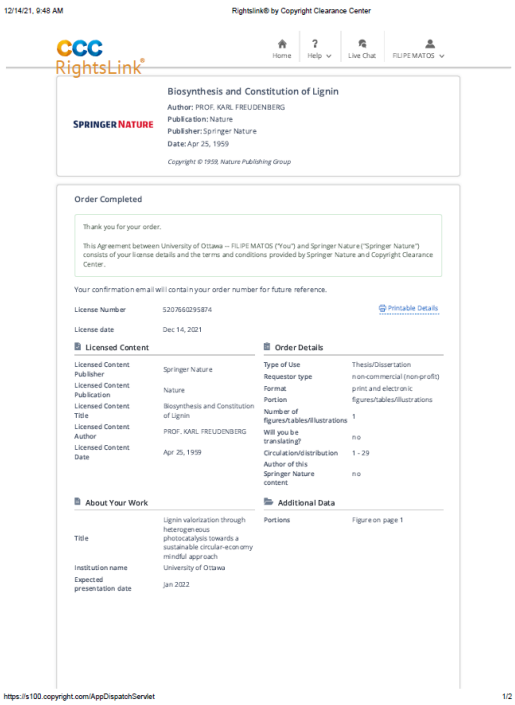

Figure 4 Permission Documentation

ELSEVIER LICENSE
TERMS AND CONDITIONS

Dec 14, 2021

This Agreement between University of Ottawa -- FILIPE MATOS ("You") and Elsevier ("Elsevier") consists of your license details and the terms and conditions provided by Elsevier and Copyright Clearance Center.

License Number	5207661449841
License date	Dec 14, 2021
Licensed Content Publisher	Elsevier
Licensed Content Publication	Elsevier Books
Licensed Content Title	Comprehensive Natural Products Chemistry
Licensed Content Author	Norman G. Lewis,Laurence B. Davin,Simo Sarkanen
Licensed Content Date	Jan 1, 1999
Licensed Content Pages	129
Start Page	617
End Page	745
Type of Use	reuse in a thesis/dissertation
Portion	figures/tables/illustrations

Figure 5 Permission Documentation (as provided)

Keywords: biobased polymer, compostable plastics, lignin modification, lignin properties, sustainable thermoplastics, natural adhesives, lignin compatibility

Citation: Glasser WG (2019) About Making Lignin Great Again—Some Lessons From the Past. Front. Chem. 7:565. doi: 10.3389/fchem.2019.00565

Received: 07 March 2019; Accepted: 24 July 2019;

Published: 29 August 2019.

Edited by:

Florent Allais, AgroParisTech Institut des Sciences et Industries du Vivant et de L'environnement, France

Reviewed by:

Paul-Henri Ducrot, INRA UMR1318 Institut Jean Pierre Bourgin, France

Gregory Chatel, Université Savoie Mont Blanc, France

Jean-Michel Lavoie, Université de Sherbrooke, Canada

*Correspondence: Wolfgang G. Glasser, wglasser@vt.edu

Figure 7 Permission Documentation

SPRINGER NATURE LICENSE
TERMS AND CONDITIONS

Dec 14, 2021

This Agreement between University of Ottawa -- FILIPE MATOS ("You") and Springer Nature ("Springer Nature") consists of your license details and the terms and conditions provided by Springer Nature and Copyright Clearance Center.

License Number	5207670875497
License date	Dec 14, 2021
Licensed Content Publisher	Springer Nature
Licensed Content Publication	Korean Journal of Chemical Engineering
Licensed Content Title	LaMer diagram approach to study the nucleation and growth of Cu2O nanoparticles using supersaturation theory
Licensed Content Author	Shahrzad Arshadi et al
Licensed Content Date	Jul 31, 2014
Type of Use	Thesis/Dissertation
Requestor type	academic/university or research institute
Format	print and electronic
Portion	figures/tables/illustrations
Number of figures/tables/illustrations	1